Tidal marsh restoration for flood risk mitigation. The effectiveness of managed realignment at Freiston Shore, Lincolnshire, UK

Dissertation

zur Erlangung des Doktorgrades
der Mathematisch-Naturwissenschaftlichen Fakultät
der Christian-Albrechts-Universität zu Kiel

vorgelegt von

Joshua Kiesel

Kiel, Juli 2021

Erster Gutachter: Prof. Dr. Athanasios T. Vafeidis

Zweiter Gutachter: Dr. Mark Schürch

Tag der mündlichen Prüfung: 25.10.2021

gez. Prof. Dr. Frank Kempken, Dekan

für Mama & Papa

The ocean throwing its waters over the broad reef appears an invincible, all-powerful enemy, yet we see it resisted and even conquered by means which at first seem most weak and inefficient.

—Charles Darwin (1839)

Acknowledgements

I can still recall warning voices from the end of my Master's thesis, when I was looking for a position to do a doctorate, telling me that a PhD would be a struggle offering ups for sure, but similarly some substantial downs. Ultimately, I got to understand what they were trying to say. I guess this is one of the situations in life where it is really advantageous not knowing in advance the details of what one is about to commit to. Nevertheless, if I would be in a position to choose again, I wouldn't decide any different. The reason for this attitude is that I now appreciate that a doctorate is never solely a one-man job and with the support I got from my supervisors, family, friends and colleagues during all those years, I would always be able to finally finish.

Here I would like to acknowledge some very important human beings who made this thesis possible. The first one on the list is a veritable doctor father, my first supervisor Nassos Vafeidis. Nassos, you have not only supervised me during my doctorate, but essentially since you encouraged me to study Geography in early summer 2011, almost exactly ten years ago. Thank you for your trust and support through all those years. Whenever I started panicking because things were not going as expected, you kept me down to earth and gave me the feeling that we would find a solution. It turned out: you were right! I would like to thank you too, Mark Schürch. You have committed to supervise me right from the start and I am glad that I found a supervisor with such enthusiasm and expertise in the topic and whose comments, ideas and critical questions were crucial for the quality of this thesis. My research stay at Cambridge University was an unforgettable experience and your support during these months,

particularly in the field, set the baseline for this thesis. In this regard, I would also like to thank the whole family Schürch and my colleagues at the Cambridge Coastal Research Unit, who made me enjoy my stay apart from the science. A special thanks goes out to Professor Tom Spencer, who enabled my stay at the CCRU and Professor Iris Möller. Working with you was a great source of inspiration for my work in the past years and your contributions were a benchmark for this thesis.

Mum and dad: It is difficult to put the gratitude I feel into words. You have always supported me, encouraged me in my plans, helped me out whenever help was needed and gave me the feeling that you are proud of me, regardless of whether I would succeed in my ventures or not. For example, when I switched from studying Sociology and Political Sciences to Geography back in 2011, you supported and encouraged me and gave me the feeling that I was doing the right thing. I don´t take this for granted. Without doubt, your love brought me to where I am now. Thanks for everything! I would also like to express my gratitude for having my brother Leon and my sister Nele around during most of my studies. You made me feel like being at home and gave me the comfort and trust that is necessary to take over big tasks. In that sense, I would also like to thank my aunt Julia Prien, her husband Krischan Prien as well as Kaller Brandt and Silke Rohde-Brandt. Liebe Oma, ich möchte diese Gelegenheit nutzen und auch Dir von ganzem Herzen Danke sagen. Seit dem Beginn meiner Promotion fieberst Du mit mir mit und verfolgst interessiert, wie ich mich von Meilenstein(chen) zu Meilenstein(chen) gehangelt habe. Dein Lebensweg und die unglaubliche Fürsorge, die Du Deiner großen Familie und auch mir entgegen bringst, sind ein großer Ansporn für mich. Ich bin sehr, sehr stolz auf Dich. Danke!

Sinja, you are certainly the person who had to make up for most of my frustrations, setbacks and sorrows. With tender and loving care you always brought me back on track and it is fair to say that I would not have finished my thesis without you. I can't recall the number of practice talks you had to listen to, how many days you had to cheer

me up and how often you had to drive away my sorrows. Without complaining, you were always there for me and always up for celebrating published papers, conference talks and anything else. I can't express how grateful I am to have you on my side. You are the most wonderful person. I love you.

With a little help from my friends. I am glad to live embedded in a safety net of incredible friends. Your contribution has been crucial through all those years. You always remind me of what really is important in life. Big shout out to my Nordic crew Malte Janssen, Patricia Wiff, Fabian & Svenja Aschenbach, Jan Lange, Hannes Popken, Tobias Laufenberg, Lennart Monsees, Jasper Schwampe, Tim Neumann, Lennart Bach, Basti Karkossa, Ina Borchert, Nils Dehn and my gang from the south Timo Eilert, Max & Jan Schöttker, Dustin Weiß, Jonas Cramer and Julian Marwede. Fortunately, two of my friends have walked with me along the long and winding road of the doctorate. Thanks Marcel König, for sharing my geeky excitement about oceans, coasts, nature in general and science, but for also diving into hour-long discussions on latest episodes of *Die Drei Fragezeichen*. It was awesome to have you around my office during the past five years. Another thank-you goes out to the best office mate in town, Claudia Wolff. I am glad that I could share my office with a friend for all those years and I am grateful that you always had an open ear for my problems and worries.

I would also like to thank some important scientists and colleagues who have supported me from the early days, shaped my scientific thinking during my Bachelor and Master studies and were significant for my decision to do a doctorate. Tobias Dolch, thank you for taking me to the AWI Wadden Sea Station on the island of Sylt, where you supervised my Bachelor thesis and brought me to some of the most incredible places I have ever visited. I am happy to call you a friend since many years. Thank you, Ingmar Unkel, for your infectious enthusiasm, which you equally spread among your students and colleagues. I am very happy to have had you as a supervisor for my Masters thesis

and I joyfully look back on many sessions of exam corrections (with loads of cookies and coffee) and commonly supervised Bachelor theses. I would also like to thank Heike Link. Without you, I would be missing the greatest and most unforgettable adventure of my life so far. Moreover, you equipped me with essential skills and knowledge and I couldn't have asked for a better preparation to do a doctorate. I would also like to thank you, Avan Antia, for your passionate commitment for the next generation of marine scientists from Kiel University. Thank you for carefully reading all of my thesis committee meeting protocols and for providing highly motivating feedback for each and every document. In each of our conversations, you managed to make me feel more positive and freshly motivated again. Among my academic companions, I would finally like to thank my colleagues and peers in the Coastal Risks and Sea Level Rise working group. I was in the lucky position to work in a supportive, productive environment and, more importantly for me, also in a friendly, comfortable atmosphere. I could equally get helpful scientific advice, talk about anything outside the scientific bubble or enjoy after-work hours in Kiel or at several conferences. I would like to thank the best colleagues ever; Lena Reimann, Sara Santamaria Aguilar, Leigh MacPherson, Bente Vollstedt, Jan Merkens, Jana Koerth, Sunna Kupfer and Maureen Tsakiris. I would also like to acknowledge the heart and soul of the Institute of Geography, Lars Michelsen. Thanks for so many in-depth discussions on the most important minor matter of the world and for the organization of several tipping and barbecue events. It was a pleasure to always have you around! Another football expert who has helped me to forget about the daily struggle for a while is Philipp Saggau. Thank you all!

Abstract

The ecosystem services delivered by coastal wetlands are among the most valuable on the planet, including the mitigation of climate related risks by sequestering carbon at rates several orders of magnitudes faster than tropical rain forests as well as the provision of natural coastal protection. Despite their ecological and socio-economic importance, coastal wetlands have been lost on a large scale in the past centuries, mostly due to human induced stress factors. The projected acceleration of Sea-Level Rise (SLR) may exacerbate the vulnerability of wetlands in the coming centuries, particularly in case of limited accommodation space due to the presence of anthropogenic infrastructure.

Increasing flood risk for low lying coasts and the continued reliance on traditional engineered solutions that have become economically and ecologically unsustainable in many locations require the development of new measures to mitigate these risks. In the last decades, Managed Realignment (MR) has been implemented with the aim to provide a cost effective and ecologically sustainable alternative to conventional coastal defence schemes. MR constitutes one of several Nature-Based Solutions (NBS) making use of the natural wave and surge attenuating capacity of coastal wetlands and their ability to build up vertically at rates often higher than historical SLR. MR involves the realignment of river, estuary or coastal defences to (re-)establish tidal exchange, supporting the formation of coastal wetlands such as mudflats and saltmarshes. Yet, an important knowledge gap constitutes lacking evidence on the true protective value of MR, which fosters political and societal opposition, ultimately counteracting large-

scale coastal restoration efforts.

This thesis tackles the above knowledge gap in a combined approach, including field measurements and hydrodynamic modelling, to study the effectiveness of High Water Level (HWL) attenuation across one of the earliest and, at time of establishment, largest coastal MR schemes of the United Kingdom: Freiston Shore, located in Lincolnshire on the east coast of England. Between August and October 2017, a series of 16 water level loggers was deployed across the MR site and the adjacent natural saltmarsh to measure the reduction of peak water levels during the highest tides of the year. Subsequently, these data were used to calibrate and validate a hydrodynamic model of the study area, which enabled studying the effects of MR scheme design on the site's HWL attenuation capacity during these tides. In a last step, the model was implemented to investigate HWL attenuation rates inside the MR site under the influence of very high storm surge levels, by additionally identifying MR width thresholds for HWL attenuation in relation to surge height and vegetation cover.

The main findings of this thesis are: 1) The MR site of Freiston Shore does not provide effective HWL attenuation under all measured conditions; 2) at the open coast of Freiston Shore, only large and wide MR sites can effectively attenuate very high tides, and the reduction of storm surges with return periods of more than ten years requires MR widths of > 1148 m (measured perpendicular to the coastline) while; 3) increased vegetation cover and larger MR widths enable the attenuation of even higher surges and; 4) breaching dikes should be preferred over complete dike removal when coastal protection is the target of MR implementation.

Three priority areas for future research are recommended: 1) Generating more *in situ* data on MR internal water level dynamics and HWL attenuations, particularly under storm surge conditions. 2) Freiston Shore's HWL attenuation function is particularly effective when tidal exchange is restricted through narrow dike breaches, which could also be achieved by applying sluices or culverts (i.e. Regulated Tidal Exchange (RTE)). However, this should be balanced against reduced sedimentation rates, limited MR

drainage and vegetation establishment, and the potential erosion and widening of dike breaches, which may all result from breaches being designed too narrow or RTE. 3) Investigating the effectiveness and applicability of several MR schemes and other NBS to mitigate flood risks on a regional scale.

Zusammenfassung

Die Ökosystemdienstleistungen von Küstenfeuchtgebieten zählen zu den wertvollsten der Welt. Zu ihnen gehören die Reduktion von Klimarisiken durch die effektive Speicherung von Kohlenstoff (um ein Vielfaches schneller als tropische Regenwälder) und die Bereitstellung eines natürlichen Küstenschutzes.

Trotz ihrer ökologischen und sozio-öknomischen Bedeutung sind Küstenfeuchtgebiete in den letzten Jahrhunderten großflächig verschwunden, was sich zumeist auf das Wirken des Menschen zurückführen lässt. Die projizierte Beschleunigung des Meeresspiegelanstiegs könnte sie noch weiter gefährden, insbesondere wenn menschengemachte Infrastruktur die landwärtige Verlagerung der Ökosysteme unterbindet.

Das Risiko von Überflutungen entlang niedrig gelegener Küstenregionen ist angestiegen und das Festhalten an konventionellen Küstenschutzpraktiken ist sowohl aus ökonomischer als auch ökologischer Sicht nicht nachhaltig. Das Entwickeln und Erproben neuer, nachhaltiger Anpassungsstrategien ist daher dringend erforderlich, um den Herausforderungen eines steigenden Meeresspiegels gerecht zu werden. Einen vielversprechenden, naturbasierten Ansatz liefert das geordnete Rückverlegen vorderster Deichlinien, was im englischen als Managed Realignment (MR) bezeichnet wird. MR macht sich die wellen- und sturmflutdämpfende Wirkung von Küstenfeuchtgebieten zunutze und baut außerdem auf dessen Fähigkeit, durch Sedimentakkumulation vertikal anzuwachsen.

Die Wiederherstellung des Wasseraustausches zwischen ehemals eingedeichten Küstenniederungen und angrenzenden Flachwasserzonen von Flüssen, Flussmündungen oder Küsten ermöglicht die Etablierung von Küstenfeuchtgebieten wie Salzwiesen. Aktuell

fehlen allerdings Studien, die die tatsächliche Schutzwirkung der im Rahmen von MR renaturierten Salzwiesen quantifizieren.

Diese Dissertation widmet sich der oben genannten Kenntnislücke in einem kombinierten Ansatz aus feldgestützter Datenerfassung und hydrodynamischer Modellierung. Das Ziel ist die Quantifizierung der Reduktion von Höchstwasserständen in einem der ältesten und zum Zeitpunkt der Rückverlegung größten MR-Gebiete des Vereinigten Königreichs: Freiston Shore in Lincolnshire, gelegen an Englands Ostküste.

Zwischen August und Oktober 2017 wurde eine Reihe von Wasserstandssensoren im MR-Gebiet und der angrenzenden natürlichen Salzwiese ausgebracht. Mithilfe der Sensoren wurde die Reduktion von Höchstwasserständen über der natürlichen und renaturierten Salzwiese während der höchsten Springtiden des Jahres erfasst. Im nächsten Schritt wurden die erfassten Daten genutzt, um ein hydrodynamisches Modell des Untersuchungsgebietes aufzusetzen. Dieses Modell war die Grundlage, um die Einflüsse des MR-Designs (Deichkonfiguration, Breite und Anzahl der kontrollierten Deichdurchbrüche) sowie die Effekte sehr hoher Sturmfluten auf die Küstenschutzfunktion zu untersuchen. Darüber hinaus wurden sturmflutspezifische Grenzwerte bezüglich der Mindestbreite(/-größe) von Freiston Shore ermittelt, unter denen keine Höchstwasserstandsreduktion mehr gewährleistet ist. Diese Ermittlung berücksichtigte die Relation zu Sturmfluthöhe (Wiederkehrperiode) und Vegetationsbedeckung.

Die wichtigsten Ergebnisse dieser Dissertation sind: 1) MR in Freiston Shore hat weder die Höchstwasserstände einer Reihe von Springtiden noch von hoch auflaufenden Sturmfluten reduziert. 2) Das Beispiel Freiston Shore zeigt außerdem, dass MR-Gebiete an offenen Küsten sehr breit(/groß) sein müssen, um effektiv die Höchstwasserstände hoher Springtiden zu reduzieren. Um darüber hinaus auch die Höhe von Sturmfluten mit Wiederkehrperioden von mehr als zehn Jahren zu dämpfen, sind MR-Breiten von >1148 m (senkrecht zur Küstenlinie gemessen) erforderlich. 3) Die Fähigkeit von MR-Gebieten, noch höher auflaufende Tiden oder Sturmfluten zu reduzieren, steigt mit höherem Vegetationsbedeckungsgrad und größeren MR-Breiten. 4) Das Durchbrechen

von Deichen sollte gegenüber der vollständigen Deichentfernung bevorzugt werden, da es zu verbessertem Küstenschutz beitragen kann.

Die vorliegende Dissertation identifiziert drei Kernbereiche für zukünftige Forschungen: 1) Es werden mehr *in situ* Wasserstandsmessungen innerhalb von MR-Gebieten benötigt, insbesondere während starker Sturmfluten. 2) Die Küstenschutzfunktion von MR-Gebieten ist besonders effektiv, wenn der Wasseraustausch durch kleine Deichbrüche oder Schleusen reduziert wird. Dies sollte gegen die sich daraus ergebenden reduzierten Sedimentationsraten, Wasserablauf, Vegetationsetablierung und die mögliche Erosion von Deichdurchlässen abgewogen werden. 3) Die Wirksamkeit und Anwendbarkeit von vielen MR-Gebieten und anderen naturbasierten Anpassungsstrategien sollten auf regionaler Ebene analysiert werden.

Contents

List of Figures

List of Tables

List of Acronyms

SLR Sea-Level Rise

IPCC Intergovernmental Panel on Climate Change

RSLR Relative Sea-Level Rise

NBS Nature-Based Solutions

UK United Kingdom

IGGI Integrated Greening of Grey Infrastructure

HWL High Water Level

MR Managed Realignment

RTE Regulated Tidal Exchange

RSPB Royal Society for the Protection of Birds

EA UK Environment Agency

ABPmer Associated British Ports Marine Environmental Research

DEFRA Department for Environment, Food & Rural Affairs

NERC Natural Environment Research Council

LiDAR Light Detection and Ranging

CASI Compact Airborne Spectrographic Imager

MSTR Mean Spring Tidal Range

MHW Mean High Water

ODN Ordnance Datum Newlyn

RTK Real Time Kinematic

NOAA National Oceanic and Atmospheric Administration

SSE South-South-East

STD Standard Deviation

NW North-West

SW South-West

SSW South-South-West

W West

S South

WNW West-North-West

OMREG Online Managed Realignment Guide

DEM Digital Elevation Model

RMSE Root Mean Square Error

ME Mean Error

MAE Mean Absolute Error

MHWD Mean High Water Depth

TP Tidal Prism

Chapter 1

Introduction

1.1 Coastal wetlands under pressure

Coastal wetlands are formed at the interface between land and sea and are characterised by regular inundation of brackish or saline water. They typically occur in sheltered environments such as estuaries, deltas, protected bays, or on the leeward side of barrier islands and sand spits (Doody, 2008). Coastal wetlands flood and drain via a dendritical tidal creek network, which is crucial for the delivery of sediments to interior parts (Reed et al., 1999). Typical ecosystems include saltmarshes, mangroves and brackish water reed swamps (Scott et al., 2014). Their ecosystem services [1] are among the most valuable on the planet (Barbier et al., 2011; Costanza et al., 1997), including storm protection (Möller et al., 2014; Barbier, 2015; Temmerman et al., 2013), carbon sequestration (Macreadie et al., 2013), water quality improvement (Valiela and Cole, 2002; Sousa et al., 2008) and provision of habitat for commercially important fish species (Barbier et al., 2011). In addition, coastal wetlands can build up vertically by sediment accretion, allowing them to keep pace with even higher rates of Sea-Level Rise (SLR) (Kirwan et al., 2016).

Despite their ecological and socio-economical importance, coastal wetlands have been

[1] Benefits people obtain from nature (MEA, 2005)

lost on a large scale in the past centuries, mostly due to human induced stress factors. For example, the exploitation and conversion of wetlands dates back to at least Roman times in Europe (Davidson et al., 1991), at least the 17th century in North America (Dahl, 1990) and southern Africa (Kotze et al., 1995); and for at least 2000 years in China (An et al., 2007; Davidson, 2014). It is therefore not surprising that coastal wetland loss has largely been attributed to overexploitation, habitat destruction due to land reclamation and embankment construction (Lotze et al., 2006; Gedan et al., 2009; Davidson, 2014; Bakker et al., 2002). The magnitude of historic loss of global coastal wetlands since 1700 ranged between 46 – 50 % and losses accelerated over the course of the 20th century, estimated at 62 – 63 % (Davidson, 2014). Relative losses since the onset of human settlement were found to sum up to 67 % (Lotze et al., 2006). These numbers reflect the particular sensitivity of coastal wetlands to environmental change (Mudd et al., 2009; Morris et al., 2002; French, 2006; Kirwan et al., 2010) and give cause for concern regarding the fate of coastal wetlands in the upcoming centuries. Particularly high-end scenarios of SLR constitute a veritable threat, which may overwhelm even fast accreting ecosystems that are generally not sediment starved (Kirwan et al., 2016). Even more vulnerable are wetlands located along the coasts of semi-enclosed ocean basins such as the Mediterranean or Baltic Seas, which are characterised by microtidal regimes. They typically lack regular inundation and thus, the continuous supply of sediments to interior parts of the ecosystem, making them more vulnerable to drowning and ponding as a consequence of SLR (Kirwan et al., 2010; Duran Vinent et al., 2021).

1.2 Future trajectories of coastal wetland change

Similar to historic wetland change, the future survival and resilience of coastal wetlands is dependent on landuse decisions (Schuerch et al., 2018; Spencer et al., 2016), but pro-

jected acceleration of global mean SLR (Kirwan et al., 2010; Nicholls and Cazenave, 2010) and the deficiency of available suspended sediments due to river damming (Syvitski et al., 2009) could further exacerbate their vulnerability. The Intergovernmental Panel on Climate Change (IPCC) reports that global mean sea-levels were rising by 1.4 mm yr^{-1} between 1901 and 1990 and 3.6 mm yr^{-1} over the period 2006 – 2015. This accelerating trend is likely to continue beyond the 21st century (Oppenheimer et al., 2019), resulting in high-end SLR projections by experts reaching 5.61 m until 2300 (Horton et al., 2020).

Relative Sea-Level Rise (RSLR) is the combined effect of eustatic SLR and vertical land movement and can exceed eustatic SLR by several orders of magnitude, particularly in subsiding delta regions (Syvitski et al., 2009; Nicholls et al., 2021). The major drivers of subsidence are accelerated soil compaction, caused by subsurface mining of oil, gas or groundwater, and flood plain engineering by dikes, levees or embankments. The embankment of low lying land is usually followed by drainage and thus, accelerated oxidation (Syvitski et al., 2009; Temmerman et al., 2013). For example, ground water extraction in the Chao Phraya Delta caused annual subsidence rates of 50 – 150 mm (Saito et al., 2007) and the Po Delta sank by > 3 m during the 20th century, mostly as a consequence of methane mining and groundwater withdrawal (Caputo et al., 1970; Corbau et al., 2019).

However, studies found that saltmarshes are generally able to grow vertically at rates equal to or exceeding historic SLR. In addition, future marsh survival is possible under most SLR scenarios, due to biophysical feedback mechanisms that are known to accelerate soil building (Kirwan et al., 2016; Schuerch et al., 2018). Yet, the projected magnitude of global wetland change over the 21st century varies between possible gains of up to 60 % (Schuerch et al., 2018) to substantial losses reaching 78 % (Spencer et al., 2016). The magnitude of wetland change (loss or gain) in the face of SLR presented above, will primarily be driven by the availability of accommodation space, allowing wetlands to migrate landwards (Schuerch et al., 2018; Spencer et al., 2016) and on

their capacity to accrete sediment and build up vertically (Kirwan et al., 2010, 2016). Lacking accommodation space will ultimately lead to coastal squeeze, which refers to the loss of coastal wetlands in front of sea defences, for example in the absence of sufficient sediment supply and simultaneous seaward erosion (Pontee, 2013; Doody, 2004).

Problematically, land reclamation and armoured shorelines, protected by dikes, groynes and seawalls, are a direct consequence of migration to coastal zones and economic development (Vousdoukas et al., 2018). Coastal zones are more densely populated than the hinterland (Small and Nicholls, 2003) and are characterised by higher rates of population growth and urbanisation (McGranahan et al., 2016). This trend is expected to continue into the future. In Europe, for example, population in the Low Elevation Coastal Zone[2] may increase from 50 million in 2000 to between 52.1 and 55.7 million in 2060, depending on socio-economic development (Neumann et al., 2015).

The combination of rising seas, land subsidence, wetland loss and population growth results in increasing flood risks for low lying coasts and projected increases in episodic flooding, particularly in regional hot-spots such as north western Europe (Kirezci et al., 2020). Consequently, adaptation costs are expected to rise in the future. Hinkel et al. (2014) estimate that in 2100 costs for building and upgrading dikes could range between 12 and 71 billion US$, but these investments are small compared to the global costs of avoided flood damages. There is consequently no alternative to increased coastal protection efforts in the future.

Hard coastal protection measures are, in contrast to coastal wetlands, non-adaptive, meaning they have to be upgraded and maintained in order to keep pace with SLR (Temmerman et al., 2013). Conventional sea defences hinder the supply of sediments by incoming tides or surges and soil drainage additionally amplifies land subsidence (Syvitski et al., 2009). Hence, Morris et al. (2020, p. 485) state that "a continued

[2]Land below 10 m elevation that is hydrologically connected to the sea (Lichter et al., 2011)

reliance on traditional defences in a future of growing societal demand for shoreline protection is economically, environmentally and socially unsustainable". Developing and identifying new measures to mitigate increasing coastal flood risks constitutes one of the most prominent challenges coastal communities are facing today (Morris et al., 2018) and will ultimately determine the fate of global coastal wetlands. A cost effective and ecologically sustainable alternative to conventional coastal defence schemes can be provided by Nature-Based Solutions (NBS).

1.3 Nature-based solutions to mitigate coastal flood risks

1.3.1 What are nature-based solutions?

NBS are often also referred to as "Building with Nature" (de Vriend et al., 2014), "Ecosystem-based coastal defence" (Temmerman et al., 2013) or "Green Infrastructure" (Pontee and Tarrant, 2017). The variety of terms coupled with a divergent understanding of what constitutes NBS can lead to confusion (Pontee et al., 2016). In this thesis and the publications therein, NBS are defined following Pontee et al. (2016, p. 30), who describe them as "consisting either wholly, or partially, of natural features that are designed to offer or improve coastal protection". According to Pontee et al. (2016) this includes:

- Fully natural solutions (reef building organisms such as mussels and corals, or intertidal vegetation in the form of saltmarshes and mangroves etc.) (Figure 1.1a)
- Managed natural solutions (including artificial reefs, beach and dune nourishment or planted saltmarsh and mangrove vegetation) (Figure 1.1b)
- Hybrid solutions combining conventional engineering with natural features (e.g. marsh-levee systems) (Figure 1.1c)

- Environment friendly structural engineering (e.g. vegetated engineering, bamboo sediment fences or brushwood groins) (Figure 1.1d)

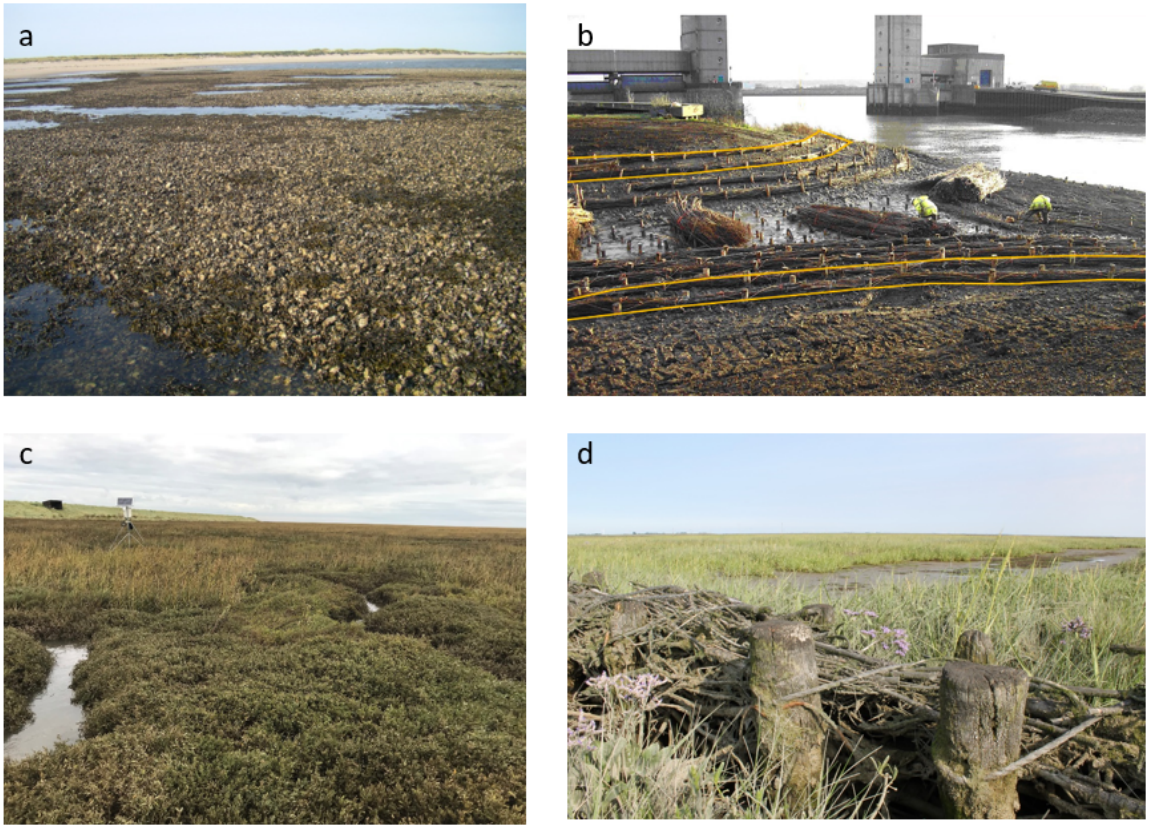

Figure 1.1 Examples of NBS: a) Reef building oyster *Crassostrea gigas* in the northern Wadden Sea, Germany (photo: Tobias Dolch); b) Saltmarsh creation in Barking Creek and tributary of river Thames, United Kingdom (UK) (Naylor et al., 2017); c) Natural saltmarsh in front of dike in Freiston Shore, UK; d) Brushwood groin in the northern Wadden Sea, Germany (photos c, d: Joshua Kiesel).

Further confusion regarding the terminology may stem from a concept called Integrated Greening of Grey Infrastructure (IGGI). IGGI can involve the creation of saltmarsh in confined spaces, such as urban areas (Naylor et al., 2017), which falls under the above definition of NBS. However, IGGI usually refers to measures that aim at enhancing the ecological value of conventionally engineered coastal defences, for example by creating arrays of holes, grooves or artificial intertidal rock pools (Hall et al., 2018; Naylor et al., 2017). Thus, in the context of the above definition, it is not the natural feature that provides or enhances coastal protection. The latter is still provided by the seawall

or dike. IGGI should therefore not be confused with NBS. In addition, Firth et al. (2020) argue that IGGI constitutes a management tool to compensate anthropogenic impacts that, despite many knowledge gaps and uncertainties, involves the potential for misuse and greenwashing. New conventional coastal engineering could appear more acceptable, thus facilitating the regulatory process (Firth et al., 2020). There is consequently potential for IGGI to even hamper the wider application of NBS in coastal defence schemes, ultimately counteracting coastal restoration efforts.

1.3.2 Benefits and functioning of ecosystems in coastal defence schemes

Decision makers and coastal managers have recently recognized the value and services provided by coastal ecosystems, which has led to increasing restoration and conservation efforts (Temmerman et al., 2013; de Vriend et al., 2014). In addition, NBS are considered to be more sustainable and cost-effective compared to conventional coastal defences (Temmerman et al., 2013; Morris et al., 2020). This reasoning is mainly based on two major functions of coastal ecosystems; first, saltmarshes, mangroves, dunes, coral and shell reefs were found to reduce the height of storm waves (Möller and Spencer, 2002; Möller et al., 2014; Vuik et al., 2016; Rupprecht et al., 2017) and surges and block their landward propagation (Barbier et al., 2008; Temmerman et al., 2012; Stark et al., 2015; Wamsley et al., 2009, 2010; Loder et al., 2009; Shepard et al., 2011); second, coastal ecosystems accrete sediments, enabling vertical growth at rates comparable to, and even exceeding, most SLR scenarios (Temmerman et al., 2013; Kirwan et al., 2016). Thus, coastal ecosystems are often referred to as ecosystem-engineers as they shape their natural environment, creating more favourable conditions for themselves and associated organisms (Jones et al., 1994). This capacity is contrary to conventional defences such as dikes, groynes and seawalls, which have to be maintained on a regular basis. Furthermore, coastal ecosystems are of great ecological importance, providing a multitude of ecosystem services to the environment

and societies. For example, mangroves and saltmarshes are among the most powerful carbon sinks on the planet, sequestering carbon at rates ~ 55 times faster than tropical rainforests (Macreadie et al., 2013; Mcleod et al., 2011). Other benefits include the maintenance of fisheries, nutrient cycling, water purification (Valiela and Cole, 2002) and the provision of raw materials and recreation (Barbier et al., 2011).

This thesis focuses on the restoration and application of saltmarshes in nature-based coastal defence schemes. Saltmarshes exist in the upper intertidal zone of shallow, sheltered embayments, river deltas or estuaries and consist of shrubby, halophytic vegetation communities adapted to regular tidal inundation (Möller, 2012). Shepard et al. (2011) divide the coastal protection function of coastal wetlands (such as saltmarshes) into wave attenuation, shoreline stabilization and High Water Level (HWL) or, dependent on the magnitude of the hydrodynamic forcing, storm surge attenuation. In this thesis, only the HWL/surge attenuation function is quantified, while implications of the other two functions are also discussed in the three publications (chapter 3, chapter 4, chapter 5). According to Smolders et al. (2015), HWL attenuation can be further differentiated into *along-estuary* and *within-wetland* attenuation. The previous refers to the contribution of estuarine intertidal wetlands to the attenuation of storm surges that propagate upstream along an estuary, which is also referred to as water retention or flood water storage (Hofstede, 2019; Cox et al., 2006; Oosterlee et al., 2018, 2020). On the other hand, *within-wetland* attenuation refers to the establishment of water surface slopes over the wetland itself and constitutes the focus of this thesis (Smolders et al., 2015).

The HWL attenuation function of saltmarshes is a result of biophysical feedbacks. Topographically complex, vegetated saltmarsh surfaces modify flow, causing the dampening of waves, tidal current velocities and turbulence, ultimately inducing water surface slopes (i.e. HWL attenuation) (Figure 1.2) (Möller et al., 1999; Christiansen et al., 2000; Ysebaert et al., 2011; Möller, 2012). Observations of tidal flow and wave height in saltmarshes have shown that mean flow velocity and energy decrease logarithmi-

cally with increasing distance from the marsh margin in direction of wave/current flow (Leonard and Croft, 2006; Christiansen et al., 2000). Saltmarsh width is consequently crucial to the coastal protection function and the delivery of ecosystem services in general (Barbier et al., 2008; Koch et al., 2009).

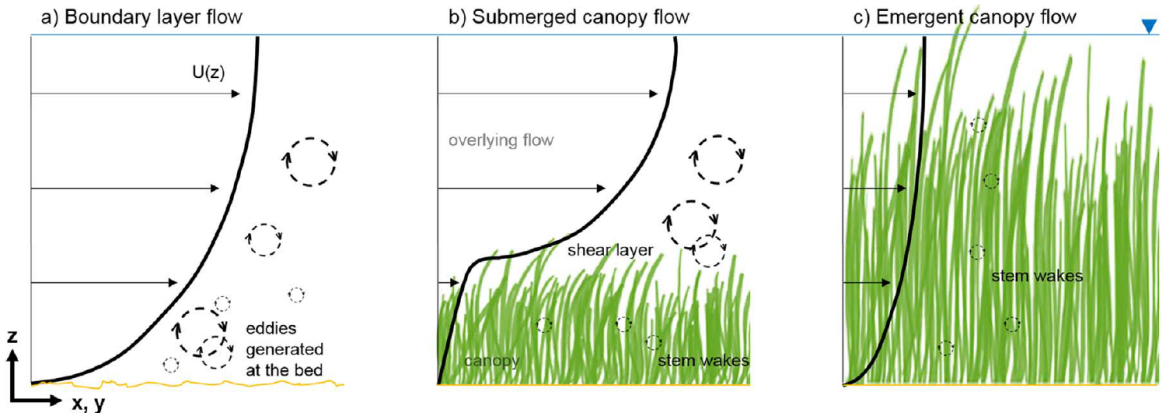

Figure 1.2 Vertical flow velocity profiles over a) unvegetated sediment; b) submerged vegetation and; c) emergent canopies. Figure adopted from Beudin et al. (2017).

The magnitude of mean flow velocity reduction is dependent on both the hydrodynamic forcing (e.g. whether submerged or emerged canopy flow occurs; Figure 1.2) and vegetation type (Anderson and Smith, 2014; Tempest et al., 2015; Möller, 2012). For example, areas of higher turbulence and velocities have been observed in zones of saltmarshes where an abrupt decline in plant (stem/shoot) density occurs (Leonard and Croft, 2006; Tempest et al., 2015). Furthermore, studies found that reductions in flow velocities are generally increasing with greater surface areas of plants, usually indicated through increased stem or shoot densities (Ysebaert et al., 2011; Tempest et al., 2015). Other vegetation properties to affect the flow of water are associated with intra- and inter-species diversity, such as variations in plant shape, dimension and architecture (Tempest et al., 2015). This is illustrated by the fact that taller vegetation types are associated with greater wave attenuation, despite similar biomass (Ysebaert et al., 2011; Möller, 2012).

In contrast, the effects of plant mechanical properties on the reduction of flow velocities are variable. Augustin et al. (2009) found that plant flexibility has limited influence

on flow resistance, while Luhar and Nepf (2013) measured two-fold increases in flow velocity over flexible compared to rigid vegetation. In their review, Tempest et al. (2015) point out that further data is needed to determine the contribution of plant flexibility on flow dissipation.

Since HWL attenuation over saltmarsh surfaces is a direct consequence of the modification of flow, it is not surprising that the drivers of flow reduction are similar to those determining the magnitude of HWL attenuation. Drivers of HWL reduction are the characteristics of the hydrodynamic forcing (e.g. the storm's track, forward speed, duration, associated water levels (Figure 1.2) etc.) (Resio and Westerink, 2008), vegetation characteristics (Temmerman et al., 2012; Barbier et al., 2013), marsh topography (Loder et al., 2009) and the presence of tidal creeks (Stark et al., 2016). Saltmarshes and mangrove forests dominated by channelized flow (through tidal creeks) provide less HWL attenuation compared to ecosystems governed by sheet flow (flow over the marsh platform) (Stark et al., 2016; Montgomery et al., 2018). Generally, the *along-estuary* associated HWL reduction capacity of saltmarshes increases with larger wetland areas (Smolders et al., 2015).

It is noted, however, that biophyiscal feedbacks and resulting HWL attenuation capacities may be altered in confined spaces or when surge heights overwhelm the depth-dependent frictional effects of saltmarsh vegetation. Both can turn HWL attenuation into amplification. Stark et al. (2015) have shown that HWL amplification can occur during very high peak water levels and have furthermore attributed spatial differences between attenuation and amplification to differences in bottom friction. Besides the effects of inundation depth, Resio and Westerink (2008) argue that longer inundation events can fill up the entire marsh storage area, ultimately causing HWL amplification. This may be particularly valid for places where the storage area is limited, for example when surrounded by dikes. Indeed, Wamsley et al. (2009) explained HWL amplification with the presence of flow-blocking levees.

In summary, the sea defence function of saltmarshes is highly complex and context

dependent, which has been stressed in recent reviews on the topic (Shepard et al., 2011; Gedan et al., 2011; Reed et al., 2018). Following Möller (2012), this means that the translation of results from scientific studies that focus on only one element of coastal protection (e.g. HWL attenuation) cannot be easily translated into engineering guidelines. The latter has to consider the full set of sea defence functionalities (HWL and wave attenuation plus shoreline stabilization) of a wetland.

One form of NBS that makes use of the multiple ecosystem services provided by saltmarshes constitutes Managed Realignment (MR), which aims at shifting the land-sea boundary in landward direction (French, 2006).

1.3.3 Managed realignment

In Europe, MR usually involves the restoration of saltmarshes on formerly reclaimed land (Garbutt and Wolters, 2008). Consequently, implementing MR in coastal protection schemes makes use of the potential of saltmarshes to provide *along-estuary* attenuation, *within-wetland* attenuation (Smolders et al., 2015), shoreline stabilization by sediment accretion (Temmerman et al., 2013) and wave attenuation (Figure 1.3) (Möller et al., 2014; Vuik et al., 2016; Rupprecht et al., 2017).

MR is implemented by realigning river, estuary or coastal defences to establish tidal exchange, supporting the formation of intertidal habitats such as mudflats and saltmarshes. In this thesis, MR is referred to as the deliberate removal or breaching of the first line of defence by simultaneously reinforcing or creating a second dike line further inland (Figure 1.3). MR schemes may involve single or multiple breaches, which is usually informed by hydrodynamic modelling studies (Esteves, 2014). Other methods of implementation are described in the literature, including controlled tidal restoration, hereafter referred to as Regulated Tidal Exchange (RTE), where defences are maintained and tidal flow into the embankment area is controlled via flood gates, culverts and sluices (Esteves, 2014; Cox et al., 2006; de Mulder et al., 2013) and managed retreat. The latter is rarely implemented in Europe, as it involves a long-term

strategy for planning radical land use changes. These are associated with the relocation of people and assets at risk from flooding (Esteves, 2014). For a more detailed description on the different MR types, the reader is referred to Esteves (2014) and Esteves and Williams (2017).

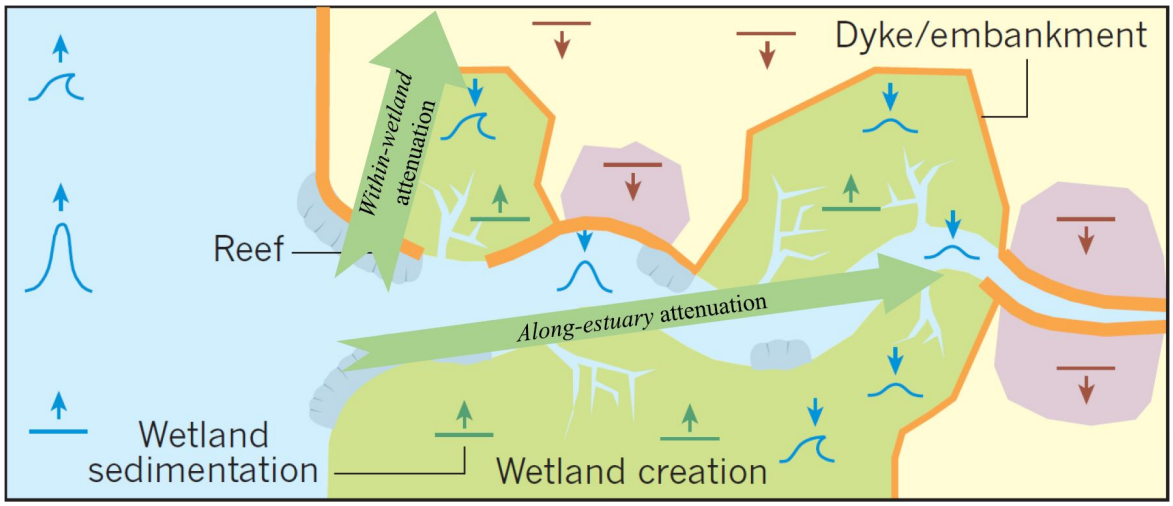

Figure 1.3 Schematic drawing of MR along an estuary. The direction of blue arrows indicates either an increase (up) or decrease (down) in the intensity of waves and water levels. Green arrows (up) indicate an increase and red arrows (down) a decrease in surface elevation. Figure taken from Temmerman et al. (2013) and adjusted by adding the concept of *within-wetland* and *along-estuary* attenuation by Smolders et al. (2015).

The different MR types emphasize varying targets. While RTE in Europe primarily aims at habitat creation and biodiversity enhancement (Esteves and Williams, 2017), the main motivation of MR (especially in the UK) is coastal protection (Pethick, 2002). Yet, MR and RTE are typically characterised by multiple targets. These are: 1) Enhancing biodiversity and creating more natural shorelines; 2) compensating for habitat loss and; 3) improving coastal protection and reduce maintenance costs of existing conventional defences (Esteves and Thomas, 2014; Esteves, 2013).

The Committee on Climate Change in the UK suggests that the length of realigned shorelines in England should reach 550 km by 2030 (approximately 10 % of England's coast). However, as of 2013, reaching the 2030 goal would require a five-fold increase in realignment rate, from 6 km to 30 km per year (Committee on Climate Change, 2013). Although some of the resistance to MR implementation can be explained by

societal and political barriers (Cooper and McKenna, 2008), slow uptake also clarifies the existence of considerable knowledge gaps, hampering the application of MR in coastal protection schemes (Bouma et al., 2014).

1.3.4 Knowledge gaps hampering the application of MR in coastal defence schemes

The need for rethinking contemporary and future adaptation to SLR and increasing flood risks is beyond doubt inevitable to tackle the multiple environmental and socio-economic pressures coasts are facing around the globe (Nicholls et al., 2021). However, the implementation of NBS and MR is hindered by societal and political opposition, which may be intensified by lasting knowledge gaps. One of the main problems is missing information on the success of existing MR schemes. Measuring success requires both the definition of precise and pre-defined targets and comprehensive and prolonged monitoring campaigns. However, pre-defined targets are widely missing or often not sufficiently concrete to enable measuring their achievement (Wolters et al., 2005). Furthermore, monitoring campaigns are often too short, focused on geo-ecological parameters such as sedimentation rates, vegetation colonisation, invertebrates and fish, and neglect complex ecosystem functions such as the provision of coastal protection (Bouma et al., 2014; Brady and Boda, 2017).

Indeed, measuring success also depends on whether the aim of restoration is the structure of an ecosystem or its functioning (Wolters et al., 2005). The structure of an ecosystem is defined as the condition at one point in time (e.g. the presence of diverse vegetation communities, elevation etc.), whereas ecosystem functioning constitutes a process that occurs over time (e.g. biogeochemical cycling or primary production) (Zedler and Lindig-Cisneros, 2000). While structural components are an integral part of many monitoring schemes, ecosystem functioning is usually neglected. Despite being targeted by many MR schemes, this involves missing assessments on the coastal protection service, the latter of which is a result of ecosystem processes such as the

alteration of flow by saltmarsh vegetation and geomorphological change years after the scheme's implementation.

In addition, studies have found that saltmarshes restored within the scope of MR differ to their natural counterparts in those structural ecosystem components that are known drivers of the coastal protection function. These differences involve vegetation characteristics (Garbutt and Wolters, 2008; Mazik et al., 2010; Mossman et al., 2012b) and topographic complexity (Lawrence et al., 2018), raising questions whether or not restored saltmarshes are equally effective in terms of coastal protection compared to adjacent natural ecosystems. There is a good body of evidence suggesting the potential of saltmarshes to effectively reduce the height of storm waves over tens of metres (Möller et al., 2014; Möller and Spencer, 2002; Vuik et al., 2016; Rupprecht et al., 2017), whereas *in-situ* measurements of peak water level reduction in coastal wetlands are scarce (Stark et al., 2015) and completely absent in MR schemes to the knowledge of the author. Studies have shown that saltmarshes are able to reduce surge and HWLs over distances of hundreds of metres (Temmerman et al., 2012; Stark et al., 2015, 2016; Resio and Westerink, 2008; Leonardi et al., 2018). Problematically, almost half (46 %) of the MR schemes in Europe as of today are smaller than 20 ha (ABPmer 2021), having the potential of effective wave height reduction, but no necessarily for HWL attenuation.

The current focus on habitat creation and missing data to support the multiple benefits (including coastal protection) of saltmarsh restoration schemes are hindering the wider implementation of MR (Esteves and Thomas, 2014). The latter is likely to be crucial for the resilience of coastal wetlands in the next centuries. Public and political acceptance for the measure is particularly dependent on evidence supporting the coastal protection case. Following Bouma et al. (2014), this involves a) quantification of the coastal protection function of saltmarshes restored in the context of MR under the most extreme events and; b) exploring the effects of potential long-term ecosystem dynamics, leading to saltmarsh deterioration and thus, reduction of the

coastal protection function. The latter has been termed by Bouma et al. (2014) as the main knowledge gap, hampering the application of intertidal ecosystems within coastal defence schemes.

1.4 Research questions and thesis structure

This thesis tackles the above knowledge gaps in a combined approach, including field measurements and hydrodynamic modelling. All assessments were made in one of the earliest and, at time of establishment, largest MR schemes of the UK, located in Freiston Shore, Lincolnshire. This thesis aims at quantifying the effectiveness of MR at Freiston Shore in terms of coastal protection under very high tides and extreme surges and seeks to find solutions for scheme design improvements. These aims are pursued by addressing the following research questions that are separated in three sections:

1. How effective is Freiston Shore in attenuating water levels of very high spring tides and can differences be identified to adjacent natural marshes?

2. How is HWL attenuation in Freiston Shore linked to MR scheme design and can the latter be used to improve Freiston Shore's effectiveness?

3. How effective is Freiston Shore in attenuating extreme surges and can MR width(/area) thresholds for HWL attenuation be identified in relation to surge height and vegetation cover?

In order to answer the above questions, this thesis is structured as follows: First, a brief history and general description of the study area is given in chapter 2. For a detailed description of the characteristics of the study area with respect to the research questions, the reader is referred to the study area sections in the three respective publications (chapter 3, chapter 4 and chapter 5). The publications are listed below and address the above research questions in order of appearance.

1. Kiesel, J., Schuerch, M., Möller, I., Spencer, T., and Vafeidis, A. T.: Attenuation of high water levels over restored saltmarshes can be limited. Insights from Freiston Shore, Lincolnshire, UK, Ecological Engineering, 136, 89–100, https://doi.org/10.1016/j.ecoleng.2019.06.009, 2019

2. Kiesel, J., Schuerch, M., Christie, E. K., Möller, I., Spencer, T., and Vafeidis, A. T.: Effective design of managed realignment schemes can reduce coastal flood risks, Estuarine, Coastal and Shelf Science, 242, 106 844, https://doi.org/10.1016/j.ecss.2020.106844, 2020

3. Kiesel, J., McPherson, L. R., Schuerch, M., and Vafeidis, A. T.: Can managed realignment buffer extreme surges? The relationship between marsh width, vegetation cover and surge attenuation, Estuaries and Coasts, https://doi.org/10.1007/s12237-021-00984-5, 2021

Finally, this thesis is closed with a general conclusion (chapter 6) and a final chapter describing suggestions for future research (chapter 7).

Chapter 2

Study area

The MR site of Freiston Shore is located at the west coast of The Wash, which is an embayment in Lincolnshire on England's North Sea coast (Figure 2.1a, b). The Wash is a comparatively shallow (average water depth < 10 m), low-energy embayment (Ke et al., 1996), comprising vast intertidal areas with various habitats such as sand- and mudflats, mussel reefs and saltmarshes (Brew and Williams, 2002). Following Pye (1995), The Wash's marshes constitute the largest single area of active saltmarsh in the UK. The Wash is characterised by a semidiurnal, macrotidal regime, with neap and spring tidal ranges of 3.5 and 6.5 m, respectively (Ke et al., 1996). The wave climate differs between the sheltered, inner parts of The Wash, where wave heights range between 0.3 and 0.5 m (Amos and Collins, 1978) and The Wash's entrance, where one year return wave heights reach > 3 m (Posford Duvivier, 1996).

The coasts of The Wash have an age-long history of land reclamation with first earth embankments probably constructed by the Romans. Greatest alterations have occurred since the late 16^{th} and 17^{th} century (Pye, 1995; Symonds and Collins, 2007b). Flood defences around The Wash protect a large area of low-lying land, from Cambridge in the south to Lincoln in the west (Brown et al., 2007; Halcrow, 1999). The latest embankment in that sequence has been completed at Freiston Shore in 1982, rising 3–4 m above the adjacent intertidal zone to protect neighbouring low lying fen-

land, urban and agricultural areas (Symonds and Collins, 2007b; Friess et al., 2012). The embanked land was used for arable cultivation (Brown et al., 2007). The latest embankment was built further seaward than the neighbouring embankments to the north and south, leading to a narrower fronting saltmarsh with less developed vegetation. This marsh has been retreating at a rate of 15 m a^{-1} after 1982 (Brew and Williams, 2002; Brown et al., 2007). Consequently, the foot of the embankment was exposed to wave attack and erosion was apparent, requiring repair and maintenance of the former owner, Her Majesty's Prison Service (Brown et al., 2007). The costs of maintaining and strengthening the flood defences in its former position were found to be considerably higher than those associated with retreating the first line of defence (Brown et al., 2007). Thus, the 1996 Shoreline Management Plan recommended realignment of Freiston Shore's coastline (Spencer and Harvey, 2012). The land was bought by the Royal Society for the Protection of Birds (RSPB) and maintenance of the flood defences was adopted by the UK Environment Agency (EA).

In 2002, 66 ha of new intertidal and shallow water habitats were restored by breaching the seaward embankment at three locations (each of ca. 50 m width) (Brown et al., 2007) and connecting 1200 m of artificially created tidal creeks within the site with creeks of the adjacent natural marsh (Figure 2.1c) (Friess et al., 2014; Symonds and Collins, 2005). This was the largest MR scheme in the UK at that time (Friess et al., 2012). Prior to breaching, new embankments were built at the back of the realignment and a 15 ha lagoon was created landward the new southern line of defence (Brown et al., 2007). The aims of MR at Freiston Shore were 1); "to create a sustainable flood defence scheme through the establishment of saltmarsh; 2) to establish a saltmarsh community of botanical value, and to provide suitable habitat for invertebrate and birds; 3) to avoid adverse impacts to existing habitat and adjacent saltmarsh and mudflat and, finally; 4) to establish new brackish habitat through the excavation of a borrow pit landward of the setback bank" (Brown et al., 2007, p. 1).

The MR site of Freiston Shore has not been embanked for a long time, which is why

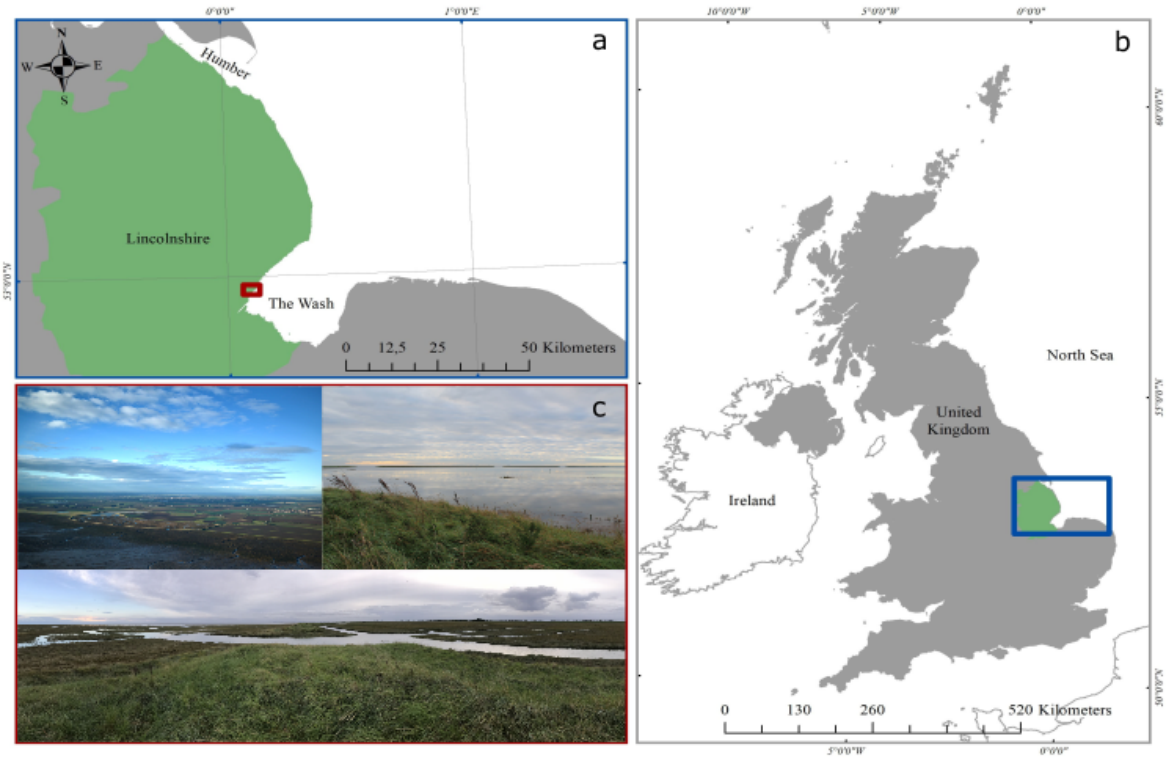

Figure 2.1 Location of the Freiston Shore MR site in b) eastern England and a) The Wash embayment. c) Top left: Oblique aerial photography of the study area from January 2017 (© Environment Agency copyright and/or database right 2019. All rights reserved); Top right: Total inundation of the MR site during one of the highest tides of the year 2017. The three breaches are visible in the background of the picture; Bottom: View from the northernmost breach in southward direction during a rising tide. On the left of the picture, the adjacent natural marsh is shown and, on the right, the MR site with flooded artificial tidal creeks is pictured (photos bottom and top right: Joshua Kiesel, October 2017).

elevations inside the opened polder were suitable for rapid vegetation development. This was confirmed by the final monitoring report, stating that in 2007, mean total vegetation cover within the MR was estimated at 86 % (Brown, 2008). When field data were collected for this thesis in 2017, vegetation cover ranged in the same order of magnitude, varying between 73 % in the south and 81 % in the north of the MR. The advanced state of vegetation development within the scheme in combination with the originally targeted coastal protection function make Freiston Shore an ideal study site to measure its effectiveness in terms of coastal protection against the originally defined aim.

Chapter 3

Attenuation of high water levels over restored saltmarshes can be limited. Insights from Freiston Shore, Lincolnshire, UK

Joshua Kiesel, Mark Schuerch, Iris Möller, Tom Spencer, Athanasios T. Vafeidis [1]

[1]This chapter is published as: Kiesel, J., Schuerch, M., Möller, I., Spencer, T., and Vafeidis, A. T.: Attenuation of highwater levels over restored saltmarshes can be limited. Insights from Freiston Shore, Lincolnshire, UK, Ecological Engineering, 136, 89–100, https://doi.org/10.1016/j.ecoleng.2019.06.009, 2019

Abstract

The Managed Realignment (MR) of flood protection on low-lying coasts, and the creation, or re-creation, of intertidal saltmarsh habitat between old and new, more landward sea defence lines is an intervention designed to help protect coastal infrastructure and communities against the impact of storm waves and surges. However, the effectiveness of such schemes has rarely been proven in the field. Environmental monitoring has generally been limited to the first few years after implementation and has focused on sediment accretion and surface elevation change, vegetation establishment and habitat utilization, to the neglect of the study of biophysical processes, such as wave energy dissipation and High Water Level (HWL) attenuation.

We address this knowledge gap by analysing HWL attenuation rates in saltmarshes from within, and in front of, the open coast MR site of Freiston Shore (Lincolnshire, United Kingdom (UK)). For this purpose, a suite of 16 pressure transducers was deployed along four sections (two within and two outside the MR) of identical setup to measure water level variations during the highest spring tides of the year 2017.

Our results show that for the conditions encountered during the field monitoring period, the capacity of the Freiston Shore MR site to provide HWL attenuation was limited. HWL attenuation rates were significantly higher over the natural saltmarsh (in front of the MR), where HWL attenuation ranged between 0 and 101 cm km^{-1} (mean 46 cm km^{-1}). Within the MR site, rates varied between –102 and 160 cm km^{-1} (mean –3 cm km^{-1}), with even negative attenuation (i.e. amplification) for about half of the measured tides.

We argue that the weak performance of the MR site in terms of HWL attenuation was a result of internal hydrodynamics caused by scheme design and meteorological conditions. The latter may have counteracted the HWL attenuating effect caused by the additional shallow water area provided by the restored saltmarsh.

3.1 Introduction

Acceleration of global sea level rise (Church et al., 2013; Nerem et al., 2018), land subsidence (Syvitski et al., 2009) and an expected increase in the intensity of storms and storm surges (Knutson et al., 2010) are threatening growing coastal populations

worldwide. Engineered coastal protection measures, such as dikes, seawalls or embankments are costly to construct, maintain, and upgrade in order to keep pace with sea level rise and increasing flood risk. Furthermore, embankments aggravate land subsidence by promoting soil compaction due to drainage, and at the same time impede sedimentation. In estuarine settings, embankments cause the funnelling of flow, which ultimately leads to higher water levels up-estuary than would be the case in more natural systems (Syvitski et al., 2009; Temmerman et al., 2013).

Nature-based coastal adaptation approaches are increasingly seen as a cost-effective and sustainable flood and erosion protection option (Thorslund et al., 2017). Managed realignment (MR) constitutes one approach towards nature-based coastal adaptation and often involves the breaching or removal of hard coastal defences such as seawalls and dikes and, at the same time, the construction of a new defence line further inland (Esteves, 2013; Garbutt et al., 2006; Mazik et al., 2010). This allows for regular tidal inundation of the realigned area, enabling the (re-)establishment of saltmarshes. Furthermore, once established, saltmarshes should be self-sustaining, providing they have sufficient accommodation space and sediment supply to keep pace with rates of sea level rise (Kirwan et al., 2016; Schuerch et al., 2018).

MR aims at: 1) Managing the risks associated with coastal hazards; and 2) creating, or re-creating, habitats of high biodiversity and ecological value. Target 1) can be subdivided into three elements. The first two elements have been referred to as *along-estuary* attenuation (Smolders et al., 2015) and involve i) the creation of additional flood storage and ii) the creation or re-establishment of additional wetland area providing wider and 'rougher' estuarine boundaries to slow the passage of the flood wave (Pethick, 2002; Townend and Pethick, 2002). The third aspect is represented by iii) the reduction of water levels over the wetland itself, such that at the back of the MR the new seawall can be of a lower design specification and cheaper to build and maintain than the breached outer wall (Dixon et al., 1998; Pethick, 2002). This has been referred to as *within-wetland* attenuation (Smolders et al., 2015) and constitutes the

focus of this paper. This form of attenuation is based on the simple physical relationship between the drag forces exerted by rough surfaces, such as vegetated wetlands, and resulting water surface slopes (i.e. the landward decrease in HWLs) (Resio and Westerink, 2008) and attenuation of waves (Knutson et al., 1982; Möller et al., 1999, 2014; Shepard et al., 2011).

There is good evidence that the presence of saltmarshes reduces surge and tidal levels (Stark et al., 2015, 2016; Temmerman et al., 2012) over distances of hundreds of metres (Leonardi et al., 2018; Resio and Westerink, 2008). However, as of 2013, 66 % of MR schemes in England are smaller than 20 ha (Esteves, 2013), with only a few schemes reaching several hundreds of metres in width. Thus, the dimensions of most sites have the potential for effective wave reduction but the capacity for HWL reduction remains unclear. Furthermore, it is well known that vegetation community properties (Rupprecht et al., 2017; Tempest et al., 2015) and morphological surface complexity (Loder et al., 2009; Temmerman et al., 2012) affect HWL attenuation. These marsh characteristics are less well developed in MR sites compared to natural systems (Lawrence et al., 2018; Mossman et al., 2012a). Consequently, there is room for debate as to whether or not the performance of restored saltmarshes (within MR schemes), in terms of HWL reduction, is as effective as that recorded from natural saltmarshes (Bouma et al., 2014). Answering this question involves the generation of knowledge on both i) the maximum attenuation potential of coastal wetlands and ii) the inundation thresholds up to which they are able to induce significant differences in water surface slopes.

The Committee on Climate Change in the UK have argued that the length of realigned shorelines in England needs to reach 550 km by 2030 (Committee on Climate Change, 2013). However, up until November 2013, only 66 km of England's shorelines had been realigned, suggesting that considerable challenges lie ahead in order to reach the 2030 target. Whilst some of the resistance to MR implementation can be explained by societal and political barriers to adoption (Cooper and McKenna, 2008), slow uptake

also suggests that the coastal defence case for MR has yet to be made in a sufficiently convincing manner to significantly change operational coastal management practices.

One of the largest MR schemes in the UK was established in 2002 at Freiston Shore, Lincolnshire, UK (Figure 3.1). The targeted benefits of the site were specified as: 1) the creation of more natural shorelines; 2) the reduction of flood protection costs; and 3) habitat creation (Associated British Ports Marine Environmental Research (ABPmer), (ABPmer, 2010)). The UK Government's Department for Environment, Food & Rural Affairs (DEFRA), its executive agency, the UK Environment Agency (EA) and the Natural Environment Research Council (NERC) organized a monitoring campaign between 2002 and 2006, led by the Centre for Ecology and Hydrology, NERC, with additional environmental monitoring and analysis by the Cambridge Coastal Research Unit (University of Cambridge) and Birkbeck, University of London. The monitoring programme focused on mapping from airborne platforms (aerial photography, Light Detection and Ranging (LiDAR) and Compact Airborne Spectrographic Imager (CASI) surveys), establishing rates and patterns of sedimentation and accretion, and the recording of vegetation communities, intertidal invertebrates, fish and bird population dynamics and their change over time with the re-establishment of tidal exchange (Brown et al., 2007). However those parameters initially targeted, i.e. the reduction of flood protection costs, were not monitored after scheme implementation. The incomplete evaluation of MR has often been ascribed to rather vague formulated targets (Esteves, 2013; Esteves and Thomas, 2014; Wolters et al., 2005). This was also the case at Freiston Shore. Not surprisingly, therefore, the formulation of clearly stated objectives for future MR schemes was a recommendation in the final report (Brown et al., 2007).

Addressing this coastal management knowledge gap is important, particularly when considering the expected future need for considerably more MR schemes (Committee on Climate Change, 2013). In this paper, we therefore address the following three questions:

1. Has managed realignment at Freiston Shore led to a reduction in HWLs at the landward margin of the realigned site?

2. How variable is HWL attenuation across space and over time within this MR site?

3. For a specific range of tidal inundations, can a demonstrable difference be seen in HWL attenuation between the MR scheme and the adjacent natural saltmarsh?

3.2 Study area and methods

3.2.1 Study area

Freiston Shore was the largest MR in the UK at time of establishment in 2002 and still ranks among the ten largest UK schemes (ABPmer, 2010). It is situated in The Wash embayment in Lincolnshire (UK), southern North Sea (Figure 3.1a and b). 75 % of The Wash's coastline is fronted by saltmarshes, which locally reach 1–2 km in width. The total saltmarsh area, 4199 ha, constitutes the largest coherent area of active saltmarsh in the British Isles (Pye, 1995). The tides of The Wash are characterized by a semidiurnal, macro-tidal regime (Mean Spring Tidal Range (MSTR) = 6.5 m), exhibiting flood dominated tidal asymmetry (Friess et al., 2014; Pye, 1995). Wave rider buoy measurements at the mouth of The Wash, between May 1999 and May 2000, recorded maximum and mean significant wave heights of 2.81 and 0.61 m respectively (Spencer and Harvey, 2012).

The Wash has been heavily influenced by land reclamation since Roman times. Between 1970 and 1980, 800 ha of natural saltmarsh area was reclaimed for agricultural use (Baily and Pearson, 2007) with the last embankment, hereafter referred to as the old seawall, being constructed in 1982. It has been argued that this seawall was constructed too far seaward with the result that the fronting saltmarsh sustained considerable wave erosion (Friess et al., 2014; Symonds and Collins, 2007a, 2005) and a

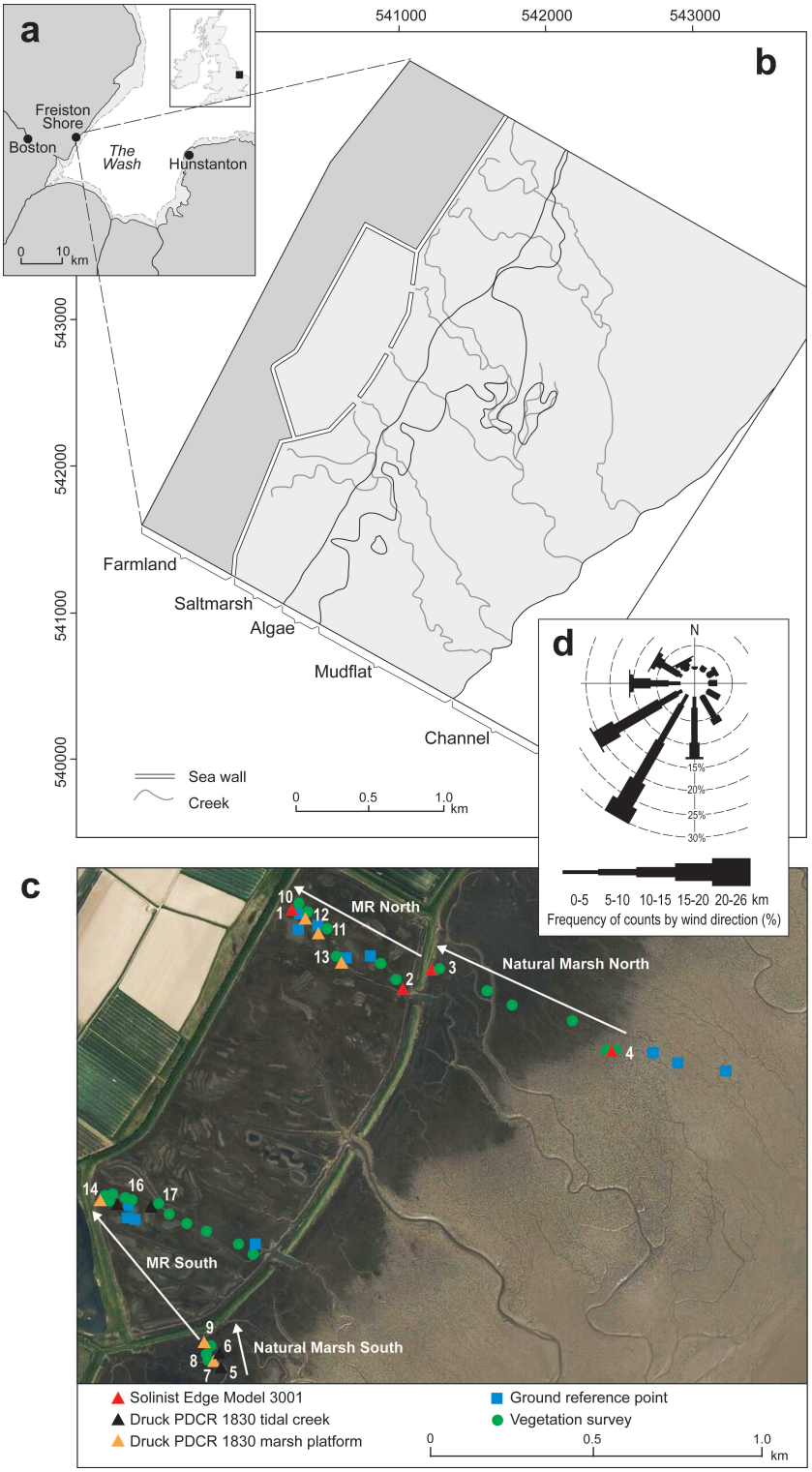

Figure 3.1 a) Location of the Freiston Shore managed realignment site in The Wash embayment, eastern England; b) schematic map of the managed realignment scheme including the adjacent natural saltmarsh and major tidal creeks; c) study design with location of pressure transducers and quadrats of the vegetation survey. White arrows indicate the four different sections along which the sensors were deployed; d) wind rose showing wind conditions for Holbeach weather station during the measurement period.

mean retreat rate of 15 m a^{-1} (Brew and Williams, 2002).

The 1996 regional Shoreline Management Plan therefore recommended realignment of this coastal segment (Friess et al., 2008), setting the coastal defence back to an earlier position and allowing for the restoration of formerly reclaimed saltmarshes over an area of 66 ha. Three breaches, each of ca 50 m width, were cut into the old seawall in August 2002 (Figure 3.1b). An artificial creek system of ca. 1200 m in total length was created within the MR and connected to the creek system of the natural saltmarsh in front of the site (Friess et al., 2014; Symonds and Collins, 2007a, 2005). It was calculated that the site would inundate fully ca. 150 times per year, with 50 % inundation 467 times per year, which would allow for the development of mid to upper marsh communities (just above Mean High Water (MHW)) (Nottage and Robertson, 2005).

At the time of MR implementation, elevations within the site varied between 2.76 m and 3.33 m Ordnance Datum Newlyn (ODN) (where 0.0 m ODN approximates to mean sea level), allowing for rapid vegetation colonization. By 2006, mean total vegetation cover within the MR was estimated at 86 % (Brown et al., 2007).

Over the period November 2002 — April 2008, mean rates of surface elevation changes on natural vegetated saltmarsh control sites (2.91 – 3.40 m ODN), at some distance seaward from the new breaches, showed rates of mean vertical accretion of 0.17 — 0.21 cm a^{-1}, comparable to elevation gains seen at other marsh surfaces in the region. Within the MR, one site close to one of the breaches showed an exceptionally high rate of mean surface elevation gain of 18.75 cm in the first 5.5 years after the re-introduction of tidal exchange, one hundred times greater than rates of increase at the control sites (Spencer and Harvey, 2012). This was most likely as a result of high localized sediment supply from breach and channel enlargement and the presence of surfaces left unnaturally low (2.76 – 2.96 m ODN) in the tidal frame as a result of the 1982 embanking. By comparison, a site in the middle of the MR (3.11 – 3.23 m ODN) showed a mean elevation gain of 5.19 cm over the same time period but still significantly higher than the external control sites. Finally, sites at the rear of the

MR, far from any of the breaches or internal channels, registered rates of mean surface elevation gain of 0.30 – 0.39 cm a^{-1}, only slightly higher than the rates of increase measured at the external control sites (Spencer and Harvey, 2012). The analysis of a LiDAR based digital terrain model from 2016 (provided by the EA) revealed that mean elevation inside the MR (3.04 ± 0.42 m ODN) as being higher than that of the adjacent natural marsh (2.88 ± 0.5 m ODN).

3.2.2 Water level assessment

Water level measurements were taken at 16 locations in saltmarsh canopies and tidal creeks within the MR scheme of Freiston Shore and in the adjacent natural marsh (Figure 3.1c). The monitoring period extended over two consecutive springtide periods between 19 September and 12 October 2017. This period coincided with the equinoctial tides, the highest spring tides of the year, which ensured the complete inundation of both the MR site and the natural marshes for several high water events. Hourly meteorological data on wind speeds and direction from Holbeach weather station, 18 km to the south of the study site, were provided by the UK Met Office for the entire monitoring period (Figure 3.1d).

Water levels were recorded with a series of 16 pressure transducers of two types (12 Druck PDCR 1830 & 4 Solinst Levellogger Edge Model 3001), both of which have an accuracy of < 1 cm. All sensors were manually calibrated to measure the height of the water column (cm). The measurement interval for the Solinst and Druck sensors was programmed to 30 s and 0.25 s, respectively. In order to eliminate the effect of waves on recorded water levels, data from both sensor types were smoothed by calculating moving averages over two minute intervals.

The geographic coordinates and elevations of each sensor (Table 3.1) were determined by a Leica Viva GS08 GNSS satellite survey Real Time Kinematic (RTK) system; all stored measurements were characterised by a 3-D coordinate quality of up to 50 mm, but typically below 20 mm.

Table 3.1 Name, coordinates and elevation of each pressure sensor.

Sensor #	**Latitude**	**Longitude**	**Elevation (m ODN)**
Loc 1	540724.04	343436.682	2.99
Loc 2	541058.77	343224.113	2.78
Loc 3	541157.14	343277.481	2.87
Loc 4	541671.59	343076.004	2.08
Loc 5	540556.04	342136.048	1.46
Loc 6	540551.82	342171.991	1.83
Loc 7	540546.43	342147.882	2.58
Loc 8	540524.98	342149.823	2.71
Loc 9	540516.16	342199.482	2.73
Loc 10	540724.04	343436.682	2.99
Loc 11	540795.27	343379.266	2.89
Loc 12	540764.41	343408.975	2.9
Loc 13	540871.92	343290.1	3.01
Loc 14	540200.98	342596.534	2.85
Loc 16	540248.96	342582.824	2.19
Loc 17	540348.24	342583.267	1.82

HWL attenuation rates (cm km^{-1}) were calculated from i) the vertical difference in water level between two pressure transducers (termed hereafter as transect), where each pressure transducer represents one location (see Figure 3.1c) and ii) the measured horizontal distance (m) between the two sensors. Positive rates refer to HWL attenuation, while negative values correspond to an amplification of HWLs along the respective transect. In order to be able to compare HWL attenuation rates across the MR and the natural marsh, but also to account for spatial variabilities within both systems, transects of variable lengths were deployed along four sections (Natural Marsh North (containing 1 transect) & South (3 transects), MR North (7 transects) & South (2 transects) (Figure 3.1c). This configuration allowed for a comparison of HWL reduction between the MR and the adjacent natural marsh transects.

As vegetation properties were considered to be constant during the measurement period, we used water depth and meteorological conditions to explain the event based variability along each transect. The northern (MR North, Natural Marsh North) and southern sections (MR South, Natural Marsh South) (Figure 3.1c) were more than 1 km apart from each other, which is why we used water depth data from nearby sensors for the respective correlations. For both sections, water depth was taken from the sensor in front of the landward seawall (Loc 1 in the north and Loc 14 in the south) (Figure 3.1c).

3.2.3 Vegetation survey

Assuming meteorological conditions to be constant across the entire study area, spatial variabilities in HWL attenuation between transects were qualitatively explained by spatial variations in vegetation properties. Vegetation sampling was conducted by following the sampling protocols of Moore (2011); these are consistent with field protocols commonly used in the National Oceanic and Atmospheric Administration (NOAA) Estuarine Research Reserve Program (Meixler et al., 2018).

Vegetation characteristics were recorded next to each pressure sensor location and along each of the four sections (Figure 3.1c). Species present, and their coverage, height and density, were measured in 39 1 $\times$ 1 m quadrats. Two quadrats were measured next to each sensor location. Additional quadrats were selected along all four sections whenever a visible change in the dominant species occurred. Finally, in order to get a representative estimate of the vegetation properties per section (MR North, MR South, Natural Marsh North and Natural Marsh South), density, height and coverage were averaged over the entire section length.

The percentage vegetation cover for each species individually, and for the entire quadrat, was visually determined to the nearest 5 %, by comparing the share of vegetation versus remaining bare ground.

Vegetation height was assessed for each species by measuring from the substrate to

the top of the plant. In order to get a representative estimate of vegetation height per quadrat, this procedure was repeated several times for each species by excluding the highest and lowest 20 % of plants present. The percentage cover and mean vegetation height of each individual species, and the total coverage of the respective quadrat, were used to calculate the mean total vegetation height.

Shoot density was determined per species, and for each 1 × 1 m quadrat as a whole, by counting the rooted stems in three 20 × 20 cm sub-quadrats. For *Puccinellia maritima*, which can form very dense carpets in the higher marsh, the frame size was reduced to 10 × 10 cm. Finally, mean shoot density was calculated per quadrat using the same procedure as for vegetation height.

In addition, to assess the general distribution and coverage of vegetation between sections, a supervised image classification (overall accuracy of 93 %) was conducted for four polygons, each representing one of the four sections. The polygons were created using QGIS software (version 2.18.12), drawing a straight line through each pressure sensor of the respective section and applying a buffer of 50 m around it. The classification used a vertical aerial photograph provided by the EA from 6 May 2016, taken around the time of low water (no aerial photographs were available for 2017). Seasonal differences in vegetation growth between the actual field survey and the aerial photography may have affected vegetation cover estimates. In order to check whether vegetation cover was different between 2016 and 2017, the extent and distribution of vegetation, mud and water was compared visually for 12 additional ground reference points (Figure 3.1c). Subsequently, the proportion of six classes for the areas of interest were assessed: mud, mud with vegetation, water, embankment, vegetation and unclassified.

3.2.4 Statistical analysis

In order to address research question 3, we tested whether or not there was a statistically significant difference in HWL attenuation between the MR site and the adjacent

natural marsh over the study period. As the data was neither normally distributed (Shapiro Wilk test p-value < 0.05) nor homoscedastic (Bartlett test p-value < 0.05), a non-parametric Mann Whitney U test was used.

We also tested whether or not HWL attenuation rates inside the MR and in the natural marsh were significantly different from 0. A Shapiro Wilk test confirmed that the data was not normally distributed (MR p-value < 0.0005; Natural Marsh p-value < 0.0005) and thus a non-parametric one-sample Wilcoxon signed rank test was applied to both datasets.

3.3 Results

3.3.1 Meteorological conditions

Hourly averaged wind speeds during each high tide's slack water period varied between 7.4 km h^{-1} and 33 km h^{-1}, with maximum gusts between 11.1 km h^{-1} and 50.0 km h^{-1}. During the measurement period, south-westerly (offshore) winds were dominant, with onshore winds (South-South-East (SSE)) only observed during two high water events. During these two events, hourly averaged wind speeds did not exceed 16.7 km h^{-1}.

3.3.2 HWL attenuation

Overall, the results showed significantly higher (p-value < 0.005) attenuation rates over the natural marsh, with values ranging between 0 and 101 cm km^{-1} (mean 46 cm km^{-1}) compared to the MR, where values ranged from -102 to 160 cm km^{-1} (mean -3 cm km^{-1}) (Table 3.2).

While the results for the natural marsh showed that HWLs were attenuated for all tides measured, about half of the measurements inside the MR revealed HWLs that were not attenuated but amplified (Figure 3.2). In addition, a one-sample Wilcoxon signed

Table 3.2 HWL attenuation rates over the Freiston Shore MR, the adjacent natural marsh and the total marsh width.

Location	**Attenuation rate (cm km^{-1})**	**Length of attenuation (km)**
Natural Marsh	0 - 101	0.036 - 0.545
MR	–102 - 160	0.091 - 0.512
Total marsh width (Loc 4–1)	0 - 18	1.015

rank test revealed that HWL attenuation rates in the natural marsh were significantly different from 0 (p-value < 0.005) which was not the case inside the MR (p-value $= 0.5$).

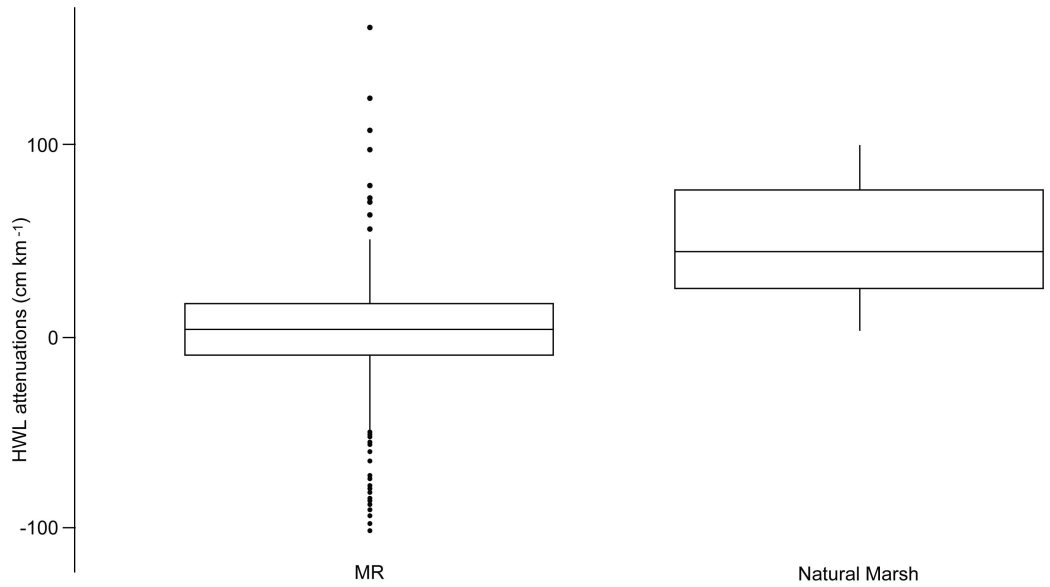

Figure 3.2 Boxplots of HWL attenuation rates within the Freiston Shore MR site and the adjacent natural marsh. The bottom and top of the box refer to the 25$^{\text{th}}$ and 75$^{\text{th}}$ percentile, while the centerline constitutes the median. The upper and lower whiskers are calculated as the upper and lower boundary of the box + 1.5* the interquartile range. Data points, which did not fall within this range, are plotted as outliers. The results of a non-parametric Mann-Whitney U test revealed that the difference between the MR and the adjacent natural marsh was significant (p-value < 0.0005).

The differences between the two systems in terms of HWL attenuation are also apparent when looking at the respective Standard Deviation (STD). The spread of measured attenuation rates along the individual transects and across the sections (MR South,

MR North, Natural Marsh South, and Natural Marsh North) revealed considerable temporal and spatial variability (Figure 3.3).

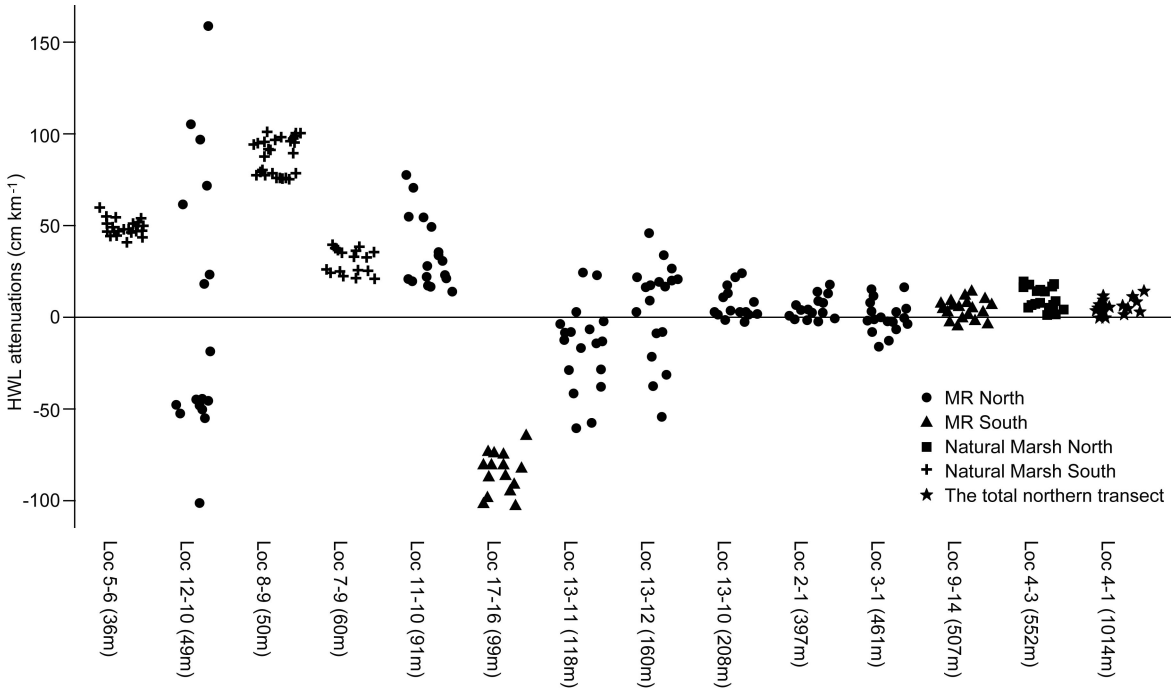

Figure 3.3 HWL attenuation rates plotted for each location and ordered by transect length. The shape of the data points indicates the respective section.

This variability was found to be exceptionally pronounced inside the MR, where mean values were considerably higher in the north than in the south (6 cm km^{-1} in the north and 33 cm km^{-1} in the south), while variability was higher in the south (STD 44 cm km^{-1} in the south and 35 cm km^{-1} in the north). In the southern natural marsh, HWL attenuation rates varied from 23 to 101 cm km^{-1} (mean 56 cm km^{-1}, STD 25 cm km^{-1}); in the northern part of the natural marsh these values were considerably lower, varying from 0 to 18 cm km^{-1} (mean 9 cm km^{-1}, STD 6 cm km^{-1}). It should be noted, however, that values in the northern natural marsh were derived from only one transect (Loc 4—3), whereas measurements in the natural marsh of the southern section included three transects.

The results further indicate that there is a nearly asymptotic relationship between HWL attenuation and the distance over which the latter was calculated (termed hereafter as transect length) (Figure 3.3).

The correlation between HWL attenuation and water depth was highly transect specific (Figure 3.4). In the north, only one transect showed a significantly negative correlation ($R^2 = 0.28$; Figure 3.4a), but otherwise no significant relationship between HWL attenuation and water depth could be detected, for either the natural marsh or the MR site. In the south, in contrast, the relationship between HWL attenuation and water depth was very different between the MR and the natural marsh (Figure 3.4b). In the latter, comparatively little variation in HWL attenuation could be explained by water depth ($R^2 \geq 0.25$), even though two out of three transects still showed a significant correlation (Loc 5—6 & Loc 8—9). As opposed to the results of the northern section, correlations in the southern natural marsh revealed a positive relationship between the two parameters. Inside the southern MR, significantly negative correlations clarified that most of the variation in HWL attenuation could be explained by water depth ($R^2 \geq 0.85$; Figure 3.4b; Loc 9—14, Loc 17—16).

Our results further indicate that besides water depth, wind direction may have affected HWL attenuation rates and also the observed differences between the MR and the natural marsh. It is shown that the effect of wind direction is section specific (Figure 3.5). While the southern natural marsh experienced above average rates of HWL attenuation during North-West (NW) (58 cm km^{-1}), South-West (SW) (59 cm km^{-1}), South-South-West (SSW) (59 cm km^{-1}) and West (W) (63 cm km^{-1}) winds (compared to an overall mean attenuation rate of 56 cm km^{-1}), the northern natural marsh showed greater than average attenuation only under South (S) (17 cm km^{-1}) winds (compared to an overall mean of 9 cm km^{-1}). The northern MR exhibited low rates of HWL attenuation and even amplification during NW (-1 cm km^{-1}), W (-5 cm km^{-1}) and West-North-West (WNW) (-3 cm km^{-1}) winds (compared to an overall mean of 6 cm km^{-1}). HWL amplification inside the southern MR predominantly occurred during NW (-46 cm km^{-1}), SW (-36 cm km^{-1}) and W (-50 cm km^{-1}) winds (compared to an overall mean of -33 cm km^{-1}). In summary, while westerly and north-westerly winds were more likely to result in above average HWL attenuation

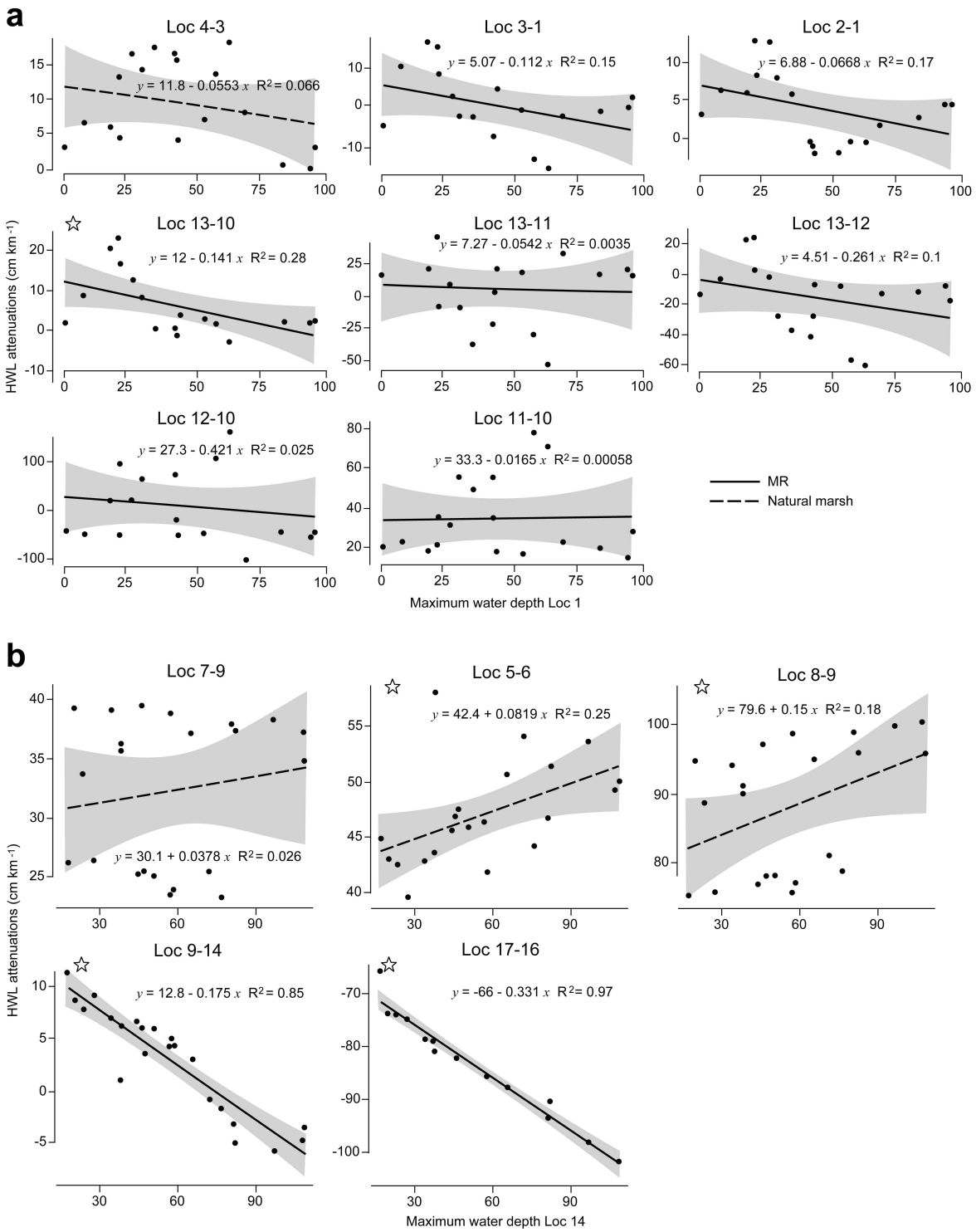

Figure 3.4 a) Scatterplot matrix showing the correlation between HWL attenuation rates and water depth at Loc 1 for all locations within the northern section. Shaded areas around the linear models represent the standard deviation and a star indicates significant trends (p-value < 0.05). The p-values for each location were calculated as follows: Loc 4–3 = 0.3; Loc 3–1 = 0.11; Loc 2–1 = 0.088; Loc 13–10 = 0.002; Loc 13–12 = 0.19; Loc 12–10 = 0.53; Loc 11–10 = 0.92. b) Scatterplot matrix showing the correlation between HWL attenuation and water depth at Loc 14 for all locations within the southern section. Shaded areas around the linear models represent the standard deviation and a star indicates significant trends (p-value < 0.05). The p-values for each location were calculated as follows: Loc 7–9 = 0.47; Loc 5–6 = 0.018; Loc 8–9 = 0.049; Loc 9–14 = < 0.0001.

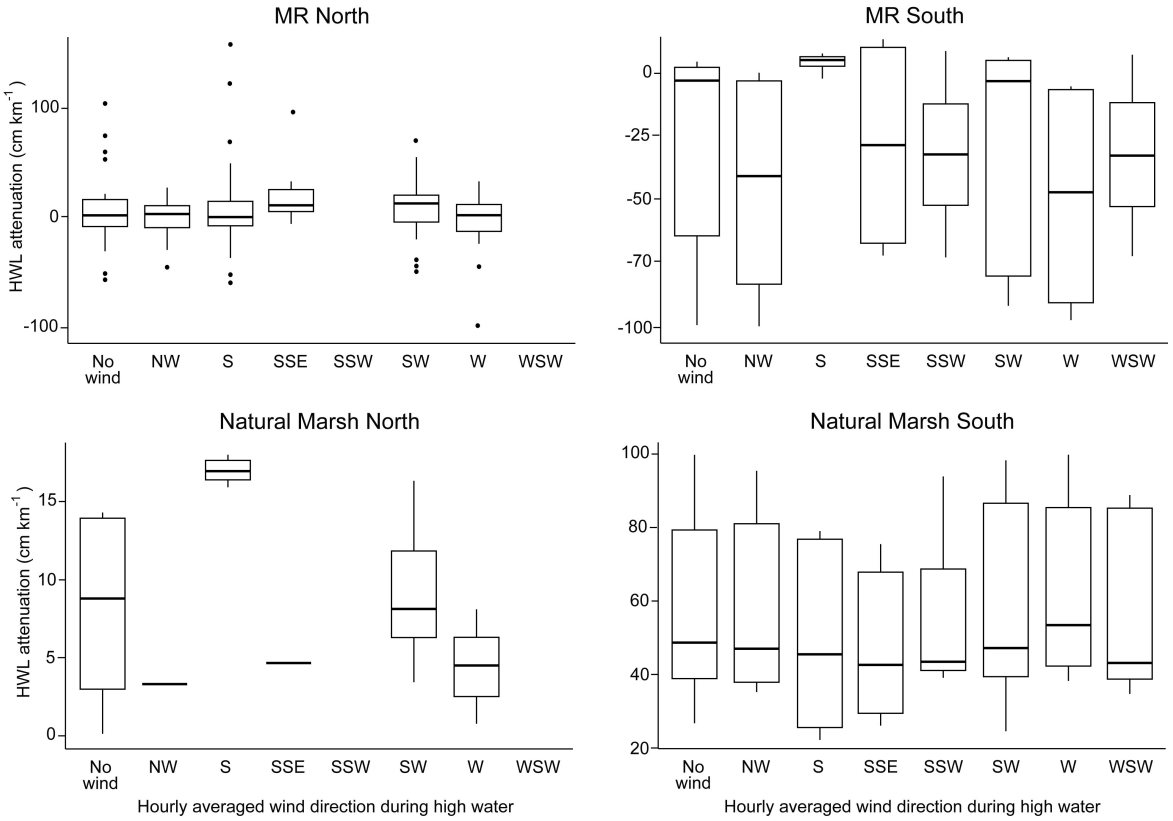

Figure 3.5 HWL attenuation rates for each section plotted against hourly averaged wind direction during high water slack. Shown are only those HWL attenuation rates, where the hourly averaged wind speed during high water slack was > 11.1 km h^{-1}. The "No Wind" category summarizes attenuation rates for all wind directions, but which were assessed during wind speeds ≤ 11.1 km h^{-1}. The bottom and top of the box refer to the 25$^{\text{th}}$ and 75$^{\text{th}}$ percentile, while the centerline constitutes the median. The upper and lower whiskers are calculated as the upper and lower boundary of the box + 1.5 * the interquartile range. Data points, which did not fall within this range, are plotted as outliers.

in the southern natural marsh, they had the opposite effect inside both sections of the MR.

3.3.3 Vegetation characteristics

The locations with highest mean vegetation height in the southern natural marsh (43.5 cm) clearly coincided with those transects over which the highest HWL attenuation rates were observed during this study. However, spatial variations in HWL attenuation along the other sections could not be explained by differences in vegetation properties

(Figure 3.6). For example, highest shoot densities were measured in the northern and southern MR (1755 stems m^{-2} and 1121 stems m^{-2}), while values in the natural marshes were significantly lower, with 287 stems m^{-2} in the northern and 224 stems per m^{-2} in the southern natural marsh. These differences likely appeared due to the locally high abundances of the common saltmarsh-grass *Puccinellia maritima*. Whilst HWL attenuation was higher in the northern MR compared to the southern MR, in accordance with the higher stem density, it was generally significantly less than that recorded in the natural marsh, despite the much lower stem densities.

Furthermore, differences in vegetation cover among the sampled quadrats did not explain the differences in HWL attenuation between the sections. Similar to shoot densities, mean vegetation cover of sampled plots inside the MR (MR North 92 % and MR South 96 %) was higher compared to the southern (74 %) and northern natural marsh (67 %). However, the assessment of vegetation cover by means of the supervised image classification (not represented in the field measurements shown in Figure 3.6) showed that vegetation cover was highest in the southern natural marsh (90 %), coinciding with the tallest vegetation (Figure 3.6) and highest HWL attenuation rates. The second highest vegetation cover was measured in the northern MR (81 %), while the northern natural marsh (74 %) and the southern MR (73 %) showed very similar cover characteristics. The lower vegetation cover in the northern natural marsh compared to the southern natural marsh may be the result of the high proportion of dissecting tidal creeks, as reflected in the high share of area classified as mud (9 % compared to 5 % Natural Marsh South; 6 % MR South 7 % MR North). The percentage of open water areas was higher inside the MR compared to the natural marsh (9 % MR North; 10 % MR South; 1 % Natural Marsh North; $<$ 1 % Natural Marsh South), reflecting both the artificial internal creek system and a high surface coverage of waterlogged areas and bare pools.

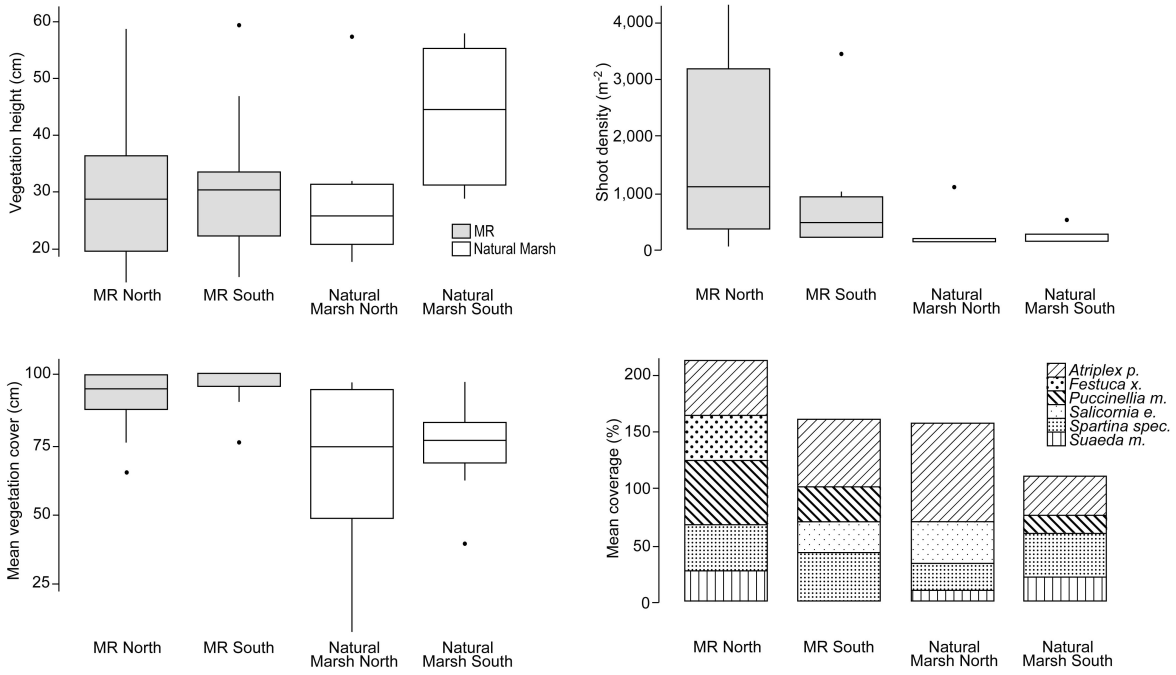

Figure 3.6 Vegetation characteristics and species per section. Only those genera are shown for which coverage exceeded 10 %.

3.4 Discussion

3.4.1 Has managed realignment led to a reduction in HWLs at the landward margin of the realignment site and how variable is HWL attenuation across space and time within this MR site?

The results of this study show that, for the conditions encountered during the field monitoring period, the capacity of the Freiston Shore MR site to provide HWL attenuation was limited. In fact, HWL attenuation rates inside the MR were not significantly different from zero. This was unexpected as the site exhibits high bed friction, due to its extensive vegetation cover and (artificial) topographic complexity resulting from the presence of excavated channels and constructed surface mounds and hollows. These results and the large HWL attenuation range observed inside the MR suggest that the existing relationship between HWL attenuation and bottom friction is more complex,

as previously suggested by Resio and Westerink (2008), and that the effects of vegetation on surge height reduction cannot be combined to a "single reduction factor" (Reed et al., 2018). This may be particularly valid in smaller enclosed basins such as MR sites. Rather, the comparatively high spatial (between transects) and event driven variability of HWL attenuation inside the scheme (Figure 3.3), indicate that internal hydrodynamics, resulting from the combined effects of variations in water depth and meteorological forcing, may have counteracted the attenuation of HWLs induced by the additional shallow water area provided by the restored saltmarsh.

This reasoning is supported by differences in the correlation between HWL attenuation and water depth between the southern MR site and the adjacent natural marsh. Inside the MR, correlations were significantly negative, while relations were positive in the adjacent natural marsh (Figure 3.4b). This indicates that for the inundation depths encountered during the monitoring period (varying between 16 and 110 cm at Loc 14), the southern natural marsh did not reach its full HWL attenuation potential. On the other hand, the same inundation depths were found to cause HWL amplification inside the southern MR. The occurrence of HWL amplification under comparatively low inundation depths may compromise the performance of the MR site under increasing inundation depths, for example during event-based storm surge conditions or, in the long term, with respect to sea-level rise. Stark et al. (2015) argued that the ideal inundation depth range for marshes to reach their highest attenuation rates lies between 0.5 and 1.0 m. At Freiston, this claim works well for the natural marsh, but not at all for the MR.

3.4.2 For a specific range of tidal inundations, can a demonstrable difference be seen in HWL attenuation between the MR scheme and the adjacent natural marsh?

The results of this study suggest considerably higher HWL attenuation rates over the natural marsh, than previously measured in the field (Table 3.3) and significantly higher than measurements inside the MR site. It can be argued that the high capacity of the natural marsh to reduce maximum water levels is a result of two factors. Firstly, during 27 % of the high tide slack water periods assessed, the wind direction was SW (i.e. offshore), a direction that was found to result in the highest HWL attenuation over the natural marsh (Figure 3.5).

Table 3.3 Observed attenuation rates in wetlands from previous field studies. Adapted from Stark et al. (2015) and Paquier et al. (2017).

Location	Description	Attenuation rate (cm km^{-1})	Length of attenuation (km)	Reference
Louisiana	Hurricane Andrew (1992) surge reduction over 37 km of marsh and open water	4.4 - 4.9	37	Lovelace (1994), Wamsley et al. (2010)
Great Marshes, Massachusetts	Mean HWL variation across tidal flats and saltmarsh channels	–2 - 11	/	Calculated by Stark et al. (2015) from figures in van der Molen (1997)
Ten thousand islands, National Wildlife Refuge, Florida	Hurricane Charley (2004) surge reduction across 5.5 km of marshes and mangroves	9.4 - 15.8	5.5	Krauss et al. (2009)
Shark River (Everglades), Florida	Hurricane Wilma (2005) surge reduction over 14 km of riverine mangrove	4.0 - 6.9	14	Krauss et al. (2009)
Cameron Prairie, Louisiana	Hurricane Rita (2005) surge reduction in marsh area	10.0	/	McGee et al. (2006), Wamsley et al. (2010)
Sabine, Louisiana	Hurricane Rita (2005) surge reduction in marsh area	25.0	/	McGee et al. (2006), Wamsley et al. (2010)
Vermillion, Louisiana	Hurricane Rita (2005) surge reduction in marsh area	4.0	/	McGee et al. (2006), Wamsley et al. (2010)
Vermillion, Louisiana	Hurricane Rita (2005) surge reduction in marsh area	7.7	/	McGee et al. (2006); Wamsley et al. (2010)
Western Scheldt estuary, Saeftinghe Marsh	Regular Spring to Neap tides including two storm surge events over saltmarsh surfaces and within tidal channels	–2 - 70	/	Stark et al. (2015), evaluated from figures
Chesapeake Bay	Measured over tides and two storm surge events	–280 - 270	0.02	Paquier et al. (2017)

Secondly, the most extreme HWL attenuation rates were measured along the shortest transects (Figure 3.3). Three out of four transects in the natural marsh were measured over comparatively short distances of less than 60 m. Previously, similar rates have only been measured by Paquier et al. (2017) and by Stark et al. (2015), also over very short vegetated marsh platform transects (Table 3.3). Two possible explanations for this phenomenon can be found in the literature. Firstly, the flow field over vegetated surfaces is dominated by high friction induced by the presence of vegetation (Stark et al., 2015; van Oyen et al., 2012, 2014). This friction is reduced over longer transects, which typically include areas of high density vegetation canopies but also mud, standing water and low and pioneer communities with widely spaced individual plant stems. Secondly, HWL attenuation is not a linear process. Rather, it is spatially highly variable, depending on local marsh morphology, vegetation and hydrodynamic forcing (Resio and Westerink, 2008; Stark et al., 2016; Temmerman et al., 2012). These arguments are supported by this study, where highest attenuation rates were observed along short transects in the southern natural marsh. These were also transects where vegetation height and cover were highest. Thus, short transects over saltmarsh surfaces may generate maximum (within highly vegetated marsh transect) or minimum friction (on bare sediments) on the water column, depending on the surface cover and topography. This effect is averaged over the entire marsh width, resulting in converging HWL attenuation rates when measured over longer distances.

The exceptionally high attenuation rates across the natural marsh alone, however, do not explain the discrepancies with respect to the MR site. The weak performance of the MR site may originate from differences in those saltmarsh characteristics, which are known to determine HWL attenuation. It is well known that the effectiveness of wetlands in attenuating HWLs is dependent upon regional and local bathymetry, including the height, width and topography of fronting mudflats and sandflats; on local surface geometry and raised-feature elevations (Resio and Westerink, 2008); the presence of a closed vegetation cover of high and flexible stems (Resio and Westerink,

2008; Rupprecht et al., 2017); and the interaction of shallow water flows with a tidal creek network (Resio and Westerink, 2008; Smolders et al., 2015; Stark et al., 2015, 2016; Temmerman et al., 2012). By analysing 19 MR sites (including Freiston Shore), Lawrence et al. (2018) found that restored saltmarshes lack the variations in topographic roughness found in natural marshes. Marsh topography affects vegetation development (Lawrence et al., 2018), which helps to explain why vegetation characteristics of MR sites established on agricultural soils, such as Freiston Shore, differ from those of natural marshes (Mossman et al., 2012b). Furthermore, a patchy vegetation cover, as found inside the Freiston Shore MR, considerably reduces HWL attenuation rates (Temmerman et al., 2012). Based on the interrelation between morphology, vegetation and HWL attenuation, the restoration of a naturally complex and diverse topography should be a key objective of future MR schemes. However, the effects of morphologic complexity (including rugosity, topographic wetness, surface curvature and distance to creek (Lawrence et al., 2018)) on HWL attenuation rates have not yet been quantified (Möller and Christie, 2018). The detailed understanding of these controls on HWL attenuation is crucial for enhancing the future performance of similar saltmarsh restoration schemes.

3.4.3 Managed realignment: scheme design, meteorological forcing and HWL attenuation

The relative importance of meteorological conditions to spatial patterns of water levels within the MR site may be related to the design of the MR scheme. This is likely to be particularly significant where seawall breaches have been used as the means of re-establishing tidal exchange and thus, much of the seawall perimeter to the site remains intact. Previous studies in natural marshes have shown that storage area limitations for flood waters, for example, may cause water blockage against dikes or other structures confining the marsh size, causing HWL amplification (Stark et al., 2016). The results from Freiston support this observation. The positioning of the seawall boundaries to

the MR site relative to tidally and meteorologically forced water levels led to HWL amplification over the study period (Figure 3.7a: Loc 12–10; Figure 3.7b: Loc 6–9 and over the course of the MR, peaking at Loc 16). Resio and Westerink (2008) further explain this phenomenon; HWL amplification by water blockage occurs when the duration of the hydrodynamic forcing is long compared to the time it takes to fill the storage area. Here we further suggest that this effect may be amplified by meteorological conditions. Consequently, the size of a MR is an important factor in determining whether or not a created, or recreated, saltmarsh can reach its full attenuation capacity. This constitutes a true wetland restoration dilemma, as site size is often a major limiting factor towards MR implementation. In 2013, 66 % of MR sites in England were smaller than 20 ha (Esteves, 2013). In addition, this finding raises questions regarding the performance of the already existing MR schemes across the UK, which are mostly smaller than Freiston Shore (66 ha), with a mean size of currently 48 ha (Boorman and Hazelden, 2017).

Inside the MR, prevailing W and SW winds were found to result in exceptionally low rates of HWL attenuation inside the MR. We suspect that the effect of wind drag is greater on an almost enclosed body of water than for an open body of water, such as encountered outside the MR in the natural marsh. This effect may be amplified when wind speeds exceed those encountered during our monitoring period. It is clear that scheme design is likely to have considerable implications for the potential of any MR to reduce maximum water levels. Yet problematically, in many cases, constraints around land ownership and availability will most likely leave little choice regarding the actual location or orientation of the MR. These findings may also revive the debate on whether to perform bank removal or breach restoration, which has been termed “one of the unresolved problems facing the UK intertidal restoration program” (Pethick, 2002, p. 434).

Extensive application of nature-based coastal defences is still hampered by a lack of knowledge regarding their performance in terms of reducing the risk of coastal flooding,

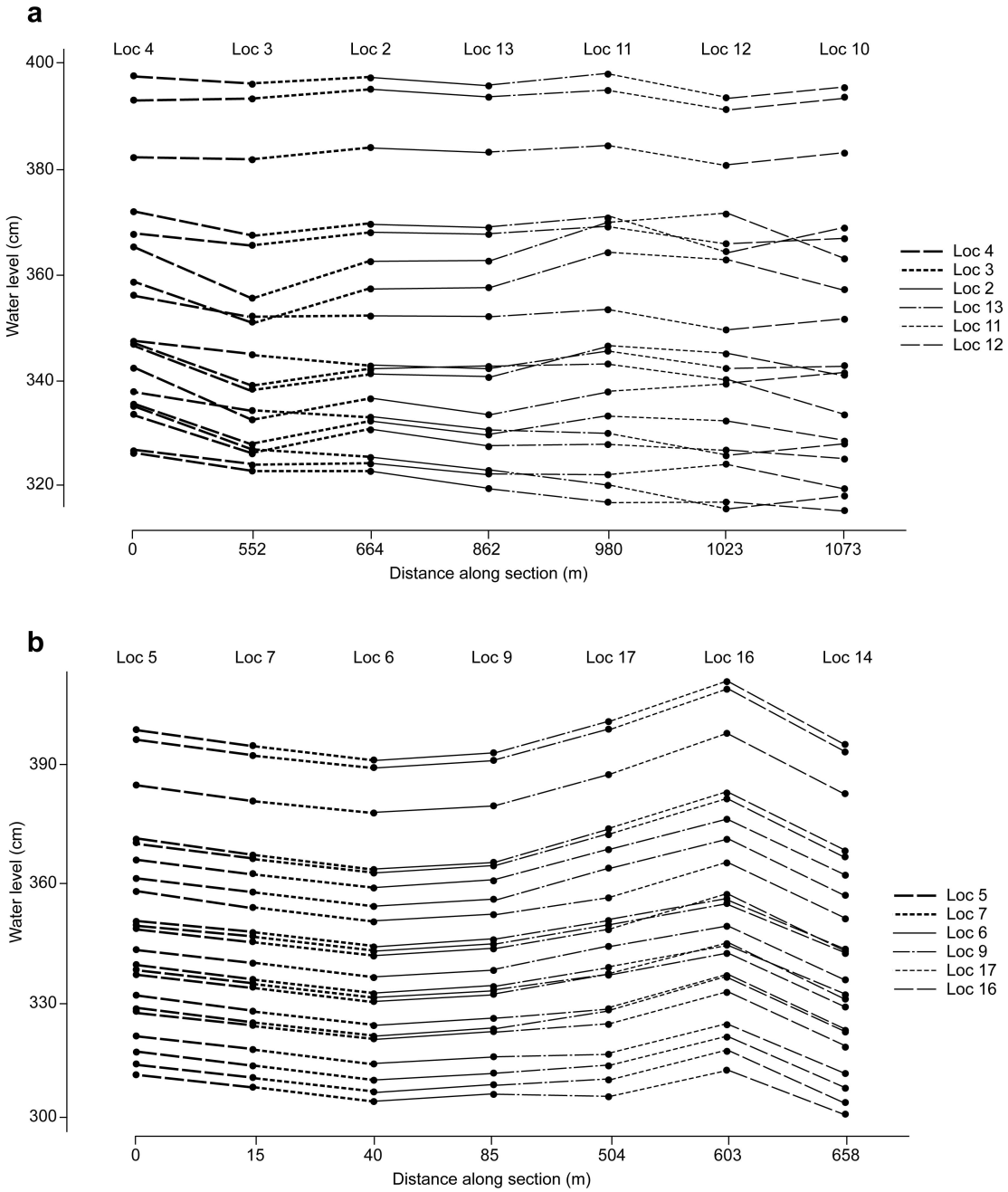

Figure 3.7 a) Cross section of water levels for both northern sections (including Natural Marsh North and MR North). Water levels are plotted for every sensor (shape) and every tide (line) on the y-axis, while distance is placed on the x-axis and measured in m from the most seaward sensor (Loc 4) in landward direction. b) Cross section of water levels for both southern sections (including Natural Marsh South and MR South). Water levels are plotted for every sensor (shape) and every tide (line) on the y-axis, while distance is placed on the x-axis and measured in m from the most seaward sensor (Loc 5) in landward direction.

as well as by a general lack of comprehensive design guidelines (Bouma et al., 2014; Reed et al., 2018). In establishing these guidelines, adequate consideration of the effects of site geometry, meteorological conditions, and restored surface characteristics on site internal hydrodynamics is urgently required.

3.5 Conclusions

For the conditions encountered during the field monitoring period, the capacity of the Freiston Shore MR site to provide HWL attenuation was limited. HWL attenuation rates were significantly higher in the natural saltmarsh (in front of the MR), where HWL attenuation ranged between 0 and 101 cm km^{-1} (mean 46 cm km^{-1}). Within the MR site, rates varied between -102 and 160 cm km^{-1} (mean -3 cm km^{-1}), with even negative attenuation (i.e. amplification) for about half of the measured tides.

The weak performance of the MR site in terms of HWL attenuation was a result of internal hydrodynamics caused by scheme design and meteorological conditions, counteracting the HWL attenuating effect caused by the additional shallow water area provided by the restored saltmarsh.

The findings of this study make clear that current design, monitoring and assessment approaches at MR sites may result in unrealized (HWL attenuation) potential (Spencer and Harvey, 2012). In order to fully exploit this potential in future MR schemes, forthcoming research should examine more closely the driving forces of HWL attenuation in space (site geometry and orientation, surface morphology, tidal creek network characteristics, vegetation canopy types and their site coverage) and time (wind strength, duration and direction and associated wave fields and water depths). The results of such studies should then be used to establish better guidelines for MR scheme design and implementation, to result in more effective HWL attenuation.

This in turn should enable the wider implementation of managed realignment at the coast, by fostering stronger, scientific evidence based coastal management and public

support and confidence.

3.6 Declaration of competing interest

The authors declare that they have no known competing financial interests or personal relationships that could have appeared to influence the work reported in this paper.

3.7 Acknowledgements

JK thanks the German Academic Exchange Service (Grant ID 57314604) and the Future Ocean Excellence Cluster (University of Kiel) for funding his stay in Cambridge, as a member of the Department of Geography's Visiting Scholar Programme. We thank B. Evans and E. Christie, Cambridge Coastal Research Unit, for technical and field assistance. The authors thank the Royal Society for the Protection of Birds, for access for research at the Freiston Shore reserve and the UK Environment Agency, for the supply of vertical aerial photography and LiDAR data.

Chapter 4

Effective design of managed realignment schemes can reduce coastal flood risks

Joshua Kiesel, Mark Schuerch, Elizabeth K. Christie, Iris Möller, Tom Spencer, Athanasios T. Vafeidis [1]

[1]This chapter is published as: Kiesel, J., Schuerch, M., Christie, E. K., Möller, I., Spencer, T., and Vafeidis, A. T.: Effective design of managed realignment schemes can reduce coastal flood risks, Estuarine, Coastal and Shelf Science, 242, 106 844, https://doi.org/10.1016/j.ecss.2020.106844, 2020

Abstract

Managed Realignment (MR) constitutes a form of nature-based adaptation to coastal hazards, including sea level rise and storm surges. The implementation of MR aims at the (re)creation of intertidal habitats, such as saltmarshes, for mitigating flood and erosion risks and for creating more natural shorelines. However, some evidence suggests that the desired coastal protection function of MR schemes (in terms of High Water Level (HWL) attenuation) may be limited and it was hypothesized that this was due to the configuration of the remaining seawalls, which we refer to as scheme design.

Here we present the results of a hydrodynamic model application, which we used to analyse the effects of scheme design on within-site HWL attenuation by applying six scheme designs that differ in terms of breach characteristics and water storage capacity. In specific, we vary the configuration of the seaward defence line (including the seawall breaches) and the position of the landward dike by modifying the digital elevation model of the site.

Our results show that changes in scheme design, particularly storage area and number and width of breaches, had significant effects on the site's HWL attenuation capacity. Decreasing the tidal prism by changing the number and size of breaches, with the site area kept constant, leads to increased modelled HWL attenuation rates. However, average HWL attenuation rates of >10 cm km^{-1} are only achieved when site size increases. The mean high water depth of each scheme design scenario, calculated by dividing tidal prism by MR area, explains most of the variation in average HWL attenuation between all scenarios. Attention to potential within-site hydrodynamics at the design stage will aid the construction of more effective MR schemes with respect to coastal protection in the future.

4.1 Introduction

Managed Realignment (MR) constitutes a form of nature-based adaptation for low lying coasts, aiming at the restoration or creation of intertidal habitats, such as saltmarshes, for the long-term management of flood and erosion risks. Saltmarshes can attenuate HWLs (Smolders et al., 2015; Stark et al., 2015, 2016; Temmerman et al., 2013), waves (Möller et al., 2014; Möller and Spencer, 2002; Rupprecht et al., 2017;

Spencer et al., 2015) and provide flood water storage, thus contributing to mitigating coastal flooding. Furthermore, saltmarshes constitute intertidal habitats which offer additional benefits such as nutrient cycling, carbon storage, preservation of high water quality, increased biodiversity and cultural services including recreation (Burden et al., 2013; Esteves, 2014; Luisetti et al., 2011; Spencer and Harvey, 2012).

Despite these multiple benefits, the assessment of the extent to which MR schemes provide the desired functions is difficult, as data on long-term individual project performance are scarce and of limited geographic coverage. In combination with societal and political resistance (Cooper and McKenna, 2008; Ledoux et al., 2005), the limited evaluation of MR may explain why the wider implementation is still hindered by funding constraints, availability of suitable land and uncertainties related to natural coastal evolution (Esteves and Williams, 2017). Nevertheless, MR schemes have been increasingly implemented in several countries, with large scale examples in Belgium (Sigma Plan, 2011), the USA (Day et al., 2007; United States Environmental Protection Agency, 2013), Germany (Schernewski et al., 2018a,b) and the UK (Cross, 2017; Esteves and Thomas, 2014; Turner et al., 2007). In December 2015, a total of 140 European sites were established (Esteves and Williams, 2017). In the UK, for example, the Online Managed Realignment Guide (OMREG) listed 51 MR projects in 2013 (Esteves and Thomas, 2014), which increased to 74 MR sites by 2019 (ABPmer, 2019). This growing interest needs to be accompanied by more comprehensive and longer-term monitoring, which could help to evaluate the sustainability and performance of MR and thus inform better MR design.

So far, there have been various types of MR scheme designs. These can be grouped into four classes, namely: (1) the complete removal of flood defences; (2) single breach schemes; (3) schemes with more than two breaches; and (4) regulated tidal exchange. The latter is excluded from the analysis presented in this paper, as the primary aim of regulated tidal exchange in Europe constitutes habitat creation (Esteves and Williams, 2017). The remaining three approaches have various objectives, such as the creation

of more natural shorelines, the promotion of biodiversity and, particularly in the UK, the enhancement of flood protection (including the reduction of flood protection costs and flood storage provision) (ABPmer, 2019; Esteves, 2013; Ledoux et al., 2005).

Across all different scheme designs, studies have shown that restored saltmarshes within MR schemes are different from their natural counterparts. These studies have identified differences in vegetation properties (Garbutt and Wolters, 2008; Mazik et al., 2010; Mossman et al., 2012b), biogeochemical cycling (Burden et al., 2013), topographic complexity (Lawrence et al., 2018) and HWL attenuation (Kiesel et al., 2019). Burden et al. (2013) and Garbutt and Wolters (2008) suggested that the difference between natural and restored saltmarshes may be a function of time, as it may take up to 100 years for a restored marsh to reach equivalence. The discrepancies between natural and restored saltmarshes reveal that substantial knowledge gaps still exist when it comes to recreating both the habitat and its ecosystem functioning.

These knowledge gaps may originate from the complex nature of coastal evolution and its interaction with the original scheme design. Erosion and sedimentation induce changes in site morphology (e.g. breach evolution: (Friess et al., 2014; Vandenbruwaene et al., 2015)), which in turn provides new environmental conditions to the process regime. Such interrelationships are further complicated by changing baselines, such as longer-term changes in external forcing from modified storm climates, coastal sediment availability and, in the future, accelerated sea-level rise (van Goor et al., 2003). This significantly complicates the numerical modelling of the MR site's morphodynamic evolution before and after breaching (Friess et al., 2014; Symonds et al., 2008).

Esteves (2014) argued that it is important to assess whether the selected breach design allows for the complete tidal drainage of a MR site of a particular size, especially during high water events. Similarly, Stark et al. (2016) found that storage area limitations for floodwater might cause water blockage against dikes, which in turn may result in HWL amplification. This may explain why the close coupling between inundation

depth and HWL attenuation within saltmarshes (Stark et al., 2015) may be altered within MR sites (Kiesel et al., 2019). In order to establish effective design guidelines for MR sites at the open coast, and to foster a stronger public support and confidence for this management practice, detailed knowledge on the effects of scheme design (size and breach design) on within-site HWL attenuation needs to be obtained.

For example, the size of MR and its specific breach design determines the volume of water between mean low and mean high water (i.e. the tidal prism) (Friess et al., 2014), which drives site internal inundation depths. The latter has been shown to be correlated with HWL attenuation (Stark et al., 2015, 2016). It is therefore crucial to revive the debate on whether to perform bank removal or breach restoration, which arguably still constitutes "one of the unresolved problems facing the UK intertidal restoration program" (Pethick, 2002, p. 434).

This problem has been illustrated in the MR site of Freiston Shore, where HWL amplifications were observed during a field survey (Kiesel et al., 2019). Thus, the coastal protection function for which Freiston was designed is not fully realised. In this study, we present the results of a 2-D hydrodynamic model, calibrated and validated against field measurements of the highest spring tides of the year between August and October 2017, taken within, and seaward of, the Freiston Shore MR site (Kiesel et al., 2019). We investigate six potential adaptations to Freiston Shore (termed hereafter as scheme design scenarios) in order to explore the potential of improving the HWL attenuation of the MR site. We structure the scenarios in three groups; 1) two scenarios with three breaches and varying MR areas, 2) three single breach scenarios of different breach widths and 3) one bank removal scenario. We furthermore discuss the implications of potential morphodynamic adjustments within each of these adaptations, by providing an analysis of bed shear stress for each scenario. Bed shear stress constitutes a useful parameter for this purpose, as it provides insights into depositional and erosional dynamics of intertidal areas (Callaghan et al., 2010; Li et al., 2019; Widdows et al., 2008).

4.2 Material and methods

4.2.1 Study area

The Freiston Shore MR site is located on the shores of The Wash embayment in Lincolnshire, eastern UK (Figure 4.1).

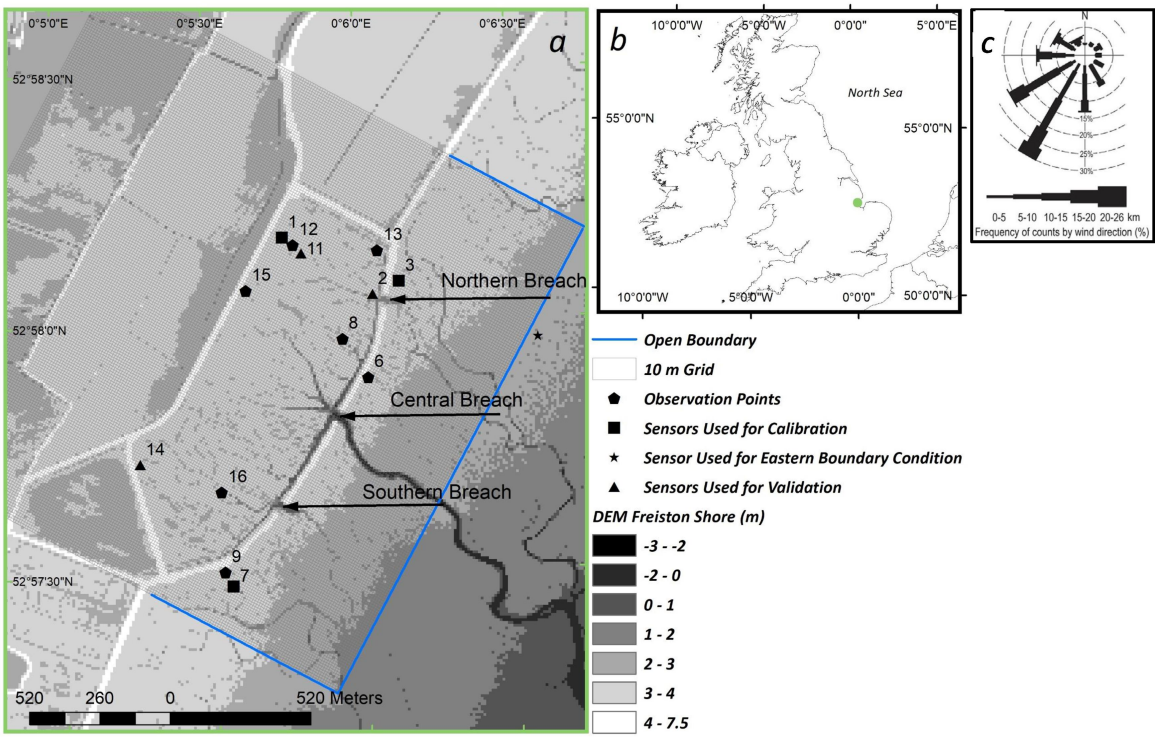

Figure 4.1 Location of the Freiston Shore MR site (green dot) in eastern England, UK (b). Panel a) shows the model domain and observation points used for model calibration, validation and for the assessment of HWL attenuation rates. The underlying 10 x 10 m digital elevation model was derived from a 2016 Light Detection and Ranging (LiDAR) survey and was provided by the UK Environment Agency (EA). Panel c was taken from Kiesel et al. (2019) and shows the wind conditions during the measurement period at Holbeach weather station, 18 km to the south of the study site. UK Met Office provided the wind data.

The Wash comprises an area of about 600 km^2 (ca. 25 km long from southwest to northeast, approximately 18 km wide from northwest to southeast at its seaward margin, and about 25 km wide towards its landward southwestern margin) with an average depth of $<$ 10 m and maximum depths between 40 and 50 m. The coastline

of The Wash has a total length of 110 km, which is fringed by intertidal environments including saltmarshes, mud- and sandflats (Brew and Williams, 2002). Southwesterly winds are dominant in The Wash, which was also the case during the measurement period in 2017 (Figure 4.1c). The Wash has a semi-diurnal, macro tidal regime. Mean neap and spring tidal range is 3.5 m and 6.5 m respectively, with flood-dominated tidal asymmetry at the coastal margins (Friess et al., 2012; Ke et al., 1996; Pye, 1995). Between May 1999 and May 2000, wave rider buoy measurements at the entrance to the Wash recorded maximum wave heights of 2.81 m and mean significant wave heights of 0.61 m. These conditions make The Wash a relatively low-energy embayment, which acts as a sink of marine sediments (Spencer et al., 2012), while fluvial sediment inputs are minimal (Ke et al., 1996). Sediment transport is consequently dominated by tidal currents, although waves have significantly shaped the morphology of The Wash's margins (Pye, 1995).

Hill and Randerson (1987) stated that 10 % of the UK's saltmarsh area was located in The Wash at the time of their investigation, comprising a total of 4199 ha. In the 1990's, 75 % of The Wash's coastline was fronted by saltmarsh (Pye, 1995). The shallow intertidal flats of The Wash have been subject to extensive land reclamations since the medieval period up until the 1980's (Doody, 1987). Between 1970 and 1980 alone, 800 ha of natural saltmarsh area was reclaimed for agricultural use (Baily and Pearson, 2007). The latest seawall in this sequence was created at Freiston Shore in 1982 (Symonds and Collins, 2005, 2007a,b), resulting in the retreat of the seaward edge of the fronting natural saltmarsh at rates of 15 m a^{-1} (Brew and Williams, 2002). Because of the reduced buffer zone, which left the seawall at high risk of breaching, the 1996 regional Shoreline Management Plan recommended realignment of this part of The Wash (Friess et al., 2008). This was finally realised in August 2002 by setting the coastal defence back to an earlier position, allowing for the restoration of formerly reclaimed saltmarshes over an area of 66 ha.

Besides the reinforcement of the landward seawall (0.4 — 0.5 km inland), the realign-

ment was undertaken by excavating three breaches (each of ca. 50 m width) in the seaward embankment. These breaches connected 1200 m of artificially created tidal creeks within the site with those of the adjacent natural marsh in front of the site (Friess et al., 2014; Symonds and Collins, 2005, 2007a,b). It was anticipated that the Freiston Shore MR site would fully inundate 150 times per year, which would allow for the development of mid to upper marsh communities, located above mean high water level (Nottage and Robertson, 2005).

Monitoring of the MR was organized by the UK Government's Department for Environment, Food & Rural Affairs (DEFRA), the EA and the UK's Natural Environment Research Council (NERC) and included the Cambridge Coastal Research Unit (University of Cambridge) and Birkbeck, University of London. The monitoring involved an assessment on vegetation development, accretion rates and invertebrates (Brown et al., 2007; Friess et al., 2012). The results confirmed the suitability of the site for rapid vegetation development; by 2007, the mean total halophytic vegetation cover within the MR was estimated at 89 %. In late summer 2017, the most abundant species present were *Salicornia europaea*, *Suaeda maritima*, *Puccinellia maritima*, *Atriplex portulacoides* and *Aster tripolium* (Kiesel et al., 2019). The established vegetation and the additional shallow water area provided by the restored saltmarsh were expected to provide "*within-marsh* attenuation" of waves and water levels (Smolders et al., 2015), allowing the landward seawall to be of a lower design specification and thus, cheaper to build and maintain (Dixon et al., 1998; Pethick, 2002).

In 2005, elevations at 41 surface elevation table locations within the MR varied between 2.76 m and 3.26 m Ordnance Datum Newlyn (ODN), where 0.0 m ODN approximates to mean sea level. In the first five years after breaching (2002 — 2007) most monitoring sites built up between 6 and 73 mm sediment, while some sites nearest to the central breach showed an exceptionally high total sedimentation of up to 215 mm (Brown et al., 2007). The latter sedimentation rates were most likely a result of high localized sediment input from breach and channel enlargement (Friess et al., 2014; Symonds and

Collins, 2007b) and the comparatively low surfaces as a result of the 1982 embanking (Spencer et al., 2012). After MR implementation, average internal elevations used to be lower (generally < 0.3 m) compared to the adjacent natural marsh (Friess et al., 2012). Sediment accretion inside the scheme has presumably sustained beyond the scope of the monitoring report, as in 2016 the mean elevation inside the MR (3.04 ± 0.42 m ODN) was higher compared to the external natural marsh (2.88 ± 0.5 m ODN) (Kiesel et al., 2019).

4.2.2 Model setup

Flow of water over the model domain was simulated using the Delft3D-FLOW (version 4.00.02) model (Delft Hydraulics, 2003). Delft3D-FLOW allows for the computation of flow and sediment transport over a multi-dimensional (2D (depth averaged) and 3D) finite, rectilinear or curvilinear difference grid (Delft Hydraulics, 2003; Temmerman et al., 2012). In our application, a 2D computation was used to solve the unsteady shallow-water equations.

Two-dimensional tide-induced flow was simulated on a Cartesian grid using the horizontal momentum equations, the continuity equation and 2D turbulence, which was modelled based on a constant horizontal eddy viscosity coefficient (1 m^2 s^{-1}). The modelled period extended over the highest spring tides of the year 2017, from the 20^{th} of September to the 16^{th} of October, applied at a time-step of 6 s. The model domain covered an area of 1.97 km width and 1.95 km length, extending from the pioneer zone of the natural saltmarsh in front of the MR over the MR itself in landward direction, up to the neighbouring agricultural fields (Figure 4.1a).

A 2 x 2 m LiDAR based Digital Elevation Model (DEM) from 2016 (provided by the EA) was used to implement the bathymetry and topography of the Freiston Shore coastal zone. This dataset was resampled to a 10 x 10 m and 5 x 5 m resolution grid (the latter only for calibration purposes; see subsection 4.2.3) in order to reduce computational costs. A bilinear resampling technique was applied in both cases, which

uses the average of the four nearest cells weighted by distance to define the new value of a cell. The bathymetry in the model domain is consequently not reflecting the highest surface levels, but accounts for sub grid scale features such as smaller tidal creeks, which are important for the undisturbed flow in the study site.

Key surface covers were differentiated for the application of bottom roughness coefficients. A supervised image classification (from Kiesel et al. (2019); overall accuracy of 93 %) was used to distinguish between four different surface cover classes (saltmarsh, water, mud and pasture). This classification was based on vertical aerial photography of 20 x 20 cm resolution, which was taken on May 6, 2016 during low tide for the EA. The results of the classification were validated by comparing twelve classified pixels to ground reference measurements (Kiesel et al., 2019).

The model was forced with hourly meteorological data on wind speed and direction measured at Holbeach weather station, 18 km south of the study site (Kiesel et al., 2019). It was assumed that the wind pattern was homogeneously distributed over the comparatively small model domain.

The hydrodynamic forcing of the eastern open boundary was defined in 10-min intervals, using water levels measured in 2017 in the direct vicinity (Figure 4.1, Kiesel et al. (2019)). The two neighbouring open boundaries, situated perpendicular to the eastern boundary, were not forced, but allowed to exchange water with the water body outside the model domain.

4.2.3 Model calibration and validation

The model was calibrated with tidal water depths measured at three locations (Loc 1, Loc 3, Loc 7) within and outside the Freiston Shore MR site (Figure 4.1). In order to test the model performance, we compared between modelled and measured water depth. The deviation between both was assessed by calculating the Root Mean Square Error (RMSE), Mean Error (ME) and Mean Absolute Error (MAE) for the entire inundated period, as well as the RMSE ($RMSE_{HWL}$) and MAE (MAE_{HWL}) of

HWLs.

During calibration, the model was analysed for variations in the following model setups and parameters: mesh size (10 m vs. 5 m), 2D, 3D (the latter exhibiting both five and two layers), Manning's n roughness coefficients for saltmarsh surfaces (0.035 – 0.09), wind (including two sets of wind drag coefficients and one model run without wind included), reflection parameter alpha (250, 500, 750 and 1000), boundary conditions (only eastern boundary forced vs. all three boundaries forced) and time step (0.01, 0.05 and 0.1 min). Best results were obtained by retaining Delft3D-FLOW's default wind drag coefficients, a grid size of 10 x 10 m, a reflection parameter (alpha) of 500, 2D model grid, forcing only the eastern open boundary and by applying a time step of 6 s.

The influence of wind on the modelled water levels is calculated in Delft3D-FLOW through the relationship between drag force and wind speed described by three break point drag and wind speed conditions. The influence of these coefficients was calibrated by running the model with a) no wind drag, b) default Delft3D-FLOW wind drag coefficients (breakpoint A coefficient = 0.00063 at windspeed 0 m s^{-1}; B coefficient = 0.00723 and C = 0.00723, both at windspeeds of 100 m s^{-1}, and c) varying drag coefficients and breakpoint windspeeds for breakpoints A (0.0015 at 0 m s^{-1} and B (0.005 at 40 m s^{-1} (Bastidas et al., 2016; Delft Hydraulics, 2003).

The effects of a range of values for Manning's n coefficient for saltmarshes (0.035, 0.06, 0.07, 0.08 and 0.09) on modelled water depths were tested against the field measurements. All coefficients (besides 0.09 and 0.06) were taken from the literature (Lawrence et al., 2004; Stark et al., 2016, 2017; Temmerman et al., 2012; Wamsley et al., 2010). Generally, the Freiston Shore model was not sensitive towards varying values of Manning's n coefficient. The range of mean MAE_{HWL} for the calibration points varied between 0.047 m (MAE_{HWL} Loc 1 = 0.03, Loc 3 = 0.03 and Loc 7 = 0.08) for a Manning's n value of 0.06 and 0.08 (MAE_{HWL} Loc 1 = 0.03, Loc 3 = 0.03 and Loc 7 = 0.08) and 0.057 m for a Manning's n coefficient of 0.09 (MAE_{HWL} Loc

1 = 0.07, Loc 3 = 0.03 and Loc 7 = 0.07). Consequently, the Manning's n values of 0.06 and 0.08 gave the best fit to the observation data. A Manning's n coefficient of 0.08 was selected for our model runs as this value has been used widely in similar studies for saltmarsh areas and proven to be suitable for approximating the roughness of saltmarsh surfaces (Loder et al., 2009; Stark et al., 2016; Temmerman et al., 2012). To account for the bottom roughness of other surface cover classes present in the model domain, Manning's n coefficients for additional types of surface covers were assigned as follows: tidal flat (0.03), open water (0.02) and pasture (0.06). These values have been shown to be suitable for representing the drag forces of rough surfaces in a range of hydrodynamic model applications (Garzon and Ferreira, 2016; Hossain et al., 2009; Lawrence et al., 2004; Liu et al., 2013; Smolders et al., 2015; Stark et al., 2016; Temmerman et al., 2012; Wamsley et al., 2010, 2009).

Validation was performed by comparing modelled and measured water depths at three additional locations (Loc 2, Loc 11 and Loc 14) (Figure 4.1, Table 4.1). Model validation (based on $\mathrm{MAE_{HWL}}$) confirmed that water depths were well represented by the model across the site. The model outputs showed a phase shift of typically 10 min, and a maximum of 20 min. We therefore applied a constant correction of 10 min.

Table 4.1 Results of model validation at three locations. Error measurements represent the difference between modelled and measured water depths.

	RMSE (m)	**ME (m)**	**MAE (m)**	**$\mathrm{RMSE_{HWL}}$ (m)**	**$\mathrm{MAE_{HWL}}$ (m)**	**Mean $\mathrm{MAE_{HWL}}$ (m)**
Loc 2	0.060	–0.030	0.050	0.060	0.040	
Loc 11	0.050	0.0200	0.030	0.030	0.030	0.030
Loc 14	0.060	0.030	0.030	0.020	0.020	

We used bed shear stress as an indicator for expected morphological adjustments, which are triggered by changes in scheme design and used the status quo to assess the validity of this approach. We looked at the difference between two LiDAR derived DEMs of Freiston Shore (both provided by the EA) from the years 2002 (the year of

the original breach) and 2016, in order to assess areas within Freiston Shore, which have accreted or were eroded in the respective period. In a next step, we compared the morphologic evolution of the MR to the spatial distribution of bed shear stress. This comparison shows that, in accordance with the spatial distribution of bed shear stress, morphological change has mostly focussed around the breaches, within, and next to, the artificial tidal creeks (Appendix A, Figure A.1).

4.2.4 Scheme design scenarios

In order to investigate whether changing the design of the Freiston Shore MR site would affect HWL attenuations, the scheme design was artificially changed by manipulating both the dike and breach topography in the model grid.

For this analysis a baseline scenario (status quo) was modelled, which represents the original implemented scheme. Additionally, six MR site modifications were applied, based on the most commonly used MR designs for the purpose of coastal protection in the UK: entire bank removal (Scenario 1), single breach design (Scenarios 2.1, 2.2 and 2.3) and schemes with more than two breaches (Scenarios 3.1 and 3.2) (Figure 4.2). The site design characteristics of each scenario are displayed in Table 4.2. We tested multiple variations in width of the central breach within the single breach designs (Scenarios 2.1, 2.2, 2.3), ranging from 30 m to 99 m. The latter breach width was implemented to account for any potential breach widening consequent upon changes in site hydrodynamics (Friess et al., 2014; Symonds and Collins, 2007b). Additionally, two variations in MR area for schemes with two or more breaches were tested (Scenario 3.1 and 3.2) to study the influence of site size on HWL attenuation (Table 4.2). For these scenarios, the storage area of the Freiston Shore MR site was increased by 118 % and 73 % for Scenario 3.1 and 3.2, respectively (Table 4.2, Figure 4.2).

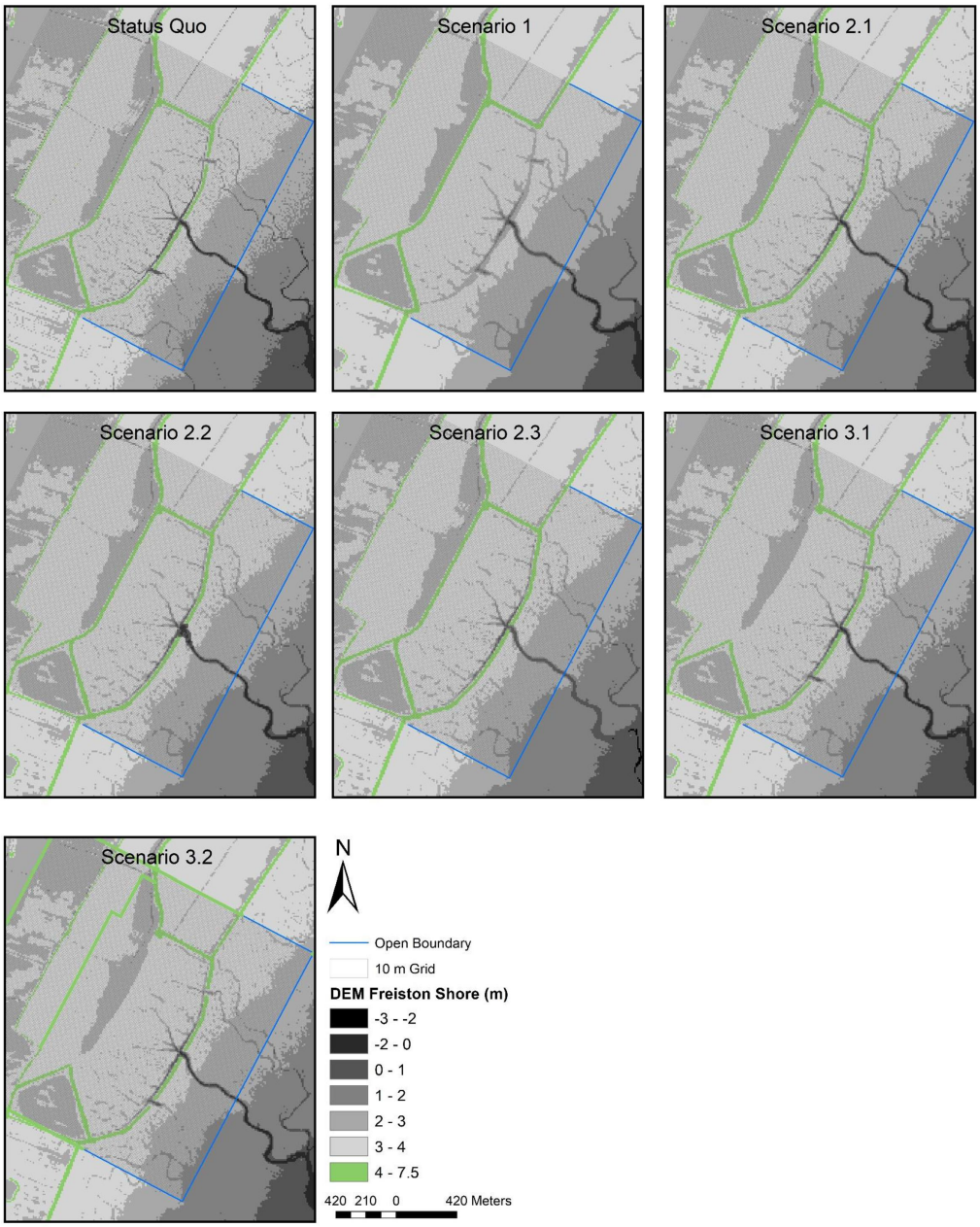

Figure 4.2 Scheme design scenarios at the Freiston Shore MR site. The status quo constitutes the baseline scenario to which other models were compared. Scenario 1 represents a scheme design where the entire seawall has been removed. Scenario 2.1 depicts an alternative option with only one breach, while Scenario 2.2 constitutes a single breach scenario with an enlarged centre breach, accounting for expected morphologic adjustments. In Scenario 2.3, the centre breach is decreased in size, in order to test the effects of a decreased tidal prism. In Scenario 3.1, the MR is significantly increased in size by removing the landward seawall to the back of the site. Scenario 3.2 is similar to Scenario 3.1, but characterised by a slightly smaller area. See Table 4.2 for further details.

Table 4.2 Number of breaches, total breach width and area for every MR scheme design scenario including the status quo.

	Status Quo	**Scenario 1**	**Scenario 2.1**	**Scenario 2.2**	**Scenario 2.3**	**Scenario 3.1**	**Scenario 3.2**
number of breaches	3	1	1	1	1	3	3
total breach width (m)	127	1475	45	99	30	127	127
MR area (m^2)	650,067	650,067	650,067	650,067	650,067	1,416,350	1,124,400

4.2.5 Calculation of HWL attenuation rates, tidal prism and bed shear stress

HWL attenuation rates (cm km^{-1}) were calculated from the vertical difference in water level (elevation based on bathymetry (see Table 4.3) + water depth) between two observation points (termed hereafter as transect) and the measured horizontal distance (m) between the two sensors. The following transects were assessed: Loc 13–1, Loc 3–1, Loc 2–1, Loc 11–1, Loc 8–15, Loc 6–15, Loc 16–14, and Loc 9–14 (Figure 4.1). In order to assess the coastal protection function of the Freiston Shore MR site and the tested scenarios, we calculated HWL attenuation over transects, which range from the breached seaward dike to the reinforced landward dike (Loc 3–1, Loc 6–15 and Loc 9–14). We additionally measured five transects from inside the MR to the landward seawall (Loc 13–1, Loc 2–1, Loc 11–1, Loc 8–15 and Loc 16–14). Positive rates refer to HWL attenuation, while negative values correspond to an amplification of HWLs along the respective transect (Kiesel et al., 2019).

The tidal prism (m^3) for each scenario was assessed by calculating the volume of water between average high and low water level within the MR during the measurement period. We used mean low water level and not just the marsh's surface elevation to

Table 4.3 Name, location and elevation of observation points used in our model application. Elevation was extracted from the model bathymetry and the coordinates are given in British National Grid coordinate system.

Sensor	Latitude	Longitude	Elevation based on model bathymetry (m ODN)
Loc 1	540,728	343,438	3.48
Loc 2	541,059	343,229	3.23
Loc 3	541,154	343,281	3.4
Loc 6	541,044	342,920	3.39
Loc 7	540,544	342,144	3.13
Loc 8	540,949	343,061	3.24
Loc 9	540,518	342,202	3.54
Loc 11	540,799	343,378	3.29
Loc 12	540,768	343,405	3.32
Loc 13	541,076	343,390	3.1
Loc 14	540,205	342,594	3.32
Loc 15	540,590	343,239	3.32
Loc 16	540,503	342,494	3.04

calculate the tidal prism, because tidal creeks and depressions inside the MR always retained some water, even during low tide.

Bed shear stress was extracted from the model results for each cell and each time step. Afterwards, we averaged bed shear stress for every grid cell by exclusively taking periods of inundation into account.

4.2.6 Statistical analyses

Since the data was neither normally distributed (Shapiro Wilk pvalue < 0.0005) nor homoscedastic (Bartlett p-value < 0.0005), the non-parametric One-Way Wilcoxon rank sum test and a Mann Whitney U test were used for statistical analysis. The latter was used to test the hypothesis (H_0) that HWL attenuation rates of every scenario were not significantly different from the status quo. The One-Way Wilcoxon

rank sum test was used to investigate the hypothesis (H_0) that HWL attenuation rates were not significantly different from zero.

4.3 Results

4.3.1 The effects of MR scheme design on HWL attenuation

To determine the overall effect of the MR on mean HWL attenuation rates for every scenario, we first averaged attenuation rates over all measured transects and all high water events. Hereafter, positive rates refer to the attenuation of HWLs, while negative values show that HWLs were amplified.

Our results reveal statistically significant effects of the Freiston Shore MR scheme design on HWL attenuation rates. HWL attenuation rates in all scenarios were significantly different from zero and, besides Scenario 1, all scenarios were significantly different from the status quo (Figure 4.3, Table 4.4).

Table 4.4 Mean HWL attenuation rates, tidal prism and area for every scheme scenario including status quo. Standard deviations as well as p-values for the respective statistical tests are shown.

	Status Quo	**Scenario 1**	**Scenario 2.1**	**Scenario 2.2**	**Scenario 2.3**	**Scenario 3.1**	**Scenario 3.2**
Mean attenuation (cm km^{-1})	–1	–1	4	2	6	16	11
Standard deviation (cm km^{-1})	3	1	7	5	8	11	12
One-Way Wilcoxon rank sum test (p-values)	0.002	<0.0005	<0.0005	<0.0005	<0.0005	<0.0005	<0.0005
Mann Whitney *U* test (p-values)	/	0.5	<0.0005	<0.0005	<0.0005	<0.0005	<0.0005
Tidal prism (m^3)	296,891	307,435	263,762	270,122	256,034	498,752	420,997
Area (m^2)	650,067	650,067	650,067	650,067	650,067	1,416,350	1,124,400

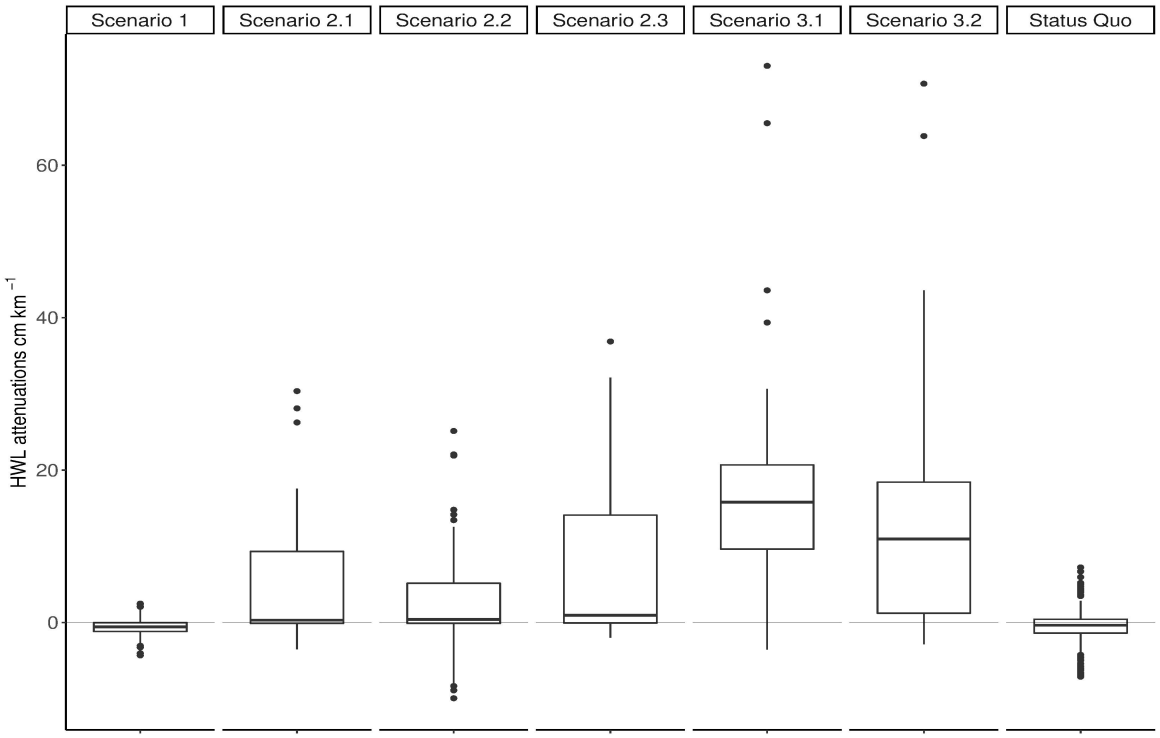

Figure 4.3 HWL attenuation rates for all tested scheme design scenarios. Every boxplot represents the variation of HWL attenuation rates over all transects and all high water events of the respective scenario. The bottom and top ends of the box refer to the 25^{th} and 75^{th} percentile and the centreline constitutes the median. Both whiskers are calculated as the upper and lower boundary of the box + 1.5 * the interquartile range. Data points, which did not fall within this range, are plotted as outliers.

While the status quo and Scenario 1 produced average attenuation rates of –1 cm km^{-1}, indicating the amplification of HWLs, all other scenarios produced average HWL attenuation, even though their minimum values reveal occasional amplification of HWLs (Figure 4.3). HWL attenuation rates were highest for those scenarios where the three breaches remained intact and the MR area was substantially increased (Scenarios 3.1 and 3.2). Scenario 3.1 exhibited the highest attenuation rates reaching up to 73 cm km^{-1}.

The comparison of HWL attenuation rates between individual transects shows no distinct spatial trends and great variability across the MR in Scenario 1 and the status quo (Figure 4.4). However, spatial patterns can be observed for Scenarios 2 and 3. In Scenarios 2.1, 2.2 and 2.3 we found above average attenuation rates for transects Loc

3–1, Loc 6–15 and Loc 9–14. In contrast to the other transects, these were measured starting from in front of the old and breached dike. This trend is also evident in Scenarios 3.1 and 3.2, but less distinct. In Scenario 3.1 and 3.2, comparatively low attenuation rates were assessed for transect Loc 16–14.

4.3.2 Correlation of HWL attenuation with Mean High Water Depth (MHWD)

All scenarios, as well as the status quo, differ in terms of tidal prism (Table 4.4). The latter is determined by MR area and breach design. Variations in both parameters determine the MHWD in each scenario, which is described by

$$\text{MHWD} = TP/A \tag{4.1}$$

where TP refers to the site's tidal prism (m^3) and A to MR area (m^2). Our results indicate the dependency of HWL attenuation rates on MHWD, as a significantly negative correlation (p-value of polynomial model < 0.0005) was found across all scenarios (Figure 4.5).

Similarly, we found significant correlations (described by polynomial functions) between average HWL attenuation and mean high water depth of each individual high water event within each scenario (Figure 4.6). The threshold, which divides between attenuation and amplification, is very different between scenarios. While for the status quo the threshold is approximately 0.4 m of mean high water depth, it increases by more than two-fold for scenarios 2.1, 2.2 and 3.2. For scenarios 2.3 and 3.1, the threshold water depth was not reached during the measurement period.

4.3.3 Bed shear stress

Our results show that areas of comparatively high bed shear stress are in all scenario families mostly concentrated around the breaches. In Scenario 1 bed shear stress is

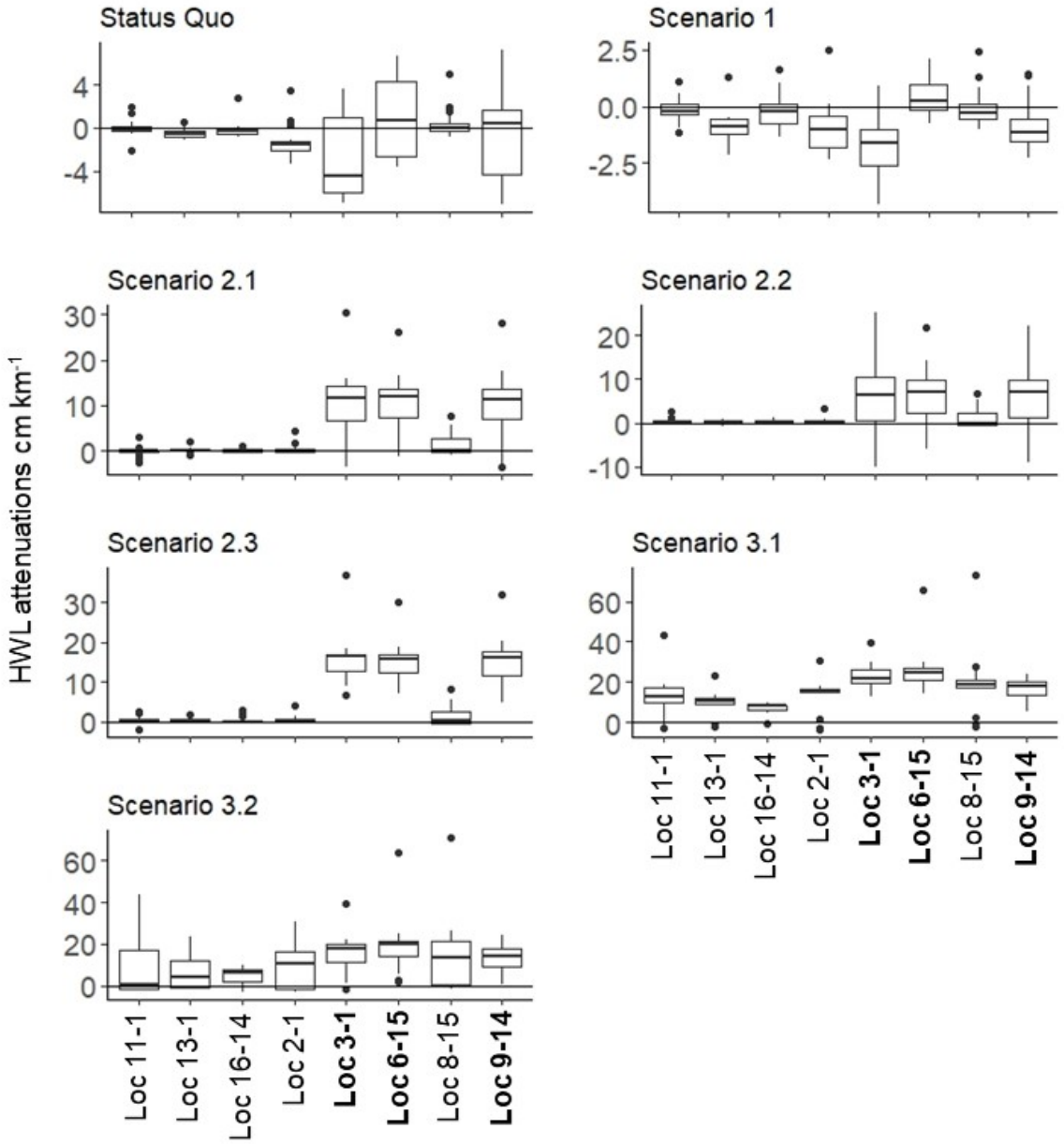

Figure 4.4 HWL attenuation rates for every transect of each scenario. Every boxplot represents the variation of HWL attenuation rates over all high water events of the respective scenario. Note that the y-axes vary in scale in order to enhance readability. Transects written in bold letters on the x-axes range from outside the breached seaward seawall to the new landward seawall. The bottom and top ends of the box refer to the 25^{th} and 75^{th} percentile and the centreline constitutes the median. Both whiskers are calculated as the upper and lower boundary of the box + 1.5 * the interquartile range. Data points, which did not fall within this range, are plotted as outliers.

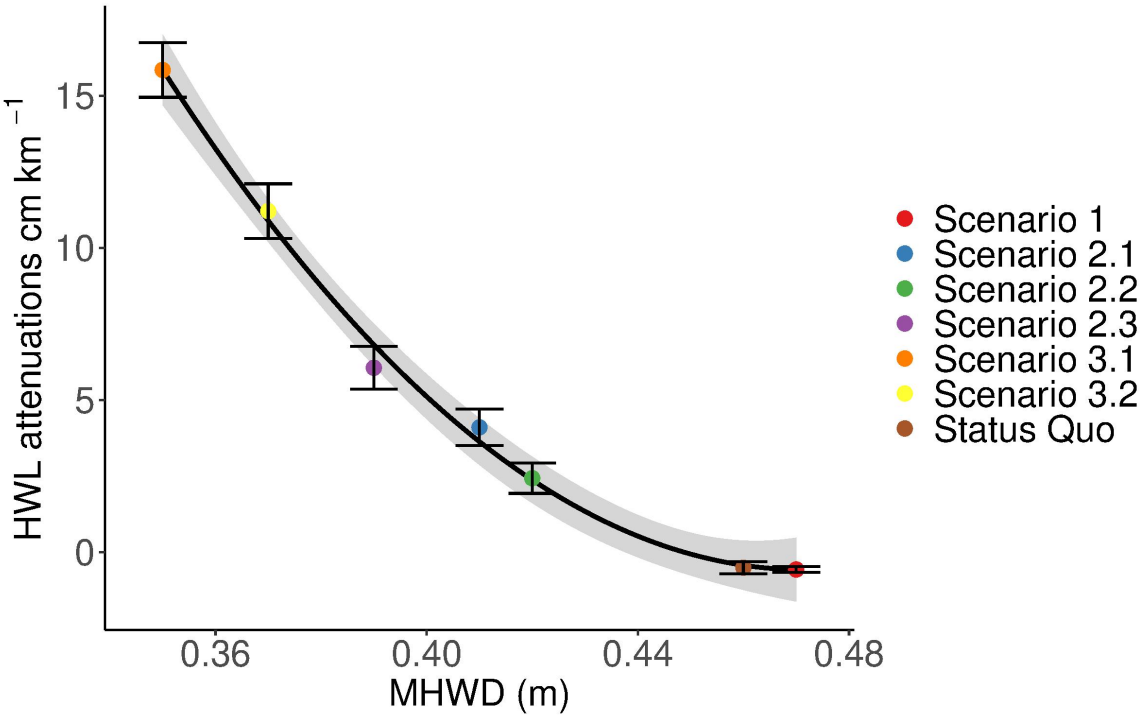

Figure 4.5 The correlation between mean HWL attenuation of each scenario and MHWD. The error bars show the standard error of the mean and the shaded area around the polynomial model indicates the 95 % confidence interval. Formula: y = 5.5—14 x + 4.3 x^2; R^2 = 0.996; adjusted R^2 = 0.994; p < 0.0005.

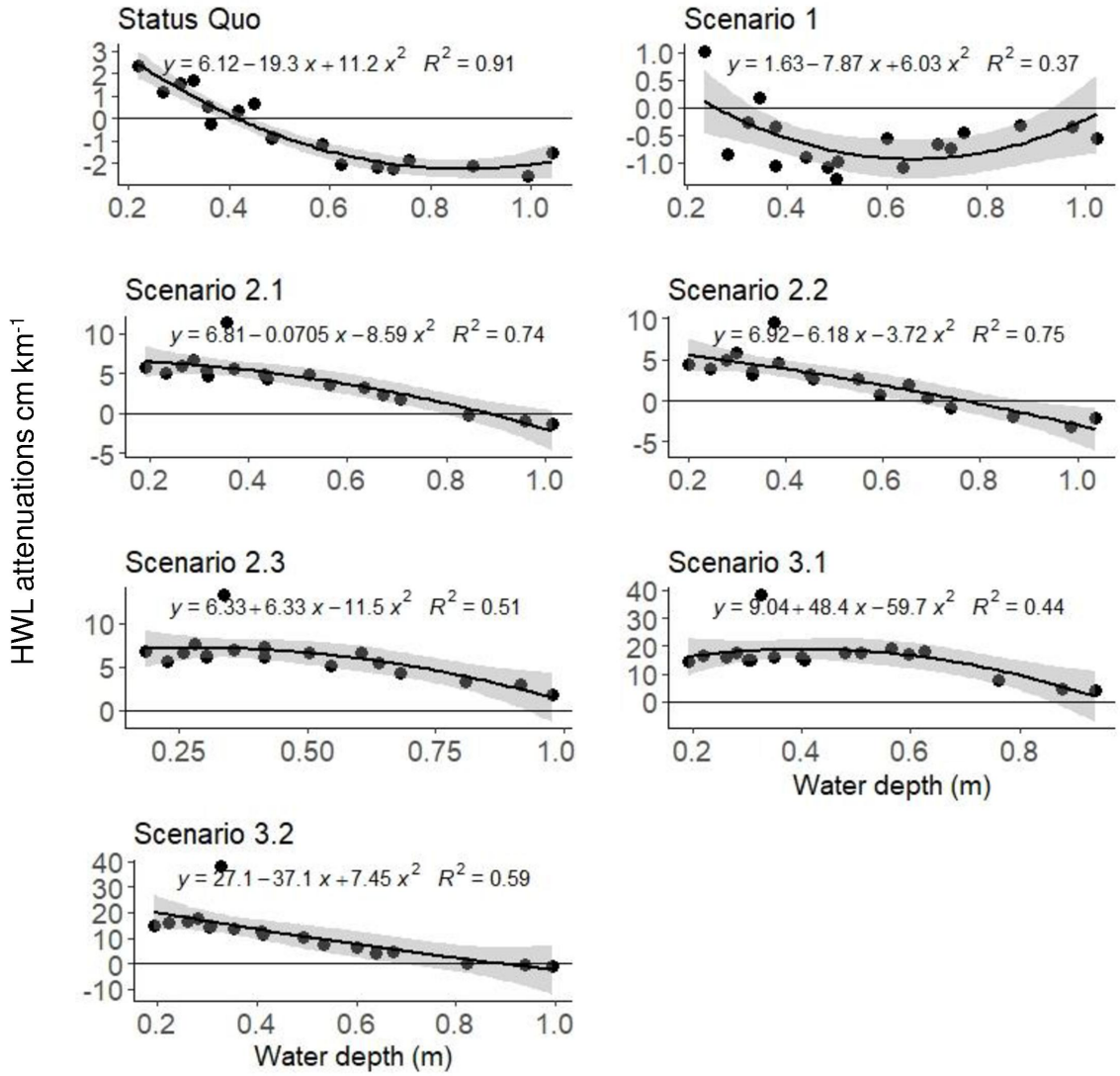

Figure 4.6 Correlation between average HWL attenuation and mean high water depth. HWL attenuation has been averaged for every individual high water event during the simulated period by using all available transects. Mean high water depth has been calculated for every high water event and over all observation points within each MR scenario. The shaded area around the polynomial model represents the 95 % confidence interval.

extensively spread along the removed seawall (Figure 4.7).

In Scenario 2.1, the highest values of bed shear stress are concentrated around the central breach, whereas areas to the back of the site, including the northern and south-western parts, are characterised by comparatively low bed shear stress. In Scenario 3.1, high values of bed shear stress also concentrate around the three breaches, but in comparison to Scenarios 1 and 2.1, they are more scattered towards the northwest of the site, where the landward seawall has been removed.

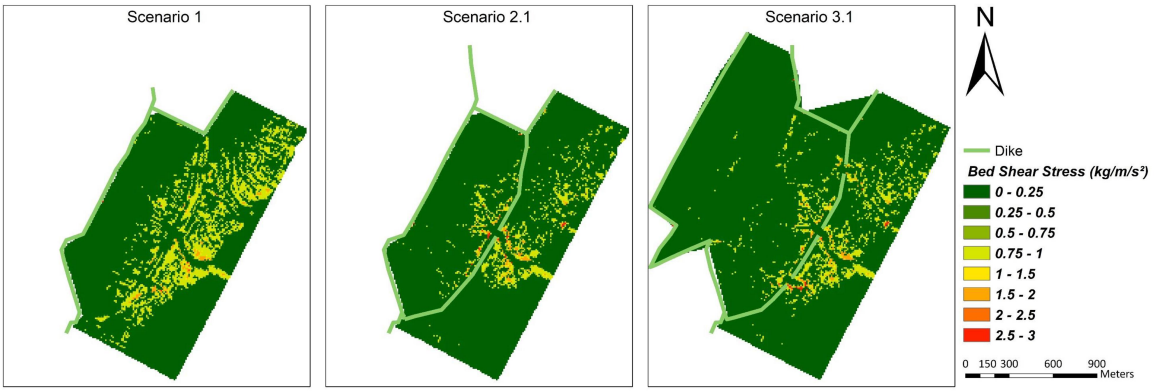

Figure 4.7 Bed shear stress within the three scenario families. Bed shear stress was averaged over the study period, excluding times when the site was not flooded.

4.4 Discussion

4.4.1 Implications for MR scheme design

Storage area and breach design of the Freiston Shore MR site have had a significant effect on the site's HWL attenuation capacity. Furthermore, HWL attenuation was affected by variations in breach design. For example, when the storage area of the Freiston Shore MR site was kept constant (as in Scenario 1, 2.1, 2.2, 2.3 and the

status quo), modelled HWL attenuation rates increased with decreasing tidal prism. In these scenarios, the tidal prism was controlled by changing the number and the widths of the breaches. However, our results show that effective coastal protection in terms of higher HWL attenuation rates (i. e. > 10 cm km^{-1}) can only be obtained if the MR area is of sufficient size. The maximum modelled HWL attenuation rates were observed for Scenarios 3.1 and 3.2 (up to 73 cm km^{-1}), which contained the largest storage areas and consequently exhibited the largest tidal prisms. Stark et al. (2015) measured comparable maximum HWL attenuation rates (up to 70 cm km^{-1}) over short transects in the extensive natural Saeftinghe marsh in the Western Scheldt estuary (Netherlands). We note, however, that a larger MR surface area provides also more space for wind waves to develop within the scheme, which may affect the development of vegetation, sedimentation patterns and ultimately, hydrodynamics (Nottage and Robertson, 2005).

Scenario 3.1 and 3.2 produced the highest attenuation rates because of their association with the lowest MHWD. This relationship helped explain most of the variation in mean HWL attenuations across scenarios, which was also observed for each scenario individually (Figure 4.5, Figure 4.6). However, previous studies have shown that also MR site orientation, meteorological conditions, vegetation characteristics and local tidal regime are important drivers of HWL attenuation (Kiesel et al., 2019; Paquier et al., 2017; Resio and Westerink, 2008; Sheng et al., 2012; Stark et al., 2015; Wamsley et al., 2009, 2010). This hinders the extrapolation of HWL attenuation rates, measured at a given study site for a specific range of high water events and meteorological conditions, to other MR sites. The diverse driving forces of HWL attenuation help explaining why flood level reduction is highly variable between wetlands, specific wetland locations as well as individual high water events (Temmerman et al., 2012). This variability may be reflected in weaker correlations between HWL attenuation and the mean high water depth of each high water event (Figure 4.6), compared to the overall trend (Figure 4.5).

We hypothesize that the close coupling between MHWD and HWL attenuation suggested by this study may vary depending on whether MR sites or natural marshes are considered. For example, this study suggests that scheme scenarios with MHWDs of approximately > 0.4 m (status quo and Scenario 1) may already result in overall HWL amplification. This finding raises two major issues: i) problematically, HWL attenuation is particularly important when inundation depths are well above 0.4 m, for example during storm surge conditions; and ii) Stark et al. (2015), analysing field data, showed that for the extensive (natural) Saeftinghe marsh along the Western Scheldt estuary (Netherlands), HWL attenuation rates peaked during inundation depths ranging between 0.5 and 1 m. The latter provides reference that MR schemes (15 years of age) may not be as effective as natural marshes when it comes to the magnitude of HWL attenuation.

Consequently, future MR design needs to account for the altered correlation between MHWD and HWL attenuation within MR schemes and for the strong internal dynamics in attenuation rates. The former may enable the optimization of MR scheme designs for the purpose of "*within-wetland*" (Smolders et al., 2015) attenuation and thus, coastal protection. By measuring water depth as a function of MR area and local tidal prism, the usage of MHWD may help estimate the HWL attenuation potential of existing MR sites. This could enable the identification of sites with low or even negative HWL attenuation potential. For such sites, it could be possible to retro-fit an improved scheme design, by managing the site's tidal prism and/or the number, and width/s, of seawall breaches.

Breach design can be essential for coastal protection. Across most scenarios (all but Scenario 1), median and/or maximum HWL attenuation rates were highest for transects, which were measured from in front of the breached seawall (Figure 4.4). For sites with a bank removal design, the approach to retro-fit an improved scheme design may, however, come too late.

At Freiston Shore, breach width and depth was, in the early stages of site evolution, de-

pendent on the local tidal prism. This explains why after site implementation, breach channels increased in width by up to 950 % within only 2.5 month and shows that if breaches are designed with a cross sectional area insufficient to accommodate the tidal exchange, they are very likely to erode (Friess et al., 2014; Townend et al., 2016; Vandenbruwaene et al., 2015). This means that the breach design is restricted by local environmental circumstances.

However, such adverse effects could be prevented for sites, where the tidal prism is managed via regulated tidal exchange (21 of 74 UK MR sites) (ABPmer, 2019). In the UK, regulated tidal exchange is usually not implemented for the purpose of coastal protection but, according to our results, it may yet prove to be efficient in terms of HWL attenuation. However, regulated tidal exchange may only offer a degree of control as the effects of meteorological conditions acting on an enclosed body of water could still lead to adverse internal hydrodynamics and HWL amplification (Kiesel et al., 2019).

Our findings emphasise the importance of breach design and regulated tidal exchange for MR implementation. In contrast to bank removal (Scenario 1), breach design enables, even if only to a limited extent, the regulation of the site's tidal prism and consequently, inundation depths, which in turn determine the degree to which HWLs are attenuated within the MR site. Furthermore, the remaining structure maintains a certain degree of protection for the restored saltmarsh within the MR, leading to increased HWL attenuation rates (Figure 4.4), reduced erosional effects of storm waves and tidal currents and enhanced sedimentation. This may also be true for sites managed through Regulated Tidal Exchange (RTE), as defences are maintained and flow into the restoration site is controlled via culverts and sluices (Cox et al., 2006; Esteves, 2014).

4.4.2 Considerations on the effects of site topography on modelled HWL attenuations

In this paper, we evaluate the model results of each scenario based on the original topography of the Freiston Shore MR site in 2016 (represented by a LiDAR derived digital elevation model from 2016). We acknowledge that the morphology within each of the scheme design scenarios would develop differently compared to the status quo, as tidal prism and related hydrodynamics determine within-site sedimentation (Dale et al., 2017). This is indicated by the spatial distribution of bed shear stress within the three scenario families (Figure 4.7). Changes in marsh topography might be particularly expected for tidal channel geometry, as the latter is a function of the tidal prism (Friess et al., 2014). Marsh topography in terms of surface elevation and presence of tidal creeks affect HWL attenuation (Loder et al., 2009; Stark et al., 2016; Temmerman et al., 2012), which is why we expect HWL attenuation rates to change over time in each of the scenarios.

The morphological evolution of MR sites can therefore be critical to the coastal protection function in the long-term. Stark et al. (2016) suggest that saltmarshes dominated by highly channelized flow provide less attenuation compared to marshes, which are dominated by sheet flow. It is therefore reasonable to assume that HWL attenuation rates presented for scenarios 3.1 and 3.2 are overestimated, as the newly created saltmarsh area to the back of the site would develop tidal creeks in order to drain and those creeks near the breaches would further expand in order to accommodate the increased tidal prism (Figure 4.7). Unlike Scenarios 3.1 and 3.2, we assume that HWL attenuation rates are underestimated for scenario family 2. In Scenario 2.1, bed shear stress is low (compared to the status quo; Figure A.1, Figure 4.7) in the northern and south-western parts. We would therefore assume the tidal creeks in these areas to fill up with sediments over time, resulting in increased sheet flow and ultimately, increased HWL attenuation rates for transects Loc 11–1, Loc 13–1, Loc 16–14, Loc

2–1 and Loc 8–15. On the other hand, we found HWL attenuations to be exceptionally high for transects Loc 3–1, Loc 6–15 and Loc 9–14 (reaching from in front of the breached dike to the landward dike). Due to exceptionally high loads of bed shear stress within and next to the breaches of all scenarios (and particularly in the remaining central breach for scenario family 2), these transects will be most affected by expected changes in channel morphology such as deepening and erosion and are thus likely to be overestimated as well.

4.4.3 Model reproduces water depths but not variability in HWL attenuations

The model is well suited for the reproduction of measured water depths at several locations (Table 4.1). In addition, mean HWL attenuation for the status quo was found to be in the same order of magnitude between the model (–1 cm km^{-1}) and the field survey (–3 cm km^{-1}) (Kiesel et al., 2019).

However, the exceptional variability of HWL attenuation rates measured inside the MR during the original field survey (Standard Deviation (STD): 40 cm km^{-1}) could not be reproduced by the model application (STD: 3 cm km^{-1}). The reasons for this discrepancy may involve the following four aspects: 1) the transects over which HWL attenuations were measured differed between the original field survey and this modelling study. 2) Uniform Manning's n coefficients were used for all vegetated surfaces, even though vegetation types assessed in the field revealed considerable variations and 3), due to the use of averaged bathymetry and elevation data (10 x 10 m), the model exhibited reduced topographic complexity. Furthermore, the reduced variability within the model may be ascribed to 4) differences in elevation measurements at the pressure sensor locations.

The elevation measurements in the field (Leica Viva GS08 GNSS satellite survey Real Time Kinematic (RTK)) are associated with an accuracy of up to 50 mm, but typically below 20 mm (Kiesel et al., 2019). The bathymetry for the model presented in this

study was derived from a 2 x 2 m LiDAR Digital Elevation Model (DEM) measured in 2016 (provided by the EA) and provided a vertical accuracy of ±20 cm. In fact, this study found a systematic elevation difference between the 10 x 10 m model bathymetry and the RTK measurements of, on average, 0.47 m. Model bathymetry elevations were consistently higher than the RTK measurements. It is known that due to the dense and low vegetation within saltmarshes, LiDAR systems can fail to distinguish centimetre-scale variations between the vegetation canopy (digital surface model) and the bare ground (digital terrain model) (Hopkinson et al., 2004; Schmid et al., 2011). Schmid et al. (2011) ascribed this problem to the poor penetration of the laser pulse through the marsh vegetation, which may result in digital terrain models to be less accurate and significantly varying between different surface types. This effect may be amplified by the high spatial heterogeneity of vegetation and topographic features (Fernandez-Nunez et al., 2017).

This deviation can have a large effects on the calculation of HWL attenuation rates, particularly over shorter marsh transects (Kiesel et al., 2019). The identified differences in elevation measurements underline the difficulties that marsh vegetation and small scale topographic variations pose on the derivation of elevation and bathymetry data. The identified differences in elevation measurements highlight the importance of high-resolution input data for the application of hydrodynamic models in coastal protection studies. This may even be valid for areas with comparatively good data coverage, such as Freiston Shore.

4.5 Conclusions

MR schemes are generally designed based on well-established relationships between scheme design (e.g. surface area, breach dimensions/number and tidal prism) and hydrodynamic processes. The dependency of HWL attenuation on MR scheme design in this study has shown that these relationships do not necessarily predict HWL

attenuation rates several years after breaching, particularly if site morphology and associated hydrodynamics change over time. We therefore stress the need for continued monitoring efforts in MR schemes.

We show that HWL attenuation is strongly dependent on within-site MHWD. The latter correlation is not only a function of the well established relationship between water depth, surface roughness and HWL attenuation but also incorporates the parameters of tidal prism and MR site area. Thus, once the available area for a MR site is known, the width(s) of the seawall breach(es) can be designed in order to accommodate a tidal prism, which leads to the lowest possible MHWDs.

We suggest that breach design and regulated tidal exchange should be the preferred design options for MR sites that are implemented for the purpose of coastal protection. The reason is that both enable controlling the tidal prism (and consequently inundation depths) and because the breached seawall may additionally enhance HWL attenuation rates.

We also show that our hydrodynamic model application may not be able to capture the within-site dynamics of HWL attenuation. It is important to account for these dynamics, particularly when the protection standard of new seawalls at the landward margins of MR sites need to be determined. For now, the prediction of the effects of meteorological conditions and extreme events on the relationship between MHWD and HWL attenuation is not fully understood. There is an urgent need for further field investigations of water level dynamics within MR sites, particularly under storm surge conditions.

4.6 Declaration of competing interests

The authors declare that they have no known competing financial interests or personal relationships that could have appeared to influence the work reported in this paper.

4.7 CRediT authorship contribution statement

Joshua Kiesel: Conceptualization, Methodology, Formal analysis, Investigation, Writing - original draft, Visualization. Mark Schuerch: Conceptualization, Writing - review & editing, Supervision, Project administration. Elizabeth K. Christie: Methodology, Writing - review & editing. Iris Moeller: Writing - review & editing, Supervision. Tom Spencer: Writing - review & editing, Supervision. Athanasios T. Vafeidis: Conceptualization, Resources, Writing - review & editing, Supervision, Project administration.

4.8 Acknowledgements

The work presented in this paper is based on field data obtained during JK's research stay at the Department of Geography's Visiting Scholar programme of the University of Cambridge. JK particularly thanks B. Evans (Cambridge Coastal Research Unit) for technical and field assistance. Furthermore, JK thanks Pushpa Dissanayake for his helpful introduction to the Delft3D modelling environment and the Integrated School of Ocean Science as part of the Future Ocean Excellence Cluster (University of Kiel) for funding the original field campaign. The authors thank the EA, for the supply of vertical aerial photography, LiDAR data and for their fast and helpful responses to our requests regarding the data. Furthermore, the authors would like to thank Deltares Delft Hydraulics for providing the Delft3DFLOW model. This is a contribution towards UKRI NERC BLUECoast project (NE/N015878/1).

Chapter 5

Can managed realignment buffer extreme surges? The relationship between marsh width, vegetation cover and surge attenuation

Joshua Kiesel, Leigh R. MacPherson, Mark Schuerch, Athanasios T. Vafeidis [1]

[1]This chapter is published as: Kiesel, J., McPherson, L. R., Schuerch, M., and Vafeidis, A. T.: Can managed realignment buffer extreme surges? The relationship between marsh width, vegetation cover and surge attenuation, Estuaries and Coasts, https://doi.org/10.1007/s12237-021-00984-5, 2021

Abstract

Managed Realignment (MR) involves the landward relocation of sea defences to foster the (re)creation of coastal wetlands and achieve nature-based coastal protection. The wider application of MR is impeded by knowledge gaps related to lacking data on its effectiveness under extreme surges and the role of changes in vegetation cover, for example due to sea-level rise. We employ a calibrated and validated hydrodynamic model to explore relationships between surge attenuation, MR width(/area) and vegetation cover for the MR site of Freiston Shore, United Kingdom (UK). We model a range of extreme water levels for four scenarios of variable MR width. We further assess the effects of reduced vegetation cover for the actual MR site and for the scenario of the site with the largest width. We show that surges are amplified for all but the largest two site scenarios, suggesting that increasing MR width results in higher attenuation rates. Substantial surge attenuation (up to 18 cm km^{-1}) is only achieved for the largest site. The greatest contribution to the attenuation in the largest site scenario may come from water being reflected from the breached dike. While vegetation cover has no statistically significant effect on surge attenuations in the original MR site, higher coverage leads to higher attenuation rates in the largest site scenario. We conclude that at the open coast, only large MR sites ($>$ 1148 m width) can attenuate surges with return periods $>$ 10 years, while increased vegetation cover and larger MR widths enable the attenuation of even higher surges.

5.1 Introduction

The combination of accelerated sea-level rise (Dangendorf et al., 2019; Nerem et al., 2018) and projected increases in episodic flooding, particularly in regional hotspots such as north western Europe (Kirezci et al., 2020), is expected to lead to increased flood risk for low lying coasts and higher adaptation costs (Hinkel et al., 2014). Problematically, conventional protection measures such as dikes and seawalls are challenged by rising maintenance costs and ecologically disadvantageous side effects such as limited accommodation space due to coastal squeeze (Temmerman et al., 2013; Doody, 2004; Schuerch et al., 2018).

The availability of accommodation space that allows for wetland inland migration will determine the survival of global coastal wetlands over the 21st century. Traditional hold-the-line approaches for adaptation to rising sea levels and associated flooding limit accommodation space and can lead to large scale losses of coastal wetlands. Such losses may therefore be prevented by changing adaptation practices towards nature-based solutions (Spencer et al., 2016; Schuerch et al., 2018).

Nature-based coastal adaptation can provide a cost-effective alternative (Reguero et al., 2018) or complement conventional coastal defence schemes, as studies from the United Kingdom (UK) and the Scheldt estuary (Belgium) have shown (Turner et al., 2007; Broekx et al., 2011). Such practices additionally involve the creation or restoration of coastal wetlands such as saltmarshes (Temmerman et al., 2013), which can substantially reduce flood impacts (Barbier et al., 2013) and at the same time contribute to the conservation and restoration of biodiversity and more natural shorelines.

Two options are regularly implemented in Europe, Managed Realignment (MR) and Regulated Tidal Exchange (RTE) (ABPmer, 2021). RTE constitutes a more controlled way of re-establishing tidal exchange, by fully maintaining the first dikeline and applying water control structures such as sluices, culverts or tide gates (Oosterlee et al., 2020; Cox et al., 2006). Here, we focus on managed realignment, which aims at the re-establishment of coastal ecosystems to sustainably manage flood and erosion risks (Esteves, 2013). MR constitutes the relocation of sea defences to more landward positions, followed by the breaching or removal of the old, seaward line of defence (French, 2006). A detailed description of various MR types is given in Esteves (2014), but they all involve the breaching of existing defences to re-establish tidal exchange.

Using saltmarshes as a buffer zone for preventing low lying coastal areas from flooding is based on evidence from a multitude of studies, which show the potential of vegetated surfaces to provide High Water Level (HWL) (Paquier et al., 2017; Sheng et al., 2012; Smolders et al., 2015; Stark et al., 2015, 2016; Wamsley et al., 2010) and wave attenuation (Möller and Spencer, 2002; Möller et al., 2014; Rupprecht et al., 2017).

According to Smolders et al. (2015), HWL attenuation can be distinguished between *within-wetland* attenuation and *along-estuary* attenuation. The latter refers to the contribution of estuarine intertidal areas to reduce the height of storm surges that propagate upstream along an estuary, which is also referred to as water retention or flood water storage (Hofstede, 2019; Oosterlee et al., 2020; Cox et al., 2006; Smolders et al., 2015). *Within-wetland* attenuation occurs over the wetland itself, due to shallow water depths and the resistance of vegetation (Stark et al., 2015, 2016; Temmerman et al., 2012; Loder et al., 2009; Wamsley et al., 2010, 2009). Several studies provide HWL attenuation rates in the range of 4 cm km^{-1} (Lovelace, 1994; McGee et al., 2006; Wamsley et al., 2010) to 25 cm km^{-1} (McGee et al., 2006; Wamsley et al., 2010), all of which were measured over several kilometres. These rates clarify that marshes of $>$ 1 km width are required for the provision of effective *within-wetland* attenuation.

Among the drivers of HWL attenuation are the characteristics of the surge (Resio and Westerink, 2008), vegetation community properties (Temmerman et al., 2012; Barbier et al., 2013), marsh topography (Loder et al., 2009) and the presence of tidal creeks (Stark et al., 2016). Stark et al. (2016) found that saltmarshes dominated by channelized flow provide less HWL attenuation compared to those governed by sheet flow, which has also been shown for mangrove ecosystems (Montgomery et al., 2018). Mean flow velocity decreases logarithmically with increasing distance from the marsh margin in the direction of the current flow (Leonard and Croft, 2006; Christiansen et al., 2000). Therefore, both *within-wetland* and *along-estuary* attenuation of HWLs should increase with larger wetland surface areas, even though *along-estuary* attenuation does not further increase above a certain threshold in site area (Smolders et al., 2015). The relationship between *within-wetland* attenuation and marsh width raises questions regarding the suitability of small wetland restoration schemes for providing HWL attenuation. Some studies suggested that the HWL attenuation potential of saltmarshes may be restricted by certain thresholds in inundation depth above the marsh platform. While Stark et al. (2015) found maximum attenuation rates for a water

depth range between 0.5 — 1.0 m, Wamsley et al. (2010) and Loder et al. (2009) show that very high storm surges may overwhelm the attenuating capacity of the ecosystem. The example of Freiston Shore, Lincolnshire, UK, suggests that the effectiveness of saltmarshes restored within the scope of MR to reduce high water levels is highly variable and may not be equivalent to adjacent natural ecosystems (Kiesel et al., 2019). This may not be surprising, as previous studies have shown that HWL attenuation rates over saltmarshes generally vary in space and time and cannot be summarised to a single reduction factor (Resio and Westerink, 2008; Reed et al., 2018). Differences in the HWL attenuation potential between natural and restored saltmarshes may originate from MR scheme design and differences in those ecosystem properties that drive their coastal protection function. These properties include, for example, vegetation characteristics (Mazik et al., 2010; Garbutt and Wolters, 2008; Mossman et al., 2012a) and topographic complexity (Lawrence et al., 2018).

Results from studies based on hydrodynamic modelling suggest that the coastal protection function of MR schemes can be improved by applying a scheme design (i.e. configuration of breaches and dikes) that aims at keeping internal water depths low, but attenuation rates > 10 cm km^{-1} are only achieved by establishing vast and wide shallow water areas (Kiesel et al., 2020). Problematically, MR sites are typically smaller than Freiston Shore (66 ha). According to the Online Managed Realignment Guide (OMREG) (ABPmer 2021), 71 % of the MR schemes registered in January 2021 across Belgium, Denmark, France, Germany, Netherlands, Spain and UK are smaller than Freiston Shore and 46 % smaller than 20 ha. Thus, the majority of MR schemes may not have the potential for effective *within-wetland* attenuation (Hofstede, 2019). We note, however, that the majority of sites smaller than Freiston Shore and smaller than 20 ha (72 % and 73 %, respectively) are located in estuarine settings and may therefore still be effective in providing *along-estuary* attenuation.

Two of the main knowledge gaps impeding the wider application of MR in coastal defence schemes are 1) missing studies on the effectivity of saltmarshes restored in the

context of MR to attenuate the most extreme events and; 2) shortage of information on long-term ecosystem dynamics under the influence of sea-level rise and more frequent flooding, which potentially lead to reduced ecosystem resilience and vegetation die-off. The latter can diminish the HWL attenuation potential of the ecosystem (Bouma et al., 2014; Wamsley et al., 2009; Temmerman et al., 2012; Barbier et al., 2013; Narayan et al., 2016). Saltmarsh vegetation may fail to establish in newly created MR schemes (Brooks et al., 2015) or die-off as a consequence of storm surges and associated wave climates (Rupprecht et al., 2017) and sea-level rise, directly followed by conversion to tidal flats (Kirwan et al., 2010; Marani et al., 2007) or ponds. Studies have indicated that the latter may result in a patchy distribution of vegetation (Schepers et al., 2020; Mariotti, 2020; Duran Vinent et al., 2021).

Here we address these knowledge gaps by studying the effectiveness of HWL attenuation over the Freiston Shore MR site under a range of extreme water levels (10-, 50-, 100-, 200- and 1000-year event) and three reduced vegetation scenarios, which assume patchy vegetation die-off. Further, we investigate thresholds to the HWL attenuation function of Freiston Shore in relation to marsh width by simulating the propagation of storm surges over four MR width scenarios. We additionally study how the largest MR width alters the relationship between extreme water level, vegetation scenarios and HWL attenuation. For this purpose, we use a hydrodynamic model of the Freiston Shore MR site, setup in Delft3D-Flow (Delft Hydraulics, 2003), which has been calibrated and validated against field measurements of the highest spring tides for the year 2017 (Kiesel et al., 2020).

5.2 Study area and methods

5.2.1 Study area

The MR site of Freiston Shore is situated in Lincolnshire, UK, at the west coast of The Wash embayment (Figure 5.1b, c), a shallow (average water depth < 10 m)

and sheltered embayment on the east coast of England. The intertidal areas of the bay comprise various habitats such as saltmarshes, sand- and mudflats (Brew and Williams, 2002). Tides in the embayment are semidiurnal and macrotidal, with neap- and spring-tide ranges of 3.5 and 6.5 m, respectively (Ke et al., 1996).

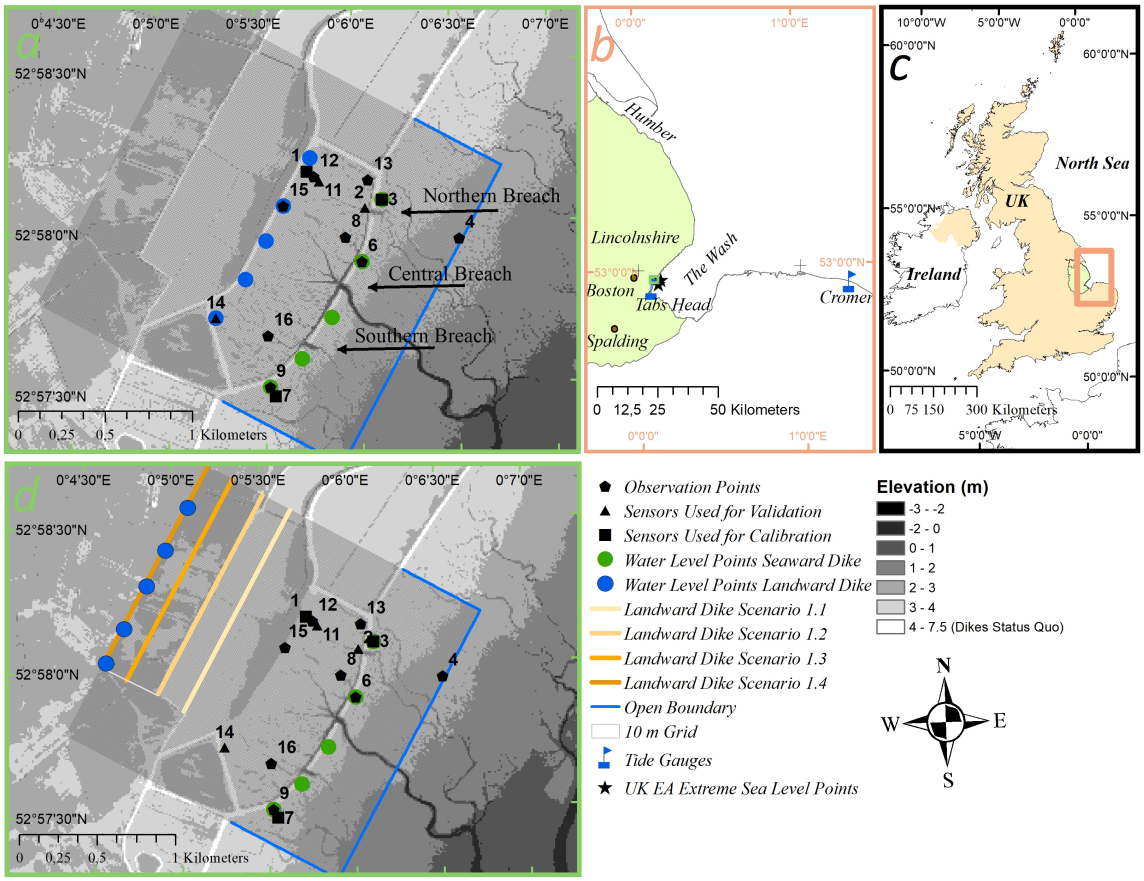

Figure 5.1 a) The model domain (indicated by 10 m grid) covers the Freiston Shore MR site, the adjacent natural marsh and neighbouring arable lands. Seaward open boundaries of the model domain (blue lines) are used to force the model with hydrographs of selected return water levels (see section 2.3). In our model application, only the eastern side was forced, while the other two were allowed to exchange water with outside the model domain. The observation points are used to calculate HWL attenuation rates within the MR site. In addition, blue dots indicate observation points in front of the landward dike and green dots are situated in front of the breached, seaward dike. b) Location of the study area in The Wash embayment (green box), location of local tide gauges and points for which extreme return water levels were available. c) Location of The Wash embayment in eastern England (orange box). d) Model setup for the four tested MR width scenarios. Note, that the landward dike of the status quo has been removed and new, artificial dikes were placed at the back of the model domain in varying distances.

The Wash has experienced numerous major storm surges in the past; the most severe occurred in 1953, resulting in the deaths of 307 people along the east coast of England (Baxter, 2005). High water levels in the south-western Wash reached 5.48 m Ordnance Datum Newlyn (ODN) (where zero m approximates mean sea level) at Haven Sluice, Boston (Figure 5.1b). The total flood damage has been estimated at £1.2 billion (equivalent for the year 2014) (Wadey et al., 2015). In 2013, the storm "Xaver" caused the highest still water levels on record at several tide gauges (Spencer et al., 2015). However, in contrast to 1953, no casualties were recorded and total flood damage costs summed up to £0.25 billion (Spencer et al., 2015). Maximum water level elevations for Lincolnshire were measured at Donna Nook, reaching 5.83 m ODN (Spencer et al., 2015).

The Wash has a long history of land reclamation and the latest dike (later also referred to as breached, seaward dike) was completed at Freiston Shore in 1982, to protect adjacent low lying fenland as well as urban and agricultural areas (Friess et al., 2012). This dike was built further into The Wash than dikes to the north and south, exposing the foot of the dike to wave attack and signs of erosion required repair and maintenance by the former owner, Her Majesty´s Prisons (Brown et al., 2007). The 1996 Shoreline Management Plan recommended realignment of the coastal stretch at Freiston Shore (Spencer et al., 2012) and in 2002, 66 ha of new intertidal and shallow water habitats were restored by breaching the seaward dike at three locations (Figure 5.1a) (Brown et al., 2007). Among the aims was the creation of a sustainable flood defence scheme through the establishment of saltmarsh (Brown et al., 2007). The final monitoring report confirmed that saltmarsh restoration was successful, as in 2007 mean total halophytic vegetation cover within the MR site was estimated at 89 % (Brown, 2008).

The analysis of a 2016 Light Detection and Ranging (LiDAR) derived Digital Elevation Model (DEM) (Environment Agency, 2020) showed that the mean elevation inside the MR was 3.04 ± 0.42 m ODN (Kiesel et al., 2019).

5.2.2 Model setup and data processing

We simulated the propagation of surge water levels over the model domain (light grey mesh Figure 5.1a) using the DELFT3D-FLOW (version 4.00.02) model (Delft Hydraulics, 2003). This model calculates the flow of water over a multi-dimensional (2D (depth averaged) and 3D) finite, rectilinear or curvilinear, boundary fitted difference grid. Areas of application include coastal, river and estuarine settings (Delft Hydraulics, 2003; Lesser et al., 2004; Temmerman et al., 2012; Elahi et al., 2020). We used the model to simulate two-dimensional flow over a Cartesian grid using the horizontal momentum equations, the continuity equation and 2D turbulence, which was modelled based on a constant horizontal eddy viscosity coefficient (1 m^2 s^{-1}). For a detailed description of the model and the governing equations we refer the reader to the DELFT3D-FLOW user manual (Delft Hydraulics, 2003).

The model domain covers an area of 1.97 km in width and 1.95 km in length. It extends from the pioneer zone of the natural saltmarsh in front of the MR over the MR itself into the adjacent agricultural lands (see coverage of 10 m grid in Figure 5.1a). The model has been set up with three open boundaries (Figure 5.1a), of which only the eastern side was forced with hydrographs representing the five return water level scenarios. All boundaries were allowed to exchange water outside the model domain. The temporal resolution of the five hydrographs was 10 minutes and the model time step was 6 seconds.

Bathymetry, topography and land cover information to develop elevation and surface roughness maps of the model domain were derived from a 2 x 2 m 2016 LiDAR derived DEM (Environment Agency, 2020) and a supervised image classification (Kiesel et al., 2019), which was based on 20 x 20 cm vertical aerial photography from the same year (Environment Agency, 2019c). In order to reduce computational costs, all data were resampled onto a 10 x 10 m grid, which was the base for the model calculations (Figure 5.1a). The DEM was resampled by calculating the average of the four nearest

cells. The supervised image classification was used to distinguish between dominant surface cover classes, namely saltmarsh, water and tidal flat (either sand or mudflat). These classes were used to derive the surface roughness within the model domain, which is represented in the model by assigning Manning´s n coefficients (saltmarsh: 0.08, tidal flat: 0.03 and water: 0.02). These values have been widely used in literature in hydrodynamic model applications and were shown to be suitable for representing the drag forces exerted by the respective surface type (Garzon and Ferreira, 2016; Hossain et al., 2009; Lawrence et al., 2004; Liu et al., 2013; Wamsley et al., 2010, 2009; Smolders et al., 2015; Stark et al., 2016; Temmerman et al., 2012). Manning´s n coefficients for every cell (20 x 20 cm) were resampled onto the 10 x 10 m grid by using the same approach as for the model's elevation.

In a previous study, the model was calibrated and validated against field measurements of the highest spring tides of the year 2017. Root mean square errors between modelled and measured water depths ranged between 0.05 and 0.06 m and mean absolute errors of peak water levels between 0.02 and 0.04 m. Model calibration included a range of Manning´s n coefficients for saltmarsh surfaces (0.035 – 0.09) and revealed that the model was not very sensitive to these variations (Kiesel et al., 2020). We note, that the effects of bottom friction are also dependent on water depth (Delft Hydraulics, 2003; Loder et al., 2009; Wamsley et al., 2010; Temmerman et al., 2012) and the calibration of the model is representative of spring tide conditions.

5.2.3 Generation of extreme water level hydrographs

In order to support successful risk-based flood and coastal erosion management, the UK Environment Agency (EA) has published a consistent set of extreme sea levels around the coasts of England, Wales, Scotland and Northern Ireland. Extreme peak sea level heights for different annual exceedance probabilities are provided in the report for events with return periods that range between 1- to 10,000-years, at points every 2 km along the coastline (Environment Agency, 2019a). In order to analyse the attenuation

of extreme sea levels within the Freiston Shore MR site, we selected the 10-, 50-, 100-, 200- and 1000-year events from the EA´s report, referenced to ODN. Peak water levels for each return period were averaged from the two closest points to the Freiston Shore MR site (Figure 5.1b). Both points are approximately 1.85 km seaward of the eastern open boundary. The resulting extreme water levels are 5.24 m for the 10-, 5.54 m for 50-, 5.67 m for 100-, 5.81 m for 200- and 6.16 m for the 1000-year event. It is likely that the extreme water levels would be attenuated to some extent while propagating from these points to the boundary of the model domain. It is therefore likely that we slightly overestimate the peak extreme water levels for each event.

To create the storm surge hydrographs which force the model, we followed the procedure described in the user guide to the EA´s report (Environment Agency, 2019b). Unfortunately no significant surges were recorded at the nearest tide gauge Tabs Head, which is why we took the hydrograph of the largest surge from the tide-gauge record at Cromer (ca. 81 km air-line distance from study site; Figure 5.1b), which occurred in February 1993, with a maximum height of 2.5 m (Figure 5.2a). We extracted the surge component of the event using the UTide Matlab functions (Codiga, 2011) and combined it with tidal water levels recorded at Tabs Head (ca. 4 km air-line distance from study site; Figure 5.1b). We then scaled each timestep of the surge component by a single factor in order to meet each of the respective target extreme water levels, as suggested by the EA's report. Each timestep of the new surge component ($S(t)_{new}$) was scaled using the following equation:

$$S(t)_{\text{new}} = S(t)_{\text{orig}} \cdot (1 + \frac{dwl - pwl}{pwl}) \tag{5.1}$$

where $S(t)_{orig}$ is the original surge extracted from the tide gauge in Cromer, dwl is the targeted design water level for each extreme event tested, and pwl is the peak total water level at the tide gauge. Finally, the resulting new surge water level time series were recombined with the tidal data from Tabs Head. This procedure was repeated for each of the five design water levels and the resulting hydrographs for each return

water level were used as boundary conditions for the eastern open boundary and are shown in Figure 5.2b.

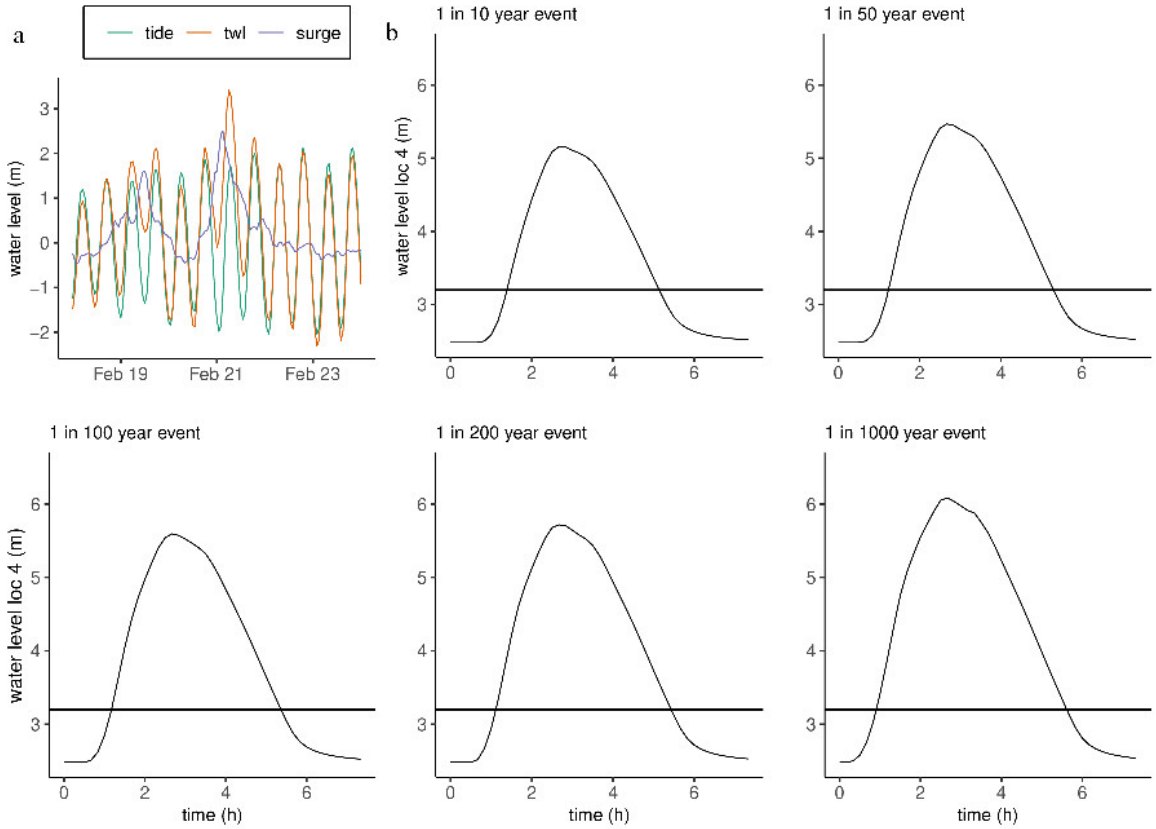

Figure 5.2 a) The largest storm surge on record for the tide gauge of Cromer (occurred in 1993). We have stretched the 1993 event to meet the five different return water levels. b) Hydrographs showing the water level curve for each extreme event at Loc 4 (see Figure 5.1a for location). The horizontal line indicates the average elevation inside the MR site. These hydrographs were used to define boundary conditions at the eastern open boundary (Figure 5.1a).

5.2.4 Marsh width scenarios

The effects of varying marsh widths (and consequently areas) were studied by removing the landward dike of the original Freiston Shore MR site (referred to as status quo) and implementing new seawalls (called thin dams in Delft3D-Flow) at the back of the site for four hypothetical (residential areas and roads are located within scenarios 1.3 and 1.4) MR width scenarios (Figure 5.1d). Marsh width was measured from the central breach perpendicular to the coastline in a landward direction. Scenario 1.1 covers an

area of 118 ha with a 900 m MR width, 1.2 145 ha and 1100 m, 1.3 180 ha and 1320 m and 1.4 205 ha and 1500 m width. We assumed full vegetation cover for all MR width scenarios.

5.2.5 Vegetation scenarios

We explore the propagation of extreme HWLs for three scenarios of reduced vegetation cover over the Freiston Shore MR site and scenario 1.4. These two model setups were chosen as they represent the greatest difference between MR widths (and areas). The original vegetation, determined from the supervised image classification (see section 2.2), was found to cover 81 % in the north of the MR and 73 % in the south (Kiesel et al., 2019). These values range in the same order of magnitude compared to findings of the monitoring report, which estimated mean total vegetation cover in 2007 to be at 89 % (Brown, 2008). This classification (also referred to as "Actual veg") constitutes the baseline from which we reduced vegetation cover by 50 %, 75 % and 100 %, the latter representing the "no vegetation" scenario. Consequently, differences in vegetation cover between areas within the MR are much smaller compared to differences between the vegetation scenarios. We induced a patchy vegetation cover for each scenario by applying a likelihood filter (50 %, 75 % and 100 %) to every cell classified as saltmarsh, determining whether that cell became tidal flat/mudflat or remained vegetated. The resulting land cover maps (Figure 5.3) were used to derive adjusted Manning's n coefficients for each changed cell.

5.2.6 Calculation of HWL attenuation rates

HWL attenuation rates (cm km^{-1}) were calculated from the vertical difference in HWL between two observation points (n = 1 for each observation point and return water level scenario), termed hereafter as transect, and the horizontal distance between them. All observation points are located on the marsh platform. In total, seven transects were established, where negative values refer to the amplification of HWLs and positive

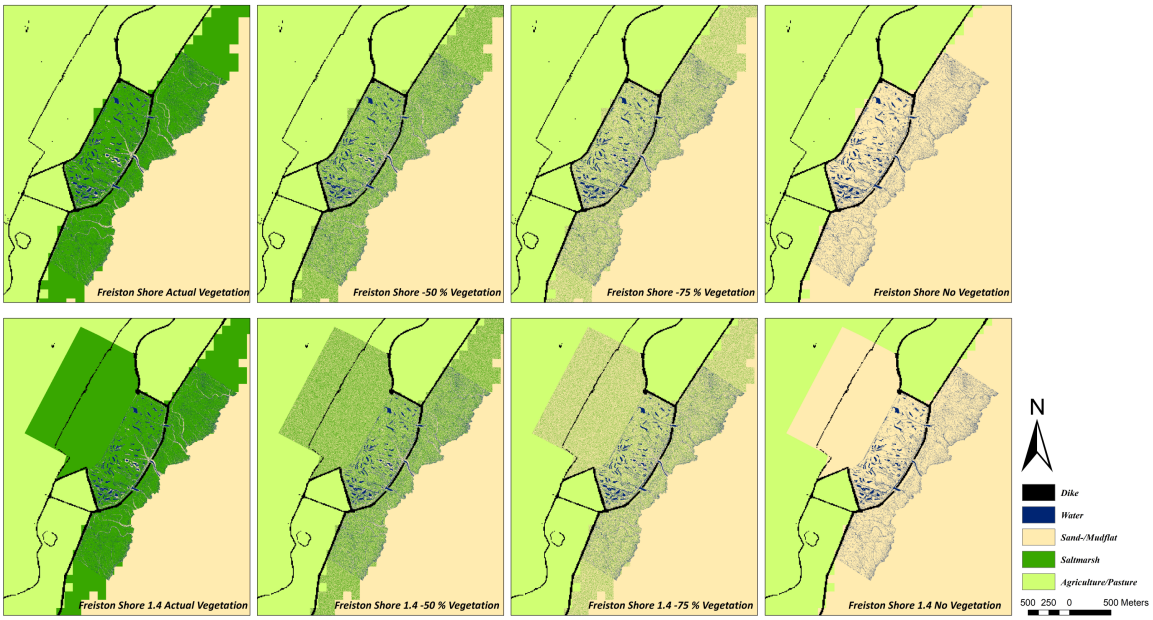

Figure 5.3 Landcover maps showing the vegetation scenarios. a) Freiston Shore and b) scenario 1.4.

values indicate attenuation. Coordinates and elevations of each location are provided in Table 5.1. We differentiate the transects based on their location, with transects Loc 3–1, Loc 6–15 and Loc 9–14 classified as "From Outside Breached to New Dike", while Loc 13–1, Loc 2–1, Loc 8–15 and Loc 16–14 are classified as "Inside MR", the latter of which refers to *within-wetland* attenuation of HWLs. Setup of these transects was the same for Freiston Shore and all MR width variations tested.

In addition to the calculation of HWL attenuation rates at the transects, we analysed differences in absolute HWLs between locations in front of the breached, seaward dike and in front of the new, landward dike for Freiston Shore and scenario 1.4. These additional locations are abbreviated with LD (landward dike) and SD (seaward dike) and are shown in Figure 5.1a and d.

Finally, we computed HWLs for locations within the three breaches, in order to compare these values with measurements from directly in front of the breached dike (Locs 3, 6, 9 and SD1 and 2).

Table 5.1 Number, coordinates and elevation of locations used to assess HWL attenuation rates. Coordinates are given in British National Grid and elevation of measurement locations was extracted from the model topography. SD and LD refer to seaward and landward dike, respectively.

Area	Function	Location #	Latitutde	Longitude	Elevation (m ODN)
Status Quo	Used to calculate HWL attenuation rates for every MR width scenario	Loc 1	540728	343438	3.48
		Loc 2	541059	343229	3.23
		Loc 3 (SD)	541154	343281	3.4
		Loc 6 (SD)	541044	342920	3.39
		Loc 7	540544	342144	3.13
		Loc 8	540949	343061	3.24
		Loc 9 (SD)	540518	342202	3.54
		Loc 11	540799	343378	3.29
		Loc 12	540768	343405	3.32
		Loc 13	541076	343390	3.1
		Loc 14 (LD)	540205	342594	3.32
		Loc 15 (LD)	540590	343239	3.32
		Loc 16	540503	342494	3.04
1.4	Used to calculate absolute HWLs at seaward and both landward dikes (SQ & 1.4)	SD1	540691	342361	3.33
		SD2	540858	342590	3.6
		LD1	540734	343514	3.42
		LD2	540511	343090	3.23
		LD3	540385	342851	3.3
		LD1.4.1	539438	343136	2.48
		LD1.4.2	539554	343358	3.07
		LD1.4.3	539699	343631	2.97
		LD1.4.4	539821	343861	2.85
		LD1.4.5	539964	344136	2.55
	Compare HWLs between SD and breaches	Breach 1	541104	343207	2.02
		Breach 2	540933	342776	0.12
		Breach 3	540734	342441	1.2

5.2.7 Statistical analyses

We tested the null-hypothesis that there are no significant differences in HWL attenuation rates between both the return water level and vegetation scenarios. For both variables, we tested the assumptions for conducting a two-way analysis of variance model (ANOVA). In those cases where data were neither normally distributed (as indicated by Shapiro-Wilk p-value < 0.05) nor homoscedastic (Bartlett p-value < 0.05), we used a Kruskal-Wallis test as non-parametric alternative. Further, we tested the null-hypothesis that there was no significant difference between the two transect types, over which HWL attenuation rates were calculated (Inside MR and From Outside Breached to New Dike) using the non-parametric Wilcoxon-rank-sum-test (assumptions for t-test not met). We also tested whether HWL attenuation rates for the status quo (original Freiston Shore MR site) were significantly different from zero and whether scenario 1.3 and 1.4 were different to the Status Quo, using the Wilcoxon-rank-sum test. Statistics and figures (despite maps) were produced with R-Studio software (R Core Team, 2019).

5.3 Results

5.3.1 Reduction of extreme HWLs over the Freiston Shore MR site

Our results show that the capacity of the Freiston Shore MR site to reduce extreme HWLs is generally low, ranging from –21 cm km^{-1} to 7 cm km^{-1} with an average of –3 cm km^{-1} for all extreme events and vegetation scenarios (negative values represent an amplification of HWLs and positive indicate HWL attenuation). We found that HWL attenuation rates do not significantly differ between individual events and vegetation scenarios (Figure 5.4). For a comprehensive overview of HWL attenuation rates and the results of statistical tests for Freiston Shore and all MR width scenarios, we refer

the reader to Table B.1, provided in Appendix B.

The results demonstrate that water levels are generally not attenuated from the seaward, breached dike to the new, landward dike. On the contrary, HWLs are generally amplified. This trend is significantly different from zero (Wilcoxon-rank-sum-test p-value < 0.0005). Looking into the transects individually shows that the negative outliers in Figure 5.4 in all scenarios mostly come from transect Loc 9–14, in the south of the study site, underlining the high spatial variability of HWL attenuation (HWL attenuation rates plotted per transect are shown in Figure B.1 in Appendix B of this thesis). The difference in HWL attenuations between the two transect types (From Outside Breached to New Dike (average –5 cm km^{-1}) and Inside MR (referring to *within-wetland* attenuation) (average –1 cm km^{-1})) is statistically significant (Wilcoxon-rank-sum test p-value < 0.0005).

On average, absolute HWLs at the landward dike were 2 cm higher compared to the breached, seaward dike. Please see Appendix B for further details (Figure B.2).

5.3.2 MR width thresholds related to HWL attenuation and reduction of extreme water levels over each MR width scenario under full vegetation cover

The modelled HWL attenuation rates of the MR width scenarios indicate that substantial areas are required to effectively reduce the highest surges at the open coast (Figure 5.4). We identified surge specific MR width thresholds for the HWL attenuation potential of Freiston Shore (Figure 5.5). When full vegetation coverage is assumed, the 10-year event would require a MR width of > 1148 m to be attenuated, the 50-year event a width of > 1247 m, the 100-year event > 1277 m and the 200-year event requires at least 1302 m. Since the 1000-year event was not attenuated in all scenarios, a width threshold could not be identified.

Scenarios 1.1 and 1.2 produced average HWL attenuation rates of –4 cm km^{-1} and

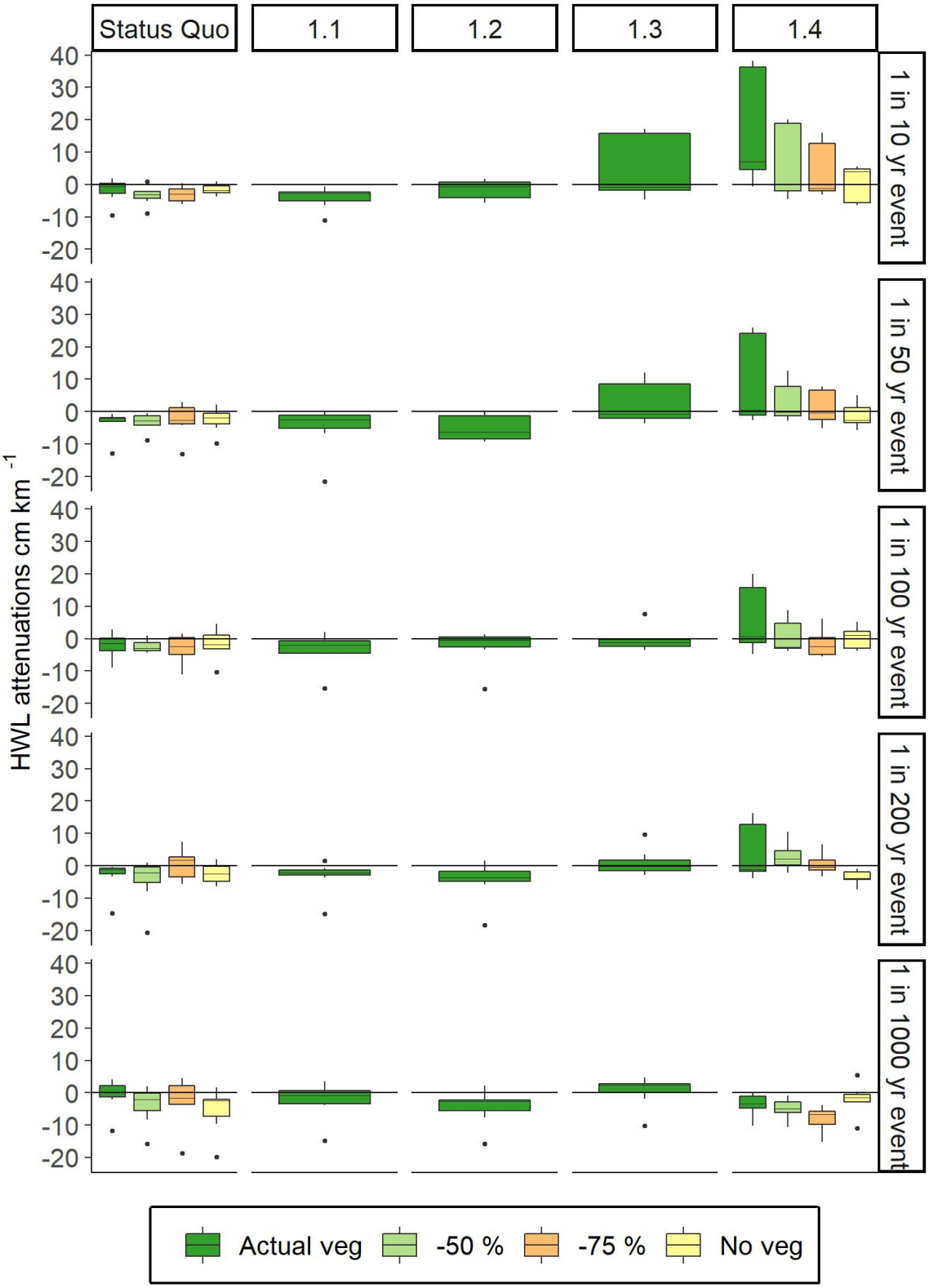

Figure 5.4 HWL attenuation rates for Freiston Shore and the MR width scenarios under all extreme water level scenarios. Freiston Shore and scenario 1.4 were additionally modelled with four scenarios of reduced vegetation cover. The boxplot is defined as follows: The bottom and top ends of the box refer to the 25th and 75th percentile and the centreline shows the median. The whiskers are calculated as the upper and lower boundary of the box + 1.5 * the interquartile range. Points that did not fall within this range are plotted as outliers.

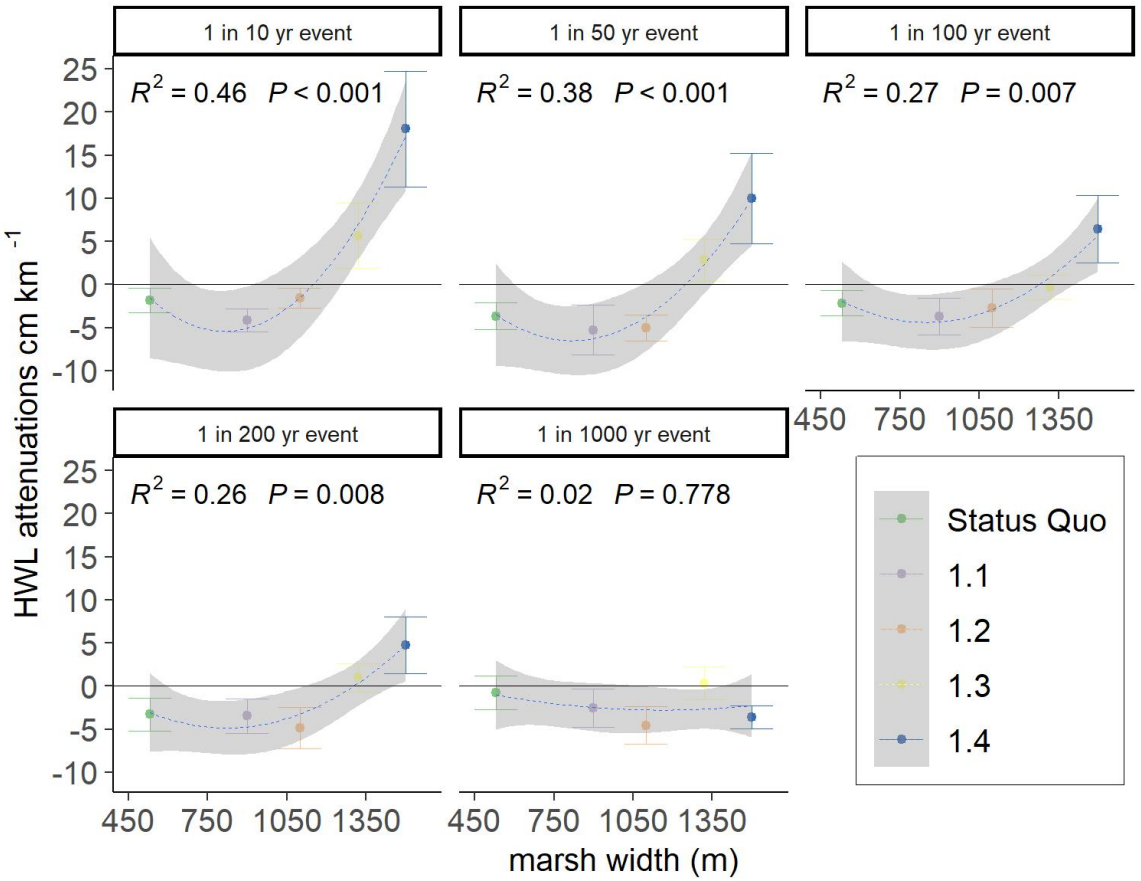

Figure 5.5 Regression between HWL attenuation rates and MR width. A second order polynomial function was fitted through the data points, which show the average HWL attenuation rate per scenario (considering only actual vegetation). The grey area around the function indicates the 95 % confidence interval and the vertical bars show the standard error of the mean.

range in the same order of magnitude compared to the original Freiston Shore MR site, despite marsh widths being approximately twice the original (900 m and 1100 m in comparison to 530 m in the Status Quo). As for the Status Quo, no statistically significant difference in HWL attenuation rates between extreme events was identified (see Appendix B Table B.1).

In contrast, average HWL attenuation rates of 2 cm km^{-1} were measured for scenario 1.3, comprising 1320 m MR width and an area of 180 ha. Even though no statistically significant difference between extreme events was found (see Appendix B Table B.1), maximum HWL attenuation rates were higher for lower surge heights. Contrary to all other scenarios tested, no amplification was observed. We note, however, that scenario 1.3 was only modelled with actual (full) vegetation cover. HWL attenuation rates were statistically significantly different compared to the Status Quo (Wilcoxon-rank-sum test p-value < 0.0005).

Scenario 1.4 comprises a total area of 205 ha and a 1500 m width, and is the only scenario which experiences substantial HWL attenuation rates. Mean HWL attenuation rate over all surges was 7 cm km^{-1}, with decreasing values as surge heights increase (Figure 5.4, Table B.1). The difference in HWL attenuation rates between extreme events was statistically significant and amplification of HWLs was only observed for the 1000-year event. HWL attenuation rates were statistically significantly different to the Status Quo (Wilcoxon-rank-sum p-value = 0.0008).

Most of the modelled attenuation in scenario 1.4 comes from transects measured from outside the breached, seaward to the landward dike, while attenuations from exclusively inside the MR are negligible (Figure 5.6). The difference between both transect types was statistically significant (Wilcoxon-rank-sum-test p-value < 0.0005). Transects from exclusively inside the MR refer to *within-wetland* attenuation. Under full vegetation cover, average *within-wetland* attenuation of HWLs exhibits –1 cm km^{-1}, while transects measured from outside breached to new dike show average HWL attenuation rates of 18 cm km^{-1}. We find that most of the attenuation from the transects

classified as "From Outside Breached to New Dike" occurs within only approximately 30 m, between locations directly in front of the breached dike and within the three breaches, or directly landward the breached dike. Over all extreme events, the average difference in HWLs between the breaches and the area in front of the breached dike is 9 cm (Figure 5.7).

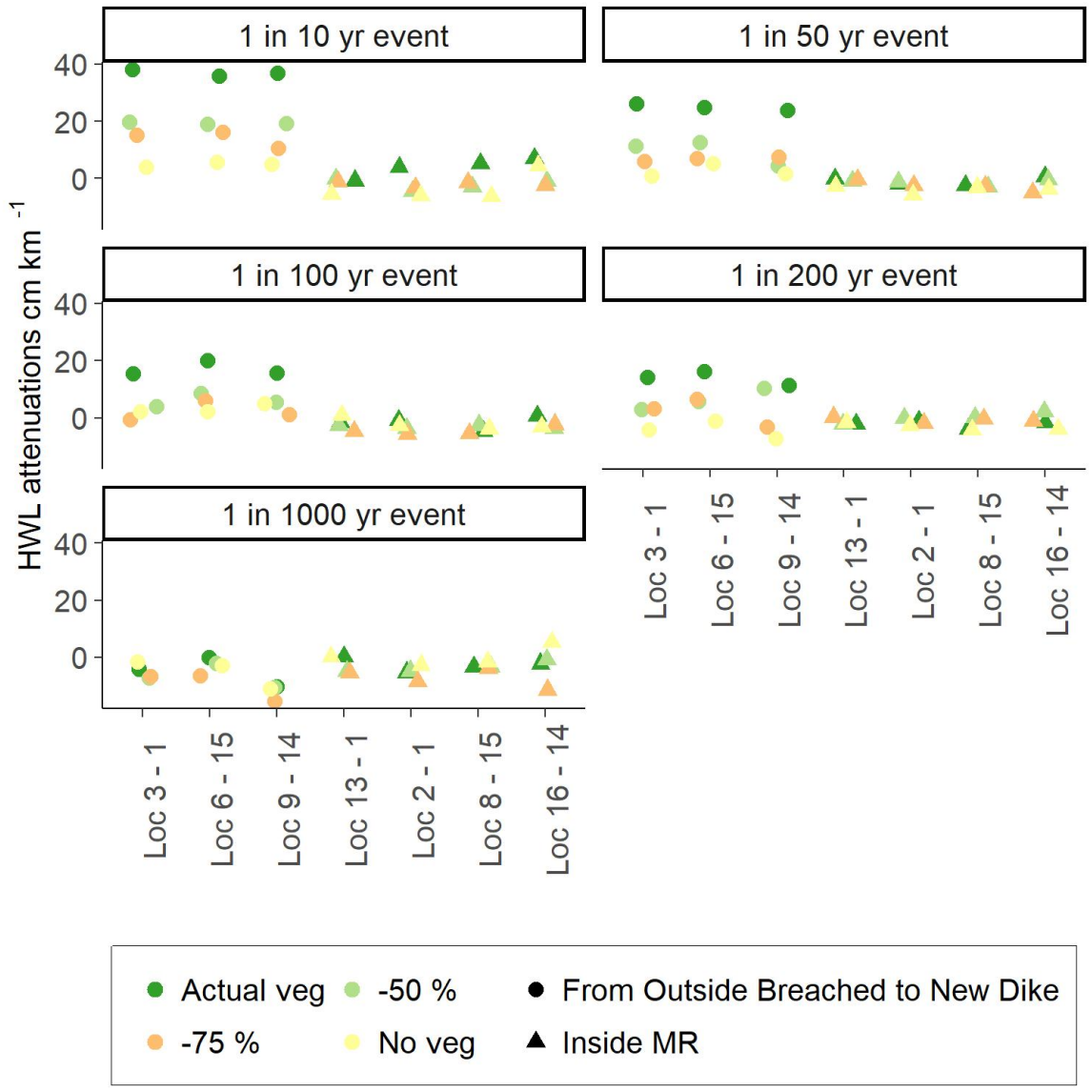

Figure 5.6 HWL attenuation rates over scenario 1.4 depicted per transect, extreme event and vegetation scenario.

Overall, HWL attenuation rates in all scenarios are characterised by high variability, expressed in standard deviations ranging from 3 to 18 cm km^{-1} (Table B.1). Higher

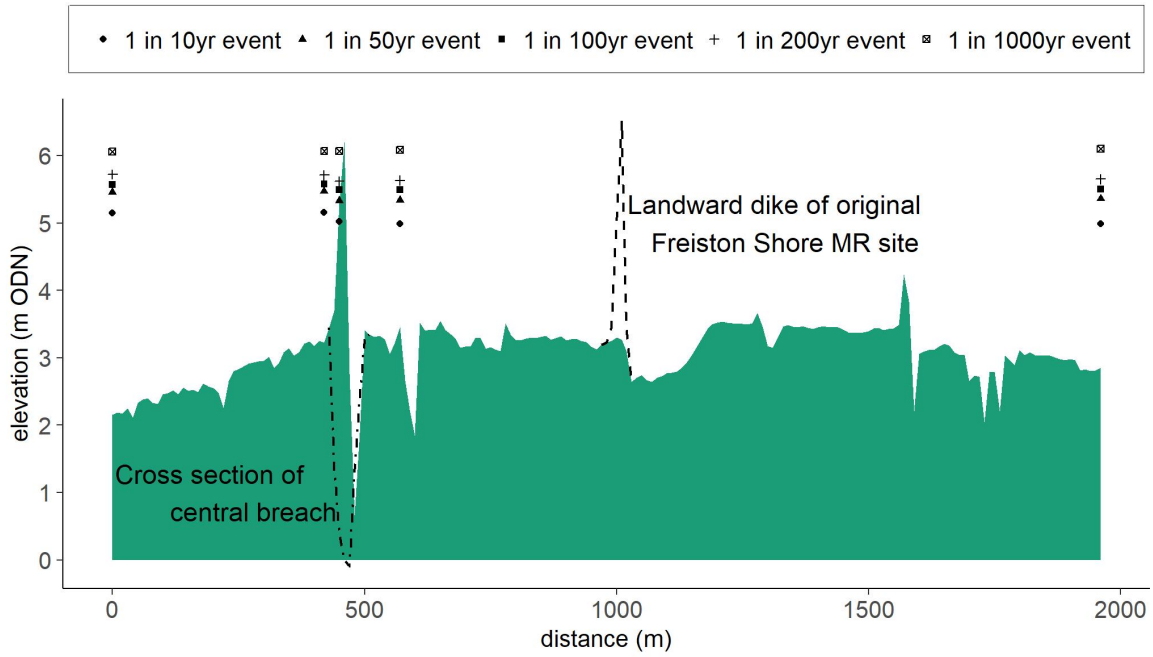

Figure 5.7 Elevation profile of scenario 1.4, measured from the pioneer zone of the adjacent natural saltmarsh via the central breach in landward direction to the end of the model domain. The shaped points show absolute HWLs for each extreme event for the respective location along the profile. These values were calculated as follows (from left to right): Loc 4; average of Locs 3, 6, 9, SD1 and 2; average HWL of southern, central and northern breach; average of Locs 2, 8, 13 and 16 and; average of LD1.4.1, 1.4.2, 1.4.3, 1.4.4 and 1.4.5.

variabilities were observed for scenarios 1.3 and 1.4, coinciding with higher attenuation rates.

5.3.3 Effects of reduced vegetation cover on HWL attenuation in scenario 1.4

Our results show that HWL attenuation rates generally decrease with decreasing vegetation cover (Figure 5.4). However, statistically significant differences were only observed for the 200- and 1000-year events (Table B.1). Looking at absolute differences in HWLs between locations in front of the breached, seaward and landward dikelines (green and blue points in Figure 5.1d) reveals that effective reductions in HWLs are observed for all but the 1000-year event, ranging from 17 cm for the 10-year event to 6 cm for the 200-year event (Figure 5.8, Table 5.2). However, the loss of vegetation reduces differences in HWLs between both dikelines to 1 cm for the 10-, 50- and 100-year events. In addition, attenuation switches to amplification for the 200-year event when vegetation is completely lost. The 1000-year event was amplified regardless of whether full or absent vegetation cover was modelled.

Table 5.2 Average HWLs measured in front of the breached and hypothetical landward dike of scenario 1.4.

	10-year		**50-year**		**100-year**		**200-year**		**1000-year**	
	Actual veg	**No veg**	**Actual veg**	**No veg**	**Actual veg**	**No veg**	**Actual veg**	**No veg**	**Actual veg**	**No veg**
HWL at breached, seaward dike (m)	5.16	5.17	5.47	5.49	5.58	5.62	5.71	5.74	6.07	6.13
HWL at hypothetical landward dike (m)	4.99	5.16	5.36	5.48	5.50	5.61	5.65	5.76	6.1	6.19
Difference (m)	0.17	0.01	0.11	0.01	0.08	0.01	0.06	–0.02	–0.03	–0.06

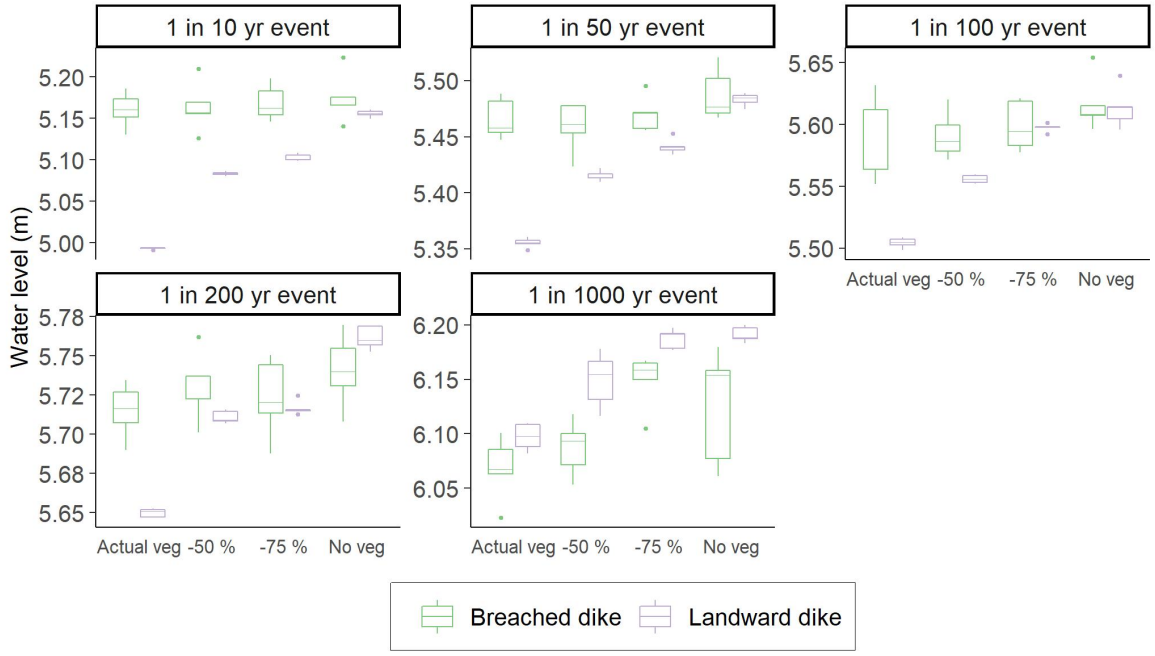

Figure 5.8 Absolute HWLs (referenced to ODN) measured seaward of both the breached and hypothetical landward dike of scenario 1.4. Locations of measurements are shown in Figure 5.1d and Table 5.1.

Transects classified as "Inside MR" suggest that *within-wetland* attenuation is low irrespective of vegetation cover. Full vegetation cover results in HWL attenuation rates of –1 cm km^{-1} and absent vegetation produces rates of –2 cm km^{-1}.

5.4 Discussion

5.4.1 Suitability of MR for effective coastal flood risk reduction and implications for management

The MR site of Freiston Shore is situated at the open coast of The Wash embayment. Thus, our findings are related to *within-wetland* attenuation of HWLs, whereas the water storage capacity (relevant for *along-estuary* attenuation) is negligible (Hofstede, 2019; Smolders et al., 2015). Our findings suggest that at the open coast, *within-wetland* attenuation has to be further grouped into transects that are measured exclusively inside the MR (which essentially equates to *within-wetland* attenuation)

and those where the first measurement point is located in front of the breached dike.

We found that the capacity of the Freiston Shore MR site to provide *within-wetland* attenuation is very limited. This has been shown before for the highest astronomical spring tides in both field and modelling studies (Kiesel et al., 2019, 2020) and, according to our results, is also valid for a range of extreme events. The comparatively weak performance of the Freiston Shore MR site is not surprising, since previous studies have shown that surge attenuation decreases if surge duration is long compared to the time it takes to fill the storage area (Resio and Westerink, 2008; Loder et al., 2009). In this study, all modelled events were long and high enough to fully inundate the original MR (and all MR width scenarios). Even though our results suggest that MR at Freiston Shore has generally led to slight amplifications of HWLs, we argue that flood risks are not exacerbated under the most extreme events since amplification rates are very small, ranging between –1 and –3 cm km^{-1} under actual (full) vegetation cover (Table B.1).

The dominant amplification of HWLs over Freiston Shore (even if mostly small) and the gradually increasing attenuation rates for larger MR widths indicate that the capacity of MR schemes equal in size or smaller than Freiston Shore to effectively provide *within-wetland* attenuation may be limited, as also discussed in Hofstede (2019) and shown in Kiesel et al. (2020). This is further clarified by previously measured and modelled HWL attenuations, ranging between 4 cm km^{-1} (Lovelace, 1994; McGee et al., 2006; Wamsley et al., 2010) and 25 cm km^{-1} (McGee et al., 2006; Wamsley et al., 2010). These rates were measured over several kilometres. Consequently, the *within-wetland* attenuation capacity of many MR schemes in Europe today may be limited, since as of 2021, 46 % of MR schemes were smaller than 20 ha (ABPmer, 2021) (compared to 66 ha in Freiston Shore). We note, however, that the capacity of smaller MR schemes to support *along-estuary* attenuation of HWLs may still be effective, particularly when placed further upstream in the estuary (Smolders et al., 2015; Leuven et al., 2019).

Our results show that at the open coast, only very large MR schemes can effectively

contribute to coastal flood risk reduction (in terms of HWL attenuation). Site dependent MR width thresholds for the tested extreme water level scenarios range between 1148 m for the 10-year event and 1302 m for the 200-year event. On the other hand, the 1000-year event was not attenuated in any of the MR width scenarios, suggesting that for such events, wider areas are required to achieve attenuation. The 200-year event illustrates the importance of a comprehensive vegetation cover, which can increase inundation depth thresholds until HWLs are effectively reduced (attenuation under full vegetation cover and amplification when vegetation is lost; Table 5.2, Figure 5.4).

Under most conditions in scenario 1.4, HWLs are substantially lower at the new, landward seawall, suggesting that it can be of a lower design specification, and thus cheaper to build and maintain (Dixon et al., 1998; Pethick, 2002). Indeed, most of this HWL attenuation presumably comes from transects measured from outside the breached, seaward dike to the new, landward one, suggesting that HWLs are affected by reflection against the dike remnants (Figure 5.6). Differences between absolute HWLs from locations in front of the breached dike, inside the three breaches and directly landwards support this idea (Figure 5.7). Over all extreme events, the average difference in HWLs between the breaches and the area in front of the breached dike is 9 cm, despite the locations being less than 30 m apart. We therefore assume that extrapolating the attenuation rates from transects "From Outside Breached to New Dike" of scenario 1.4 (on average 18 cm km^{-1} for full vegetation cover) may lead to overestimations, as much of it comes from the effects of the breached, seaward dike.

We deduce the following management implications from the findings presented in this paper:

1. At the open coast, large MR schemes can effectively reduce a large range of extreme surges, but the most extreme events are not as effectively attenuated. The potential for surge attenuation scales with MR width.

2. Most of the attenuation in scenario 1.4 may come from water piled up at the

remnants of the breached dike. However, lower water levels at the landward dike still mean that it can be of lower design specification compared to the breached dike and should thus be less expensive in terms of construction and maintenance costs.

3. When larger MR sites are implemented for the purpose of coastal protection, the successful re-establishment of vegetation is crucial to attenuate very high water levels (in this case the 200-year event). This involves careful consideration of actual (and presumably future) inundation frequencies, fostering the establishment of diverse vegetation communities (Nottage and Robertson, 2005). In addition, inundation frequency and duration are dependent on the marsh's elevation relative to tidal range and the future resilience of established vegetation depends on sustained high sedimentation rates. Marsh elevation furthermore affects bottom friction and additionally contributes to HWL attenuation (Loder et al., 2009; Wamsley et al., 2009). Sedimentation rates, site internal water depth and thus, inundation frequency and duration, can be controlled by MR design (Oosterlee et al., 2020) (width of breaches in relation to site size, via RTE or by inducing synthetic tidal regimes using novel "SmartGates" (Kiesel et al., 2020; de Mulder et al., 2013; Sadat-Noori et al., 2021)).

Inundation frequency depends on the initial surface elevation of the saltmarsh to be restored, scheme design and long-term biophysical feedback mechanisms that drive site internal sediment dynamics. The first two features can be controlled by coastal planners and practitioners at the onset of MR establishment. On Wallasea island, located close to the entrance of the Thames estuary, for example, elevations were raised by 1.5 m prior to breaching (Cross, 2017). Furthermore, the design of dike breaches can be informed by hydrodynamic modelling, and culverts and sluices enable the management of site internal inundation depths and durations. However, long-term biophysical feedback mechanisms are not yet fully understood, computationally

expensive to model on a large scale and critically dependent on the development of future hydrodynamic forcing, such as sea-level rise.

5.4.2 Our findings compared to previous studies

HWL attenuation rates modelled in this study within the MR site of Freiston Shore are generally lower (and, on average, negative) compared to previous assessments, which is also true for *within-wetland* attenuation rates in scenario 1.4. We therefore assume that the simulated extreme events may overwhelm the flow reducing capacity of the restored saltmarsh.

A good overview of saltmarsh related HWL attenuation rates from previous field studies is provided in Stark et al. (2015), which was later extended to some modelled results by Paquier et al. (2017). Their reviews reveal that HWL attenuation rates are generally highly variable and can range from –280 to 270 cm km^{-1} within a single saltmarsh (Paquier et al., 2017). However, several studies provide rates in the range of 4 cm km^{-1} (Lovelace, 1994; McGee et al., 2006; Wamsley et al., 2010) to 25 cm km^{-1} (McGee et al., 2006; Wamsley et al., 2010), all of which measured over several kilometres. When shorter transects on the vegetated marsh platform were measured, values increased and reached 70 cm km^{-1} (Stark et al., 2015) or even 270 cm km^{-1} (Paquier et al., 2017). The inverse relationship between transect length and HWL attenuation has also been suggested by Kiesel et al. (2019) for the MR site of Freiston Shore. Kiesel et al. (2019) assume that short transects over saltmarsh surfaces often generate maximum (densely vegetated) or minimum friction (bare sediments) on the water column, depending on the surface cover and topography of the respective transect. This effect may be averaged over the entire marsh width, resulting in generally lower and less variable HWL attenuation rates when measured over longer distances (Kiesel et al., 2019).

5.4.3 Model limitations

5.4.3.1 The missing link - model validation for extreme events

The model presented in this paper has been validated against field measurements of the highest spring tides of the year 2017 (Kiesel et al., 2020). These were considerably lower compared to the extreme events generated in this study. Since no measurements exist to validate the results of our model against comparative extreme water levels, we have qualitatively compared our HWL attenuation rates with results from previous assessments (subsection 5.4.2). The results are in the same order of magnitude, but without field validation data, the high storm scenarios should be viewed with caution. Since extreme surges are inherently rare events, it is not surprising that only little field data exist. However, in order to predict the effectiveness of MR schemes under relevant storm conditions, gathering data on rare events is urgently required for validating model predictions (Bouma et al., 2014). Indeed, current monitoring efforts in MR schemes devote comparatively little attention to hydrodynamic and hydrogeomorphic attributes (Spencer and Harvey, 2012), calling for extended monitoring campaigns, for example using self-contained automated monitoring systems (Bouma et al., 2014).

5.4.3.2 Considerations on vegetation scenarios and model assumptions

In this study, we have addressed the impact of vegetation die-off on the HWL attenuation function of saltmarshes restored in the context of MR. Thereby, we account for existing uncertainties around the long-term eco-geomorphological evolution of MR schemes in response to sea-level rise, which may cause prolonged inundation stress and the deterioration of vegetation (Schepers et al., 2020; Kirwan et al., 2010; Mariotti, 2020; Duran Vinent et al., 2021). However, some limitations to our approach are addressed in the following.

The vegetation induced resistance on depth-averaged flow during the very high storm tides modelled in this paper may be overestimated. We have calibrated surface rough-

ness coefficients under a range of spring tide conditions with comparatively low inundation depths, where most of the water column is influenced by vegetation induced resistance. Thus, the selected Manning´s n coefficients are representative of spring tide conditions and may be too high when applied to very high inundation depths, where most of the water column is not influenced by the presence of vegetation. However, relative differences between vegetation scenarios should not be affected by this issue. Considering patchy vegetation die-off as a consequence of sea-level rise and ponding only constitutes one mechanism of the "many faces of marsh loss" (Mariotti, 2020; Wasson et al., 2019). The complex interrelations and biophysical feedback mechanisms potentially leading to more or less homogeneous die-off are not considered. These include marsh edge erosion, for example due to increased wave loads as the marsh profile steepens (van de Koppel et al., 2005), or channel enlargement as a consequence of changes in tidal prism (Vandenbruwaene et al., 2015; Mariotti, 2018). Differences in the die-off pattern of vegetation can affect HWL attenuation rates (Temmerman et al., 2012) and, in the long-term, will affect the eco-geomorphological evolution of the site.

5.4.3.3 Considerations on the effects of morphologic site evolution on HWL attenuation rates

Modelled HWL reductions for Freiston Shore and scenario 1.4 are representative for the current biogeomorphic state of the MR and adjacent areas. In the following, we discuss likely morphologic adjustments of scenario 1.4, consequential upon the removal of Freiston Shore's landward dike and subsequent changes in the tidal prism (Friess et al., 2014; Vandenbruwaene et al., 2015; Townend et al., 2016) and anticipate potential effects on our findings.

As tidal prism and related hydrodynamics determine within-site sedimentation (Dale et al., 2017), we expect that the morphological development of all tested scenarios would be different. For example, scenario 1.4, as modelled in this paper, does not

contain any additional tidal creeks, connecting the original MR area with the new landward margin. Channel geometry, however, is a function of tidal prism (Friess et al., 2014), which would be substantially altered by increasing the size of the MR (Kiesel et al., 2020). We would therefore expect tidal creeks to develop at the landward margin of scenario 1.4 and to be morphologically altered in the area of the original scheme to accommodate for the increased tidal prism. Tidal creeks produce channelized flow, which results in lower attenuation rates compared to surfaces dominated by sheet flow (Stark et al., 2016). This is in agreement with the results of additional model runs that we conducted for scenario 1.4, where we extended the original tidal creeks of Freiston Shore to the new landward margin of the site (see Appendix B Figure B.3). The results indeed produced lower attenuation rates, suggesting that we might have overestimated HWL attenuation for scenario 1.4. However, attenuation rates measured with and without additional tidal creeks were not statistically significantly different (Wilcoxon-rank-sum test p-value = 0.22; Appendix B Figure B.4). On the other hand, differences in HWL attenuation rates between the Status Quo and scenario 1.4 with tidal creeks are not significantly different anymore, as indicated by the results of the Wilcoxon-rank-sum-test (p = 0.08).

There is an urgent need for further developing models of biophysical feedback mechanisms, enabling the projection of possible future morphologic developments within MR schemes. Recent advancements in this regard are presented by Gourgue et al. (2020), who developed a computationally efficient model to account for the impact of sub-grid-scale vegetation patches on the relationship between water flow and sediment dynamics. Such knowledge is crucial for the flood defence functionality of saltmarshes, as it defines long-term trends regarding elevation, vegetation type/coverage and features such as marsh cliffs and channels (Reed et al., 2018). The application of such models on large geographic scales and long temporal scales would be needed in order to evaluate not only the current, but also future coastal protection function of MR sites.

5.5 Conclusions

At the open coast, large MR schemes can provide effective coastal flood risk reduction, even under very high storm surge levels, as the example of scenario 1.4 has shown. Freiston Shore, on the other hand, covers 66 ha and indeed constitutes one of the larger schemes in Europe as of today. It may yet be too small to effectively reduce HWLs, but flood risks are not exacerbated. Vegetation cover and MR width/area are crucial for the coastal protection function of MR schemes, since they elevate inundation depth thresholds up to which HWL attenuation is possible. The major contribution to the effective HWL attenuation in scenario 1.4 may come from reflection of HWLs against the remnants of the breached seaward dike, as shown by differences in HWLs between locations in front of the seaward dike and within the breaches. Even if this means that the contribution of *within-wetland* attenuation is comparatively low, the landward dike can be of lower design specification compared to the breached dike and should be cheaper regarding construction and maintenance costs. We believe that the most concerning knowledge gap to be tackled by future research involves understanding long-term dynamics of biophysical feedback mechanisms and resulting eco- and morphodynamic adjustments. The latter challenges the effectivity of MR in future coastal protection schemes and thus constitutes an important research priority.

5.6 Acknowledgements

The authors thank the UK Environment Agency for their open data policy and especially for providing coastal flood boundary conditions for a multitude of return periods, which has facilitated this study considerably. We also thank Deltares Delft Hydraulics for providing the Delft3D-Flow model. Particularly, Joshua Kiesel would like to thank Professor Tom Spencer, Professor Iris Möller and Elizabeth Christie for their support and the valuable and educational input during the past years.

5.7 Conflict of interest

The authors declare that they have no conflict of interest.

Chapter 6

Conclusions

6.1 Key findings

Until recently, missing knowledge on the true protective value of restored saltmarshes in coastal defence schemes was fostering public and societal opposition and thus, hampering coastal restoration trials to apply Nature-Based Solutions (NBS) on a large scale (Bouma et al., 2014). Therefore, the overarching goal of this thesis has been to investigate the effectiveness of Managed Realignment (MR) at Freiston Shore in providing *within-wetland* attenuation of high water levels and surges (Smolders et al., 2015). The key findings from this thesis are listed below:

- The MR site of Freiston Shore does not provide effective High Water Level (HWL) attenuation under all measured conditions. On the other hand, very high storm surges are not considerably amplified.

- At the open coast of Freiston Shore, only large and wide MR sites can effectively attenuate very high tides, and the reduction of storm surges with return periods of more than ten years requires MR widths of > 1148 m (measured perpendicular to the coastline).

- The potential to attenuate even higher surges scales with MR width and vege-

tation cover.

- Breaching dikes should be preferred over complete removal when coastal protection is the target of MR implementation. Two mechanisms are responsible: 1) Via adjusting the width, dike breaches allow controlling (and lowering) site internal inundation depths, which are more effectively attenuated by saltmarsh vegetation; 2) during extreme surges, most attenuation comes from water piled up at the remnants of the breached dike, rather than from *within-wetland* attenuation. Nevertheless, the new/reinforced landward dike can still be of lower design specification given the MR site is wide/large enough.

The key findings of this thesis presented above relate to the research questions that are stated in section 1.4. The specific conclusions drawn from answering each of these questions are presented in the following.

6.2 Research questions section 1: How effective is Freiston Shore in attenuating water levels of very high spring tides and can differences be identified to adjacent natural marshes?

6.2.1 Short summary on methods and scope of respective study

In late summer of 2017, a field campaign was conducted at the MR site of Freiston Shore. During the campaign, the propagation of HWLs was measured from the pioneer zone of the adjacent natural marsh in landward direction, including areas in front of the breached dike, the MR itself and the new landward dike. For this purpose, a network of water level loggers was deployed in the adjacent natural marsh and the MR site, allowing to calculate HWL attenuation rates for both areas. The 2017 field campaign

in Freiston Shore provided a first comprehensive dataset of water level dynamics inside the largest MR site in the UK at time of establishment in 2002 (chapter 3, published in Kiesel et al. (2019)).

6.2.2 Conclusions research questions section 1

The main finding of this study was that the Freiston Shore MR site can provide very limited coastal protection benefits, with respect to its HWL attenuation capacity. This was supported by statistical analyses, clarifying that no significant deviation between HWL attenuation rates inside the scheme and zero was found (p-value = 0.5). In contrast, statistically significant differences ($p < 0.0005$) were calculated for HWL attenuation rates measured inside the MR scheme and in the adjacent natural marsh. While about half of the tides inside the MR were amplified, no amplification was recorded in the natural marsh during the studied period.

However, the evaluation of Freiston Shore's coastal protection function requires the consideration of additional aspects. One of these aspects is the nearly asymptotic relationship between transect length (distance between two water level loggers over which HWL reduction was calculated) and HWL attenuation rates (Figure 3.3). The shorter the transects, the higher and more variable was the HWL attenuation function. Three of the four transects established in the adjacent natural marsh were comparatively short, ranging between 36 m and 60 m. The latter could help explaining the exceptionally high attenuation rates measured over these locations. Similar findings were presented by Stark et al. (2015) and Paquier et al. (2017), but available data on field measurements over varying transect length under a range of conditions is still very limited (Table 3.3). Nonetheless, field observations of HWL attenuation rates measured inside and outside the Freiston Shire MR site suggest that variabilities are reduced over transects of > 200 m length (Figure 3.3 (Kiesel et al., 2019)).

Furthermore, considerable variations in HWL attenuation rates were measured inside the MR. In Kiesel et al. (2019), we explain the spatiotemporal variability in HWL

attenuation rates with vegetation characteristics, water depth, wind speed and direction, all of which known drivers of HWL reduction (Resio and Westerink, 2008; Loder et al., 2009; Sheng et al., 2012; Temmerman et al., 2012; Wamsley et al., 2009). Indeed, we found highest attenuation rates at locations where vegetation was largest (in the southern natural marsh) and a tendency of HWL attenuations to be reduced under certain wind directions and higher inundation depths. However, a significant fraction of the variability remained unexplained and it is hypothesized that the reason for this and for the comparatively poor performance of the Freiston Shore MR site to attenuate HWLs was a result of site internal hydrodynamics, caused by patterns in wind speed and direction that interacted with MR scheme design.

In summary, the results show that HWL attenuation rates inside the MR are generally low, highly variable across space and time and dependent on transect length. This supports the statement of Reed et al. (2018) that HWL attenuation can not be summarised to a single reduction factor. This may be particularly valid inside relatively small and semi-enclosed basins such as MR schemes, where site internal hydrodynamics can counteract the attenuating effect caused by the additional shallow water area provided by the restored saltmarsh (Kiesel et al., 2019). The weak correlations between HWL attenuation and assessed drivers may support this hypothesis.

6.3 Research questions section 2: How is HWL attenuation in Freiston Shore linked to MR scheme design and can the latter be used to improve Freiston Shore's effectiveness?

6.3.1 Short summary on methods and scope of respective study

The results of the field campaign posed follow up questions that are addressed in the study presented in chapter 4 (published in Kiesel et al. (2020)). The interactions between HWL attenuation and MR scheme design were investigated by implementing six modifications to the design of Freiston Shore's MR site using hydrodynamic models (Kiesel et al., 2020). These models were forced with water level measurements taken during the 2017 field campaign at the seaward margin of the adjacent natural saltmarsh. The tested scheme design scenarios include the complete removal of the originally breached dike, three single breach schemes of varying breach widths and two scenarios with substantially larger MR areas and the original three breaches in place. HWL attenuation rates were measured for transects (consisting of two water level observation points) located exclusively inside the MR and where the first observation point is located seaward of the breached dike.

6.3.2 Conclusions research questions section 2

The results showed that HWL attenuation rates were statistically significantly different between the original Freiston Shore MR site and all but the complete dike removal scenarios. In general, modifications in Freiston Shore's scheme design led to improvements of the coastal protection function in terms of HWL attenuation rates. Highest average attenuation rates of 16 cm km^{-1} (Scenario 3.1; Figure 4.3) were found for the

scenario with largest MR area.

Exceptionally high attenuation rates were observed for transects that range from in front of the seaward, breached dike to the new, landward dike, suggesting that MR sites with breach design may be particularly effective in providing coastal protection. The findings presented in chapter 4 moreover indicate that breach design may allow the improvement of HWL attenuation rates for schemes that are equal in size or even smaller than the original Freiston Shore MR site. Improvements could be achieved by reducing site internal inundation depths via the creation of smaller and/or less dike breaches (MR scheme scenarios with a single breach). In case of Freiston Shore, the latter has led to increased average HWL attenuation rates from –1 cm km^{-1}, calculated for the original MR site, to between 2 and 6 cm km^{-1}. The strong negative correlations between inundation depth and HWL attenuation rates (Figure 4.5, Figure 4.6) additionally indicated that even higher HWL reductions are possible when less water is allowed to enter the site.

We must note, however, that number and size of dike breaches have to be determined based on local hydrodynamic circumstances such as the tidal prism. If breaches are designed too small, or in insufficient numbers, they will widen and deepen, as has been the case in Freiston Shore right after implementation in 2002 (Friess et al., 2014). Breach erosion could be prevented by (re)establishing tidal inflow via Regulated Tidal Exchange (RTE), where culverts and sluices allow the passage of water. Another option may be provided by raising the MR area prior to the breach by infilling, which would reduce inundation depth and duration and thus, the site's tidal prism. An example is the MR site of Wallasea island, located close to the entrance of the Thames estuary, where elevations were initially raised by 1.5 m (Cross, 2017).

The provision of flow velocity reduction and HWL attenuation by wetlands changes non-linearly with wetland size (Koch et al., 2009; Barbier et al., 2008; Smolders et al., 2015; Leonard and Croft, 2006; Christiansen et al., 2000). Thus, if only limited space is available (smaller than Freiston Shore), adequate sizing of breaches, RTE or rais-

ing elevations to control site internal water depths may ensure that HWLs are not amplified (as in the original Freiston Shore MR site). Yet, substantial *within-wetland* attenuation of HWLs may not occur when MR size falls below a site-dependent threshold.

6.4 Research questions section 3: How effective is Freiston Shore in attenuating extreme surges and can MR width(/area) thresholds for HWL attenuation be identified in relation to surge height and vegetation cover?

6.4.1 Short summary on methods and scope of respective study

The measurements taken during the field campaign, which were later used to force the hydrodynamic model (chapter 4), covered the highest spring tides of the year 2017. These tides produced maximum water levels of 4.38 m Ordnance Datum Newlyn (ODN) in front of the northern, and 4.39 m ODN in the southern part of the landward dike. This resulted in maximum inundation depths in front of the northern and southern landward dike of 0.96 m and 1.14 m, respectively. Drawing conclusions in terms of Freiston Shore's coastal protection function, however, requires studying the impacts of very high surges on MR associated HWL attenuation rates. The latter and the identification of MR width(/area) thresholds for effective HWL attenuation in relation to surge height and vegetation cover was the aim of the the third paper of this thesis (chapter 5). In chapter 5, which is published in Kiesel et al. (2021), we have applied the validated hydrodynamic model developed in the previous paper (Kiesel et al., 2020). In contrast to the high spring tide conditions modelled in Kiesel et al. (2020), five hydrographs representing 10-, 50-, 100-, 200-, and 1000-year return water

levels were used to force the model (peak water levels varying between 5.24 m ODN and 6.16 m ODN). In addition to the original Freiston Shore MR site, four MR width scenarios were tested and gradually reduced vegetation cover (50 %, 75 % and 100 %) for the status quo and the scenario with the largest MR width.

6.4.2 Conclusions research questions section 3

The results for the original Freiston Shore MR site showed that the site may not be capable of reducing water levels of very high storm surges. Similar to the modelled spring tides, HWLs were slightly amplified (varying between –1 and –3 cm km^{-1} for all return water level scenarios and actual (full) vegetation cover). However, mean absolute HWLs were only 2 cm higher at the new, landward dike (5.64 m ODN) compared to the seaward, breached dike (5.62 m ODN) under all return water level and vegetation scenarios. This finding suggests that the Freiston Shore MR site neither provides effective coastal protection in terms of HWL attenuation, nor does it considerably exacerbate coastal flood risks. Differences in vegetation cover had no statistically significant effect on HWL attenuation.

The findings further suggest that at the open coast, only very large MR sites can effectively attenuate return water levels of > 10 years and MR width and vegetation cover can increase inundation depth thresholds until which HWLs are effectively reduced. The wider (and larger) the site, the higher the surges that can be attenuated. Critical MR width thresholds for Freiston Shore suggest that at least 1148 m are required to attenuate the 10-year event and 1302 m for the 200-year event. The results for the largest MR width scenario (1500 m MR width) further suggest that absent vegetation can turn HWL attenuation into amplification for a surge with a return period of 200 years (6 cm vs. –2 cm, respectively). Generally, HWLs were substantially lower at the hypothetical landward dike compared to the breached, seaward one in the largest MR scenario. With full vegetation cover, differences in HWLs range between 17 cm for the 10-year event and 6 cm for the 200-year event, suggesting considerable coastal

protection benefits. On the contrary, the 1000-year event is amplified under all MR width and vegetation scenarios.

Most of the attenuation in the scenario with the largest MR width (and area) may result from water that is piled up at the breached, seaward dike, while *within-wetland* attenuation from solely inside the MR is negligible (–1 cm km^{-1} when full vegetation cover is considered). This hypothesis is supported by absolute differences in HWLs between locations seaward the breached dike and from inside the three breaches (Figure 5.7). For all return water level scenarios, the average difference accounted for 9 cm, even though both areas are less then 30 m apart. Yet, the landward dike can be of lower design specification compared to the breached dike and should be cheaper regarding construction and maintenance costs.

In summary, large MR schemes can effectively reduce very high storm surge levels at the open coast, whereas the original Freiston Shore MR site, still being one of Europe's larger sites, cannot effectively reduce coastal flood risk. Vegetation cover and MR width increase inundation depth thresholds up to which HWLs are reduced. Under very high storm surge levels, most of the attenuation in the largest site scenario comes from water that is reflected at the remnants of the breached dike.

Chapter 7

Recommendations for future research

7.1 Most wanted: Field validation data for hydrodynamic models

To the knowledge of the author, this thesis presents the first comprehensive dataset of *in situ* measurements of HWL dynamics and attenuation rates inside an open coast MR scheme (chapter 3). This demonstrates that field measurements of HWL attenuation rates within restored saltmarshes, particularly inside MR schemes, are scarce and even absent under rare storm surge conditions (Stark et al., 2015; Bouma et al., 2014). Given the large variability of HWL attenuation rates found inside Freiston Shore, which could not fully be reproduced by the hydrodynamic model, and the fact that no storm surge coincided with the period of the field campaign, more field data for model validation is required. It may not be surprising that generally only little field data on extreme storm surges exist, since these are inherently rare events. To study the effectiveness of not only NBS, but also other coastal adaptation measures, field data for validating model predictions is urgently required. Bouma et al. (2014) therefore call for extended monitoring campaigns by using for example self-contained automated monitoring systems.

7.2 The balancing act: Coastal protection vs. ecological benefits?

The results of this thesis indicate that large and wide MR schemes with single or multiple dike breaches and RTE can effectively reduce HWLs and surges. For RTE, this is particularly true when implemented along estuaries, where it acts as flood water storage area (Oosterlee et al., 2018; Smolders et al., 2015). RTE may additionally prevent unexpected morphological adjustments, such as the widening and erosion of narrow dike breaches as response to increased tidal prisms. Freiston Shore constitutes a good example for this phenomenon (Friess et al., 2014).

However, studies suggest that the creation of less and smaller breaches should be balanced against hindered MR drainage and, in case of RTE, potentially reduced sedimentation rates. Oosterlee et al. (2020) compared five-year sedimentation rates between two MR sites. One was managed via RTE and the other by unhindered water exchange. Significantly higher sedimentation rates were found in the site that allows full tidal exchange, suggesting that more and wider breaches could lead to enhanced adaptive capacities of restored saltmarshes to SLR (Oosterlee et al., 2020). Indeed, a recent review by Liu et al. (2021) indicates that restored saltmarshes show generally higher sedimentation rates compared to adjacent natural marshes.

In addition to reduced sedimentation rates in case of RTE, it is suggested that restoration sites have fewer outlet channels compared to adjacent natural marshes, leading to hampered drainage (Crooks et al., 2002). A study from Puget Sound river deltas and the lower Columbia river (USA) reports that restored saltmarshes have 5-fold fewer channels compared to adjacent natural ecosystems (Hood, 2015). Inadequate drainage of restoration sites can lead to water pooling (Friess et al., 2014), which in turn results in anoxia (Crooks et al., 2002) and unfavourable biochemical conditions for vegetation establishment or persistence (Brooks et al., 2015). Anoxic soils favour pioneer plants

that are adapted to more frequent and longer inundations (Mossman et al., 2012a). In addition, if vegetation fails to establish, the development of saltmarsh ponds can be irreversible and thus constitutes a potential mechanism of marsh loss (Schepers et al., 2020).

In summary, future research on MR should focus on studying the delicate interplay between coastal protection benefits, sedimentation rates, MR drainage, vegetation establishment and the potential erosion and subsequent widening of dike breaches. As stated in the introduction to this thesis (subsection 1.3.2), the coastal protection function should then be studied more holistically, by accounting for HWL and wave attenuation in addition to shoreline stabilization. The translation of results from scientific studies that focus on only one element of coastal protection (e.g. HWL attenuation) cannot be easily translated into engineering guidelines (Möller, 2012). Ultimately, the coastal protection function, vegetation properties, sedimentation patterns and MR drainage are interrelated and refer to ecosystem functioning as a whole, which, even if usually not monitored, is a determinant of restoration success (Wolters et al., 2005).

Reducing maintenance costs of hard coastal protection measures is often targeted by MR, but success in this regard will only be achieved if maintenance of dikes is not replaced by maintenance of the restored ecosystem. Thus, a better understanding of complex natural dynamics is a pre-requisite for the successful application of coastal restoration schemes. Integrated assessments are therefore required, covering coastal protection benefits as well as MR drainage, including biogeochemical parameters and sedimentation patterns. It is clear that such studies require a concerted team effort in dedicated interdisciplinary projects. Achieving such sophisticated scientific targets is further obstructed by limited data availability (in parts stemming from insufficient MR monitoring campaigns) and computationally expensive modelling approaches. First steps in the right direction were undertaken by Gourgue et al. (2020), who have developed a novel approach to improve the representation of subgrid-scale interactions

between flow and vegetation in biogeomorphic models in a computationally efficient manner. Such modelling should also help addressing uncertainties around the future resilience of restored coastal wetlands in the face of SLR and should be pursued by the scientific community.

7.3 Effectiveness of nature-based solutions on regional scale?

Finally, studies are needed to investigate the effectiveness of diverse NBS to mitigate flood risks on a regional scale. Specific NBS, such as MR, are limited in their applicability to specific locations along the coast. For example, saltmarsh restoration requires the availability of fine sediments, low energy environments and vast low lying areas. Thus, if NBS are to be implemented on a regional scale, many different strategies are needed, including MR, beach nourishment or artificial reefs. Implementing different strategies along a coastal stretch may create synergies in terms of biodiversity and ecological functioning, but also for mitigating regional flood risks. The ECAS-BALTIC project investigates these synergies for the German Baltic Sea coast. Since November 2020, the author of this thesis works as a research associate in the project and investigates present and future flood risks for the German Baltic Sea coast with and without large-scale application of NBS.

Bibliography

ABPmer: The Online Managed Realignment Guide (OMREG), URL https://www.omreg.net/, visited on 2018-04-15, 2010.

ABPmer: The Online Managed Realignment Guide (OMREG), URL https://www.omreg.net/, visited on 2019-02-22, 2019.

ABPmer: The Online Managed Realignment Guide (OMREG), URL https://www.omreg.net/, visited on 2021-01-04, 2021.

Amos, C. L. and Collins, M. B.: The combined effects of wave motion and tidal currents on the morphology of intertidal ripple marks: The Wash, U.K, SEPM Journal of Sedimentary Research, Vol. 48, https://doi.org/10.1306/212F758B-2B24-11D7-8648000102C1865D, 1978.

An, S., Li, H., Guan, B., Zhou, C., Wang, Z., Deng, Z., Zhi, Y., Liu, Y., Xu, C., Fang, S., Jiang, J., and Li, H.: China's natural wetlands: Past problems, current status, and future challenges, AMBIO: A Journal of the Human Environment, 36, 335–342, https://doi.org/10.1579/0044-7447(2007)36[335:cnwppc]2.0.co;2, 2007.

Anderson, M. E. and Smith, J. M.: Wave attenuation by flexible, idealized salt marsh vegetation, Coastal Engineering, 83, 82–92, https://doi.org/10.1016/j.coastaleng.2013.10.004, 2014.

Augustin, L. N., Irish, J. L., and Lynett, P.: Laboratory and numerical studies of wave

damping by emergent and near-emergent wetland vegetation, Coastal Engineering, 56, 332–340, https://doi.org/10.1016/j.coastaleng.2008.09.004, 2009.

Baily, B. and Pearson, A. W.: Change detection mapping and analysis of salt marsh areas of central southern England from Hurst Castle Spit to Pagham Harbour, Journal of Coastal Research, 236, 1549–1564, https://doi.org/10.2112/05-0597.1, 2007.

Bakker, J. P., Esselink, P., Dijkema, K. S., van Duin, W. E., and de Jong, D. J.: Restoration of salt marshes in The Netherlands, Hydrobiologia, 478, 29–51, https://doi.org/10.1023/A:1021066311728, 2002.

Barbier, E. B.: Valuing the storm protection service of estuarine and coastal ecosystems, Ecosystem Services, 11, 32–38, https://doi.org/10.1016/j.ecoser.2014.06.010, 2015.

Barbier, E. B., Koch, E. W., Silliman, B. R., Hacker, S. D., Wolanski, E., Primavera, J., Granek, E. F., Polasky, S., Aswani, S., Cramer, L. A., Stoms, D. M., Kennedy, C. J., Bael, D., Kappel, C. V., Perillo, G. M. E., and Reed, D. J.: Coastal ecosystem-based management with nonlinear ecological functions and values, Science (New York, N.Y.), 319, 321–323, https://doi.org/10.1126/science.1150349, 2008.

Barbier, E. B., Hacker, S. D., Kennedy, C., Koch, E. W., Stier, A. C., and Silliman, B. R.: The value of estuarine and coastal ecosystem services, Ecological Monographs, 81, 169–193, https://doi.org/10.1890/10-1510.1, 2011.

Barbier, E. B., Georgiou, I. Y., Enchelmeyer, B., and Reed, D. J.: The value of wetlands in protecting southeast louisiana from hurricane storm surges, PloS one, 8, e58 715, https://doi.org/10.1371/journal.pone.0058715, 2013.

Bastidas, L. A., Knighton, J., and Kline, S. W.: Parameter sensitivity and uncertainty analysis for a storm surge and wave model, Natural Hazards and Earth System Sciences, 16, 2195–2210, https://doi.org/10.5194/nhess-16-2195-2016, 2016.

Baxter, P. J.: The east coast Big Flood, 31 January-1 February 1953: A summary of the human disaster, Philosophical transactions. Series A, Mathematical, physical, and engineering sciences, 363, 1293–1312, https://doi.org/10.1098/rsta.2005.1569, 2005.

Beudin, A., Kalra, T. S., Ganju, N. K., and Warner, J. C.: Development of a coupled wave-flow-vegetation interaction model, Computers & Geosciences, 100, 76–86, https://doi.org/10.1016/j.cageo.2016.12.010, 2017.

Boorman, L. A. and Hazelden, J.: Managed re-alignment; a salt marsh dilemma?, Wetlands Ecology and Management, 25, 387–403, https://doi.org/10.1007/s11273-017-9556-9, 2017.

Bouma, T. J., van Belzen, J., Balke, T., Zhu, Z., Airoldi, L., Blight, A. J., Davies, A. J., Galvan, C., Hawkins, S. J., Hoggart, S. P., Lara, J. L., Losada, I. J., Maza, M., Ondiviela, B., Skov, M. W., Strain, E. M., Thompson, R. C., Yang, S., Zanuttigh, B., Zhang, L., and Herman, P. M.: Identifying knowledge gaps hampering application of intertidal habitats in coastal protection: Opportunities & steps to take, Coastal Engineering, 87, 147–157, https://doi.org/10.1016/j.coastaleng.2013.11.014, 2014.

Brady, A. F. and Boda, C. S.: How do we know if managed realignment for coastal habitat compensation is successful? Insights from the implementation of the EU Birds and Habitats Directive in England, Ocean & Coastal Management, 143, 164–174, https://doi.org/10.1016/j.ocecoaman.2016.11.013, 2017.

Brew, D. and Williams, A.: Shoreline movement and shoreline management in The Wash, eastern England, Littoral conference 2002, the changing coast, Porto, Portugal, pp. 313–320, 2002.

Broekx, S., Smets, S., Liekens, I., Bulckaen, D., and de Nocker, L.: Designing a long-term flood risk management plan for the Scheldt estuary using a risk-based approach, Natural Hazards, 57, 245–266, https://doi.org/10.1007/s11069-010-9610-x, 2011.

Brooks, K. L., Mossman, H. L., Chitty, J. L., and Grant, A.: Limited vegetation development on a created salt marsh associated with over-consolidated sediments and lack of topographic heterogeneity, Estuaries and Coasts, 38, 325–336, https://doi.org/10.1007/s12237-014-9824-3, 2015.

Brown, S. L.: Wash banks flood defence scheme Freiston environmental monitoring 2007: R&D Technical Report FD1911/TR, Department for Environment, Food and Rural Affairs, London, 2008.

Brown, S. L., Pinder, A., Scott, L., Bass, J., Rispin, E., Brown, S., Garbutt, A., Thomson, A., Spencer, T., Möller, I., and Brooks, S. M.: Wash banks flood defence scheme Freiston environment monitoring 2002 - 2006, Department for Environment, Food and Rural Affairs, London, URL http://evidence.environment-agency.gov.uk/FCERM/en/Default/FCRM/Project.aspx?ProjectID=cd090c99-777e-4b1d-88e8-0f5ad39b5094&PageID=25ed1548-e755-452a-9d94-f2fc7d984e56, 2007.

Burden, A., Garbutt, R. A., Evans, C. D., Jones, D. L., and Cooper, D. M.: Carbon sequestration and biogeochemical cycling in a saltmarsh subject to coastal managed realignment, Estuarine, Coastal and Shelf Science, 120, 12–20, https://doi.org/10.1016/j.ecss.2013.01.014, 2013.

Callaghan, D. P., Bouma, T. J., Klaassen, P., van der Wal, D., Stive, M., and Herman, P.: Hydrodynamic forcing on salt-marsh development: Distinguishing the relative importance of waves and tidal flows, Estuarine, Coastal and Shelf Science, 89, 73–88, https://doi.org/10.1016/j.ecss.2010.05.013, 2010.

Caputo, M., Pieri, L., and Unguendoli, M.: Geometric investigation of the subsidence in the Po Delta, Bollettino di Geofisica Teorica e Applicata, 47, 187–207, 1970.

Christiansen, T., Wiberg, P. L., and Milligan, T. G.: Flow and sediment transport

on a tidal salt marsh surface, Estuarine, Coastal and Shelf Science, 50, 315–331, https://doi.org/10.1006/ecss.2000.0548, 2000.

Church, J. A., Clark, P. U., Cazenave, A., Gregory, J. M., Jevrejeva, S., Levermann, A., Merrifield, M. A., Milne, G. A., Nerem, P. D., Nunn, A. J., Payne, A. J., Pfeffer, W. T., Stammer, D., and Unnikrishnan, A. S.: Sea level change, in: Climate change 2013: The physical science basis. Contribution of Working Group I to the Fifth Assessment Report of the Intergovernmental Panel on Climate Change, edited by Stocker, T. F., Qin, D., Plattner, G. K., Tignor, M., Allen, S. K., Boschung, J., Nauels, A., Xia, Y., Bex, V., and Midgley, P. M., Cambridge University Press, Cambridge, UK and New York, NY, USA, 2013.

Codiga, D. L.: Unified tidal analysis and prediction using the UTide Matlab Functions. Technical Report 2011-01., URL `ftp://www.po.gso.uri.edu/pub/downloads/codiga/pubs/2011Codiga-UTide-Report.pdf`, 2011.

Committee on Climate Change: Managing the land in a changing climate: Chapter 5: Regulating services - coastal habitats, URL `https://www.theccc.org.uk/wp-content/uploads/2013/07/ASC-2013-Book-singles_2.pdf`, 2013.

Cooper, J. and McKenna, J.: Working with natural processes: The challenge for coastal protection strategies, The Geographical Journal, 174, 315–331, 2008.

Corbau, C., Simeoni, U., Zoccarato, C., Mantovani, G., and Teatini, P.: Coupling land use evolution and subsidence in the Po Delta, Italy: Revising the past occurrence and prospecting the future management challenges, The Science of the total environment, 654, 1196–1208, https://doi.org/10.1016/j.scitotenv.2018.11.104, 2019.

Costanza, R., d'Arge, R., de Groot, R., Farber, S., Grasso, M., Hannon, B., Limburg, K., Naeem, S., O'Neill, R. V., Paruelo, J., Raskin, R. G., Sutton, P., and van den Belt, M.: The value of the world's ecosystem services and natural capital, Nature, 387, 253–260, https://doi.org/10.1038/387253a0, 1997.

Cox, T., Maris, T., de Vleeschauwer, P., de Mulder, T., Soetaert, K., and Meire, P.: Flood control areas as an opportunity to restore estuarine habitat, Ecological Engineering, 28, 55–63, https://doi.org/10.1016/j.ecoleng.2006.04.001, 2006.

Crooks, S., Schutten, J., Sheern, G. D., Pye, K., and Davy, A. J.: Drainage and elevation as factors in the restoration of salt marsh in Britain, Restoration Ecology, 10, 591–602, https://doi.org/10.1046/j.1526-100X.2002.t01-1-02036.x, 2002.

Cross, M.: Wallasea island wild coast project, UK: Circular economy in the built environment, Proceedings of the Institution of Civil Engineers - Waste and Resource Management, 170, 3–14, https://doi.org/10.1680/jwarm.16.00006, 2017.

Dahl, T. E.: Wetland losses in the United States 1780´s to 1980´s., U.S. Department of the Interior, Fish and Wildlife Service, Washington, D.C., 1990.

Dale, J., Burgess, H. M., and Cundy, A. B.: Sedimentation rhythms and hydrodynamics in two engineered environments in an open coast managed realignment site, Marine Geology, 383, 120–131, https://doi.org/10.1016/j.margeo.2016.12.001, 2017.

Dangendorf, S., Hay, C., Calafat, F. M., Marcos, M., Piecuch, C. G., Berk, K., and Jensen, J.: Persistent acceleration in global sea-level rise since the 1960s, Nature Climate Change, 9, 705–710, https://doi.org/10.1038/s41558-019-0531-8, 2019.

Darwin, C. R.: Narrative of the surveying voyages of His Majesty's Ships Adventure and Beagle between the years 1826 and 1836, describing their examination of the southern shores of South America, and the Beagle's circumnavigation of the globe: Journal and remarks. 1832-1836, Henry Colburn, London, 1839.

Davidson, N. C.: How much wetland has the world lost? Long-term and recent trends in global wetland area, Marine and Freshwater Research, 65, 934, https://doi.org/10.1071/MF14173, 2014.

Davidson, N. C., Laffoley, D., Doody, J. P., Way, L. S., Gordon, J., Key, R., Drake, C. M., Pienkowski, M. W., Mitchell, R. M., and Duff, K. L.: Nature conservation and estuaries in Great Britain, Peterborough, UK, 1991.

Day, J. W., Boesch, D. F., Clairain, E. J., Kemp, G. P., Laska, S. B., Mitsch, W. J., Orth, K., Mashriqui, H., Reed, D. J., Shabman, L., Simenstad, C. A., Streever, B. J., Twilley, R. R., Watson, C. C., Wells, J. T., and Whigham, D. F.: Restoration of the Mississippi Delta: Lessons from hurricanes Katrina and Rita, Science (New York, N.Y.), 315, 1679–1684, https://doi.org/10.1126/science.1137030, 2007.

de Mulder, T., Vercruysse, J., Verelst, K., Peeters, P., Maris, T., and Meire, P.: Inlet sluices for flood control areas with controlled reduced tide in the Scheldt estuary: an overview, in: Proceedings of the international workshop on hydraulic design of low-head structures, edited by Bung, D. B., pp. 43–53, BAW, Karlsruhe, Germany, 2013.

de Vriend, H., van Koningsveld, M., and Aarninkhof, S.: 'Building with nature': The new Dutch approach to coastal and river works, Proceedings of the Institution of Civil Engineers - Civil Engineering, 167, 18–24, https://doi.org/10.1680/cien.13.00003, 2014.

Delft Hydraulics: User Manual Delft3D-FLOW. WL, Delft Hydraulics, Delft, The Netherlands, 2003.

Dixon, A. M., Leggett, D., and Weight, R. C.: Habitat creation opportunities for landward coastal re-alignment: Essex case studies, Water and Environment Journal, 12, 107–112, 1998.

Doody, J. P.: The impact of reclamation on the natural environment of The Wash., in: The Wash and its environment, edited by Doody, P. and Barnett, B., pp. 165–172, 1987.

Doody, J. P.: 'Coastal squeeze' – an historical perspective, Journal of Coastal Conservation, 10, 129, https://doi.org/10.1652/1400-0350(2004)010[0129:CSAHP]2.0.CO;2, 2004.

Doody, J. P.: Saltmarsh conservation, management and restoration., Springer, New York, 2008.

Duran Vinent, O., Herbert, E. R., Coleman, D. J., Himmelstein, J. D., and Kirwan, M. L.: Onset of runaway fragmentation of salt marshes, One Earth, 4, 506–516, https://doi.org/10.1016/j.oneear.2021.02.013, 2021.

Elahi, M. W. E., Jalón-Rojas, I., Wang, X. H., and Ritchie, E. A.: Influence of Seasonal River Discharge on Tidal Propagation in the Ganges–Brahmaputra–Meghna Delta, Bangladesh, Journal of Geophysical Research: Oceans, 125, 826, https://doi.org/10.1029/2020JC016417, 2020.

Environment Agency: Coastal flood boundary conditions for the UK: Update 2018: User guide: SC060064/TR7, Environment Agency, Bristol, UK, 2019a.

Environment Agency: Coastal flood boundary conditions for the UK: Update 2018: Technical summary report: SC060064/TR6, Environment Agency, Bristol, UK, 2019b.

Environment Agency: Vertical aerial photography tiles RGBN 2016 20cm: Environment Agency copyright and/or database right 2019. All rights reserved, URL `https://environment.data.gov.uk/DefraDataDownload/?Mode=survey`, 2019c.

Environment Agency: LIDAR composite DTM 2016 2m: Environment Agency copyright and/or database right 2020. All rights reserved, URL `https://environment.data.gov.uk/DefraDataDownload/?Mode=survey`, 2020.

Esteves, L. S.: Is managed realignment a sustainable long-term coastal manage-

ment approach?, Journal of Coastal Research, 65, 933–938, https://doi.org/10.2112/SI65-158.1, 2013.

Esteves, L. S.: Managed realignment: A viable long-term coastal management strategy?, SpringerBriefs in environmental science, Springer, New York, 2014.

Esteves, L. S. and Thomas, K.: Managed realignment in practice in the UK: Results from two independent surveys, Journal of Coastal Research, 70, 407–413, https://doi.org/10.2112/SI70-069.1, 2014.

Esteves, L. S. and Williams, J. J.: Managed realignment in Europe: a synthesis of methods, achievements and challanges, in: Living Shorelines: The science and management of nature-based coastal protection., edited by Bilkovic, D. M., Mitchell, M. M., Toft, J. D., and La Peyre, M. K., pp. 157–180, CRC Press/Taylor & Francis Group, 2017.

Fernandez-Nunez, M., Burningham, H., and Ojeda Zujar, J.: Improving accuracy of LiDAR-derived digital terrain models for saltmarsh management, Journal of Coastal Conservation, 21, 209–222, https://doi.org/10.1007/s11852-016-0492-2, 2017.

Firth, L. B., Airoldi, L., Bulleri, F., Challinor, S., Chee, S.-Y., Evans, A. J., Hanley, M. E., Knights, A. M., O'Shaughnessy, K., Thompson, R. C., Hawkins, S. J., and Coleman, M.: Greening of grey infrastructure should not be used as a Trojan horse to facilitate coastal development, Journal of Applied Ecology, 57, 1762–1768, https://doi.org/10.1111/1365-2664.13683, 2020.

French, J.: Tidal marsh sedimentation and resilience to environmental change: Exploratory modelling of tidal, sea-level and sediment supply forcing in predominantly allochthonous systems, Marine Geology, 235, 119–136, https://doi.org/10.1016/j.margeo.2006.10.009, 2006.

Friess, D., Möller, I., and Spencer, T.: Managed realignment and the re-establishment of saltmarsh habitat, Freiston Shore, Lincolnshire, United Kingdom, in: The Role of

Environmental Management and Eco-Engineering in Disaster Risk Reduction and Climate Change Adaptation, pp. 65–78, 2008.

Friess, D. A., Spencer, T., Smith, G. M., Möller, I., Brooks, S. M., and Thomson, A. G.: Remote sensing of geomorphological and ecological change in response to saltmarsh managed realignment, The Wash, UK, International Journal of Applied Earth Observation and Geoinformation, 18, 57–68, https://doi.org/10.1016/j.jag.2012.01.016, 2012.

Friess, D. A., Möller, I., Spencer, T., Smith, G. M., Thomson, A. G., and Hill, R. A.: Coastal saltmarsh managed realignment drives rapid breach inlet and external creek evolution, Freiston Shore (UK), Geomorphology, 208, 22–33, https://doi.org/10.1016/j.geomorph.2013.11.010, 2014.

Garbutt, A. and Wolters, M.: The natural regeneration of salt marsh on formerly reclaimed land, Applied Vegetation Science, 11, 335–344, https://doi.org/10.3170/2008-7-18451, 2008.

Garbutt, R. A., Reading, C. J., Wolters, M., Gray, A. J., and Rothery, P.: Monitoring the development of intertidal habitats on former agricultural land after the managed realignment of coastal defences at Tollesbury, Essex, UK, Marine pollution bulletin, 53, 155–164, https://doi.org/10.1016/j.marpolbul.2005.09.015, 2006.

Garzon, J. and Ferreira, C.: Storm surge modeling in large estuaries: Sensitivity analyses to parameters and physical processes in the Chesapeake Bay, Journal of Marine Science and Engineering, 4, 45, https://doi.org/10.3390/jmse4030045, 2016.

Gedan, K. B., Silliman, B. R., and Bertness, M. D.: Centuries of human-driven change in salt marsh ecosystems, Annual review of marine science, 1, 117–141, https://doi.org/10.1146/annurev.marine.010908.163930, 2009.

Gedan, K. B., Kirwan, M. L., Wolanski, E., Barbier, E. B., and Silliman, B. R.: The present and future role of coastal wetland vegetation in protecting shore-

lines: Answering recent challenges to the paradigm, Climatic Change, 106, 7–29, https://doi.org/10.1007/s10584-010-0003-7, 2011.

Gourgue, O., Belzen, J., Schwarz, C., Bouma, T. J., Koppel, J., and Temmerman, S.: A convolution method to assess subgrid–scale interactions between flow and patchy vegetation in biogeomorphic models, Journal of Advances in Modeling Earth Systems, https://doi.org/10.1029/2020MS002116, 2020.

Halcrow: Wash banks Hobhole to Butterwick low engineers report: Report to the Environment Agency, Anglian Region, 1999.

Hall, A. E., Herbert, R. J., Britton, J. R., and Hull, S. L.: Ecological enhancement techniques to improve habitat heterogeneity on coastal defence structures, Estuarine, Coastal and Shelf Science, 210, 68–78, https://doi.org/10.1016/j.ecss.2018.05.025, 2018.

Hill, M. and Randerson, P.: Saltmarsh vegetation communities of The Wash and their recent development, in: The Wash and its environment, edited by Doody, P. and Barnett, B., 1987.

Hinkel, J., Lincke, D., Vafeidis, A. T., Perrette, M., Nicholls, R. J., Tol, R. S. J., Marzeion, B., Fettweis, X., Ionescu, C., and Levermann, A.: Coastal flood damage and adaptation costs under 21st century sea-level rise, Proceedings of the National Academy of Sciences of the United States of America, 111, 3292–3297, https://doi.org/10.1073/pnas.1222469111, 2014.

Hofstede, J. L. A.: On the feasibility of managed retreat in the Wadden Sea of Schleswig-Holstein, Journal of Coastal Conservation, 23, 1069–1079, https://doi.org/10.1007/s11852-019-00714-x, 2019.

Hood, W. G.: Predicting the number, orientation and spacing of dike breaches for tidal marsh restoration, Ecological Engineering, 83, 319–327, https://doi.org/10.1016/j.ecoleng.2015.07.002, 2015.

Hopkinson, C., Lim, K., Chasmer, L. E., Treitz, P., Creed, I. F., and Gynan, C.: Wetland grass to plantation forest - estimating vegetation height from the standard deviation of lidar frequency distributions, International Archives of Photogrammetry, Remote Sensing and Spatial Information Science, 36, 288–294, 2004.

Horton, B. P., Khan, N. S., Cahill, N., Lee, J. S. H., Shaw, T. A., Garner, A. J., Kemp, A. C., Engelhart, S. E., and Rahmstorf, S.: Estimating global mean sea-level rise and its uncertainties by 2100 and 2300 from an expert survey, npj Climate and Atmospheric Science, 3, 1603, https://doi.org/10.1038/s41612-020-0121-5, 2020.

Hossain, A., Jia, Y., and Chao, X.: Estimation of Manning's roughness coefficient distribution for hydrodynamic model using remotely sensed land cover features, in: 2009 17th International Conference on Geoinformatics, pp. 1–4, IEEE, https://doi.org/10.1109/GEOINFORMATICS.2009.5293484, 2009.

Jones, C. G., Lawton, J. H., and Shachak, M.: Organisms as ecosystem engineers, Oikos, 69, 373, https://doi.org/10.2307/3545850, 1994.

Ke, X., Evans, G., and Collins, M. B.: Hydrodynamics and sediment dynamics of The Wash embayment, eastern England, Sedimentology, 43, 157–174, 1996.

Kiesel, J., Schuerch, M., Möller, I., Spencer, T., and Vafeidis, A.: Attenuation of high water levels over restored saltmarshes can be limited. Insights from Freiston Shore, Lincolnshire, UK, Ecological Engineering, 136, 89–100, https://doi.org/10.1016/j.ecoleng.2019.06.009, 2019.

Kiesel, J., Schuerch, M., Christie, E. K., Möller, I., Spencer, T., and Vafeidis, A. T.: Effective design of managed realignment schemes can reduce coastal flood risks, Estuarine, Coastal and Shelf Science, 242, 106 844, https://doi.org/10.1016/j.ecss.2020.106844, 2020.

Kiesel, J., McPherson, L. R., Schuerch, M., and Vafeidis, A. T.: Can managed realignment buffer extreme surges? The relationship between marsh width, vege-

tation cover and surge attenuation, Estuaries and Coasts, https://doi.org/https://doi.org/10.1007/s12237-021-00984-5, 2021.

Kirezci, E., Young, I. R., Ranasinghe, R., Muis, S., Nicholls, R. J., Lincke, D., and Hinkel, J.: Projections of global-scale extreme sea levels and resulting episodic coastal flooding over the 21st Century, Scientific reports, 10, 11 629, https://doi.org/10.1038/s41598-020-67736-6, 2020.

Kirwan, M. L., Guntenspergen, G. R., D'Alpaos, A., Morris, J. T., Mudd, S. M., and Temmerman, S.: Limits on the adaptability of coastal marshes to rising sea level, Geophysical Research Letters, 37, n/a–n/a, https://doi.org/10.1029/2010GL045489, 2010.

Kirwan, M. L., Temmerman, S., Skeehan, E. E., Guntenspergen, G. R., and Fagherazzi, S.: Overestimation of marsh vulnerability to sea level rise, Nature Climate Change, 6, 253–260, https://doi.org/10.1038/nclimate2909, 2016.

Knutson, P. L., Brochu, R. A., Seelig, W. N., and Inskeep, M.: Wave damping in Spartina alterniflora marshes, Wetlands, 2, 87–104, https://doi.org/10.1007/BF03160548, 1982.

Knutson, T. R., McBride, J. L., Chan, J., Emanuel, K., Holland, G., Landsea, C., Held, I., Kossin, J. P., Srivastava, A. K., and Sugi, M.: Tropical cyclones and climate change, Nature Geoscience, 3, 157–163, https://doi.org/10.1038/ngeo779, 2010.

Koch, E. W., Barbier, E. B., Silliman, B. R., Reed, D. J., Perillo, G. M. E., Hacker, S. D., Granek, E. F., Primavera, J. H., Muthiga, N., Polasky, S., Halpern, B. S., Kennedy, C. J., Kappel, C. V., and Wolanski, E.: Non-linearity in ecosystem services: Temporal and spatial variability in coastal protection, Frontiers in Ecology and the Environment, 7, 29–37, https://doi.org/10.1890/080126, 2009.

Kotze, D. C., Breen, C. M., and Quinn, N.: Wetland losses in South Africa, in: Wetlands of South Africa, edited by Cowan, G. I., pp. 263–272, Pretoria, 1995.

Krauss, K. W., Doyle, T. W., Doyle, T. J., Swarzenski, C. M., From, A. S., Day, R. H., and Conner, W. H.: Water level observations in mangrove swamps during two hurricanes in Florida, Wetlands, 29, 142–149, https://doi.org/10.1672/07-232.1, 2009.

Lawrence, D., Allen, J., and Havelock, G. M.: Salt marsh morphodynamics: An investigation of tidal flows and marsh channel equilibrium, Journal of Coastal Research, 20, 301–316, 2004.

Lawrence, P. J., Smith, G. R., Sullivan, M. J., and Mossman, H. L.: Restored saltmarshes lack the topographic diversity found in natural habitat, Ecological Engineering, 115, 58–66, https://doi.org/10.1016/j.ecoleng.2018.02.007, 2018.

Ledoux, L., Cornell, S., O'Riordan, T., Harvey, R., and Banyard, L.: Towards sustainable flood and coastal management: Identifying drivers of, and obstacles to, managed realignment, Land Use Policy, 22, 129–144, https://doi.org/10.1016/j.landusepol.2004.03.001, 2005.

Leonard, L. A. and Croft, A. L.: The effect of standing biomass on flow velocity and turbulence in Spartina alterniflora canopies, Estuarine, Coastal and Shelf Science, 69, 325–336, https://doi.org/10.1016/j.ecss.2006.05.004, 2006.

Leonardi, N., Carnacina, I., Donatelli, C., Ganju, N. K., Plater, A. J., Schuerch, M., and Temmerman, S.: Dynamic interactions between coastal storms and salt marshes: A review, Geomorphology, 301, 92–107, https://doi.org/10.1016/j.geomorph.2017.11.001, 2018.

Lesser, G. R., Roelvink, J. A., van Kester, J., and Stelling, G. S.: Development and validation of a three-dimensional morphological model, Coastal Engineering, 51, 883–915, https://doi.org/10.1016/j.coastaleng.2004.07.014, 2004.

Leuven, J. R. F. W., Pierik, H. J., van der Vegt, M., Bouma, T. J., and Kleinhans, M. G.: Sea-level-rise-induced threats depend on the size of tide-influenced estuaries worldwide, Nature Climate Change, 9, 986–992, https://doi.org/10.1038/s41558-019-0608-4, 2019.

Li, X., Leonardi, N., and Plater, A. J.: Wave-driven sediment resuspension and salt marsh frontal erosion alter the export of sediments from macro-tidal estuaries, Geomorphology, 325, 17–28, https://doi.org/10.1016/j.geomorph.2018.10.004, 2019.

Lichter, M., Vafeidis, A. T., and Nicholls, R. J.: Exploring data-related uncertainties in analyses of land area and population in the "Low-Elevation Coastal Zone" (LECZ), Journal of Coastal Research, 27, 757, https://doi.org/10.2112/JCOASTRES-D-10-00072.1, 2011.

Liu, H., Zhang, K., Li, Y., and Xie, L.: Numerical study of the sensitivity of mangroves in reducing storm surge and flooding to hurricane characteristics in southern Florida, Continental Shelf Research, 64, 51–65, https://doi.org/10.1016/j.csr.2013.05.015, 2013.

Liu, Z., Fagherazzi, S., and Cui, B.: Success of coastal wetlands restoration is driven by sediment availability, Communications Earth & Environment, 2, 169, https://doi.org/10.1038/s43247-021-00117-7, 2021.

Loder, N. M., Irish, J. L., Cialone, M. A., and Wamsley, T. V.: Sensitivity of hurricane surge to morphological parameters of coastal wetlands, Estuarine, Coastal and Shelf Science, 84, 625–636, https://doi.org/10.1016/j.ecss.2009.07.036, 2009.

Lotze, H. K., Lenihan, H. S., Bourque, B. J., Bradbury, R. H., Cooke, R. G., Kay, M. C., Kidwell, S. M., Kirby, M. X., Peterson, C. H., and Jackson, J. B. C.: Depletion, degradation, and recovery potential of estuaries and coastal seas, Science, 312, 1806–1809, https://doi.org/10.1126/science.1128035, 2006.

Lovelace, J. K.: Storm-tide elevations produced by Hurricane Andrew along the Louisiana coast, August 25-27, 1992, Open-File Report, US Geological Survey, https://doi.org/10.3133/ofr94371, 1994.

Luhar, M. and Nepf, H. M.: From the blade scale to the reach scale: A characterization of aquatic vegetative drag, Advances in Water Resources, 51, 305–316, https://doi.org/10.1016/j.advwatres.2012.02.002, 2013.

Luisetti, T., Turner, R. K., Bateman, I. J., Morse-Jones, S., Adams, C., and Fonseca, L.: Coastal and marine ecosystem services valuation for policy and management: Managed realignment case studies in England, Ocean & Coastal Management, 54, 212–224, https://doi.org/10.1016/j.ocecoaman.2010.11.003, 2011.

Macreadie, P. I., Hughes, A. R., and Kimbro, D. L.: Loss of 'blue carbon' from coastal salt marshes following habitat disturbance, PloS one, 8, e69 244, https://doi.org/10.1371/journal.pone.0069244, 2013.

Marani, M., D'Alpaos, A., Lanzoni, S., Carniello, L., and Rinaldo, A.: Biologically-controlled multiple equilibria of tidal landforms and the fate of the Venice lagoon, Geophysical Research Letters, 34, 77, https://doi.org/10.1029/2007GL030178, 2007.

Mariotti, G.: Marsh channel morphological response to sea level rise and sediment supply, Estuarine, Coastal and Shelf Science, 209, 89–101, https://doi.org/10.1016/j.ecss.2018.05.016, 2018.

Mariotti, G.: Beyond marsh drowning: The many faces of marsh loss (and gain), Advances in Water Resources, 144, 103 710, https://doi.org/10.1016/j.advwatres.2020.103710, 2020.

Mazik, K., Musk, W., Dawes, O., Solyanko, K., Brown, S., Mander, L., and Elliott, M.: Managed realignment as compensation for the loss of intertidal mudflat: A short term solution to a long term problem?, Estuarine, Coastal and Shelf Science, 90, 11–20, https://doi.org/10.1016/j.ecss.2010.07.009, 2010.

McGee, B. D., Goree, B. B., Tollett, R. W., Woodward, B. K., and Kress, W. H.: Hurricane Rita surge data, southwestern Louisiana and southeastern Texas, September to November 2005, Data Series, US Geological Survey, https://doi.org/10.3133/ds220, 2006.

McGranahan, G., Balk, D., and Anderson, B.: The rising tide: Assessing the risks of climate change and human settlements in low elevation coastal zones, Environment and Urbanization, 19, 17–37, https://doi.org/10.1177/0956247807076960, 2016.

Mcleod, E., Chmura, G. L., Bouillon, S., Salm, R., Björk, M., Duarte, C. M., Lovelock, C. E., Schlesinger, W. H., and Silliman, B. R.: A blueprint for blue carbon: Toward an improved understanding of the role of vegetated coastal habitats in sequestering CO 2, Frontiers in Ecology and the Environment, 9, 552–560, https://doi.org/10.1890/110004, 2011.

MEA: Ecosystems and human well-being: Synthesis, Island Press, Washington, DC., 2005.

Meixler, M. S., Kennish, M. J., and Crowley, K. F.: Assessment of plant community characteristics in natural and human-altered coastal marsh ecosystems, Estuaries and Coasts, 41, 52–64, https://doi.org/10.1007/s12237-017-0296-0, 2018.

Möller, I.: Bio-physical linkages in coastal wetlands – implications for coastal protection, in: NCK-days 2012 : Crossing borders in coastal research : jubilee conference proceedings, edited by Wijnberg, K., Horstman, E., and Kranenburg, W., University of Twente, Department of Water Engineering & Management, Enschede, the Netherlands, https://doi.org/10.3990/2.170, 2012.

Möller, I. and Christie, E.: Hydrodynamics and modeling of water flow in coastal wetlands, in: Coastal wetlands. An integrated ecosystem approach, edited by Perillo, G., Wolanski, E., Cahoon, D. R., and Hopkinson, C. S., Elsevier, Amsterdam, 2018.

Möller, I. and Spencer, T.: Wave dissipation over macro-tidal saltmarshes: Effects of marsh edge typology and vegetation change, Journal of Coastal Research, pp. 506–521, 2002.

Möller, I., Spencer, T., French, J. R., Leggett, D. J., and Dixon, M.: Wave transformation over salt marshes: A field and numerical modelling study from north Norfolk, England, Estuarine, Coastal and Shelf Science, 49, 411–426, https://doi.org/10.1006/ecss.1999.0509, 1999.

Möller, I., Kudella, M., Rupprecht, F., Spencer, T., Paul, M., van Wesenbeeck, B. K., Wolters, G., Jensen, K., Bouma, T. J., Miranda-Lange, M., and Schimmels, S.: Wave attenuation over coastal salt marshes under storm surge conditions, Nature Geoscience, 7, 727–731, https://doi.org/10.1038/ngeo2251, 2014.

Montgomery, J., Bryan, K., Horstman, E., and Mullarney, J.: Attenuation of tides and surges by mangroves: Contrasting case studies from New Zealand, Water, 10, 1119, https://doi.org/10.3390/w10091119, 2018.

Moore, K.: NERRS SWMP biomonitoring protocol: Long-term monitoring of estuarine submersed and emergent vegetation communities: Technical Report Series, NOAA, Silver Spring, 2011.

Morris, J. T., Sundareshwar, P. V., Nietch, C. T., Kjerfve, B., and Cahoon, D. R.: Responses of coastal wetlands to rising sea level, Ecology, 83, 2869–2877, https://doi.org/10.1890/0012-9658(2002)083[2869:ROCWTR]2.0.CO;2, 2002.

Morris, R. L., Konlechner, T. M., Ghisalberti, M., and Swearer, S. E.: From grey to green: Efficacy of eco-engineering solutions for nature-based coastal defence, Global change biology, 24, 1827–1842, https://doi.org/10.1111/gcb.14063, 2018.

Morris, R. L., Boxshall, A., and Swearer, S. E.: Climate-resilient coasts require diverse defence solutions, Nature Climate Change, 10, 485–487, https://doi.org/10.1038/s41558-020-0798-9, 2020.

Mossman, H. L., Brown, M. J. H., Davy, A. J., and Grant, A.: Constraints on salt marsh development following managed coastal realignment: Dispersal limitation or environmental tolerance?, Restoration Ecology, 20, 65–75, https://doi.org/10.1111/j.1526-100X.2010.00745.x, 2012a.

Mossman, H. L., Davy, A. J., Grant, A., and Elphick, C.: Does managed coastal realignment create saltmarshes with 'equivalent biological characteristics' to natural reference sites?, Journal of Applied Ecology, 49, 1446–1456, https://doi.org/10.1111/j.1365-2664.2012.02198.x, 2012b.

Mudd, S. M., Howell, S. M., and Morris, J. T.: Impact of dynamic feedbacks between sedimentation, sea-level rise, and biomass production on near-surface marsh stratigraphy and carbon accumulation, Estuarine, Coastal and Shelf Science, 82, 377–389, https://doi.org/10.1016/j.ecss.2009.01.028, 2009.

Narayan, S., Beck, M. W., Reguero, B. G., Losada, I. J., van Wesenbeeck, B., Pontee, N., Sanchirico, J. N., Ingram, J. C., Lange, G.-M., and Burks-Copes, K. A.: The effectiveness, costs and coastal protection benefits of natural and nature-based defences, PloS one, 11, e0154 735, https://doi.org/10.1371/journal.pone.0154735, 2016.

Naylor, L. A., Kippen, H., Coombes, M. A., and et al.: Greening the Grey: a framework for integrated green grey infrastructure (IGGI), URL `http://eprints.gla.ac.uk/150672/`, 2017.

Nerem, R. S., Beckley, B. D., Fasullo, J. T., Hamlington, B. D., Masters, D., and Mitchum, G. T.: Climate-change-driven accelerated sea-level rise detected in the altimeter era, Proceedings of the National Academy of Sciences of the United States of America, 115, 2022–2025, https://doi.org/10.1073/pnas.1717312115, 2018.

Neumann, B., Vafeidis, A. T., Zimmermann, J., and Nicholls, R. J.: Future coastal population growth and exposure to sea-level rise and coastal flooding–a global as-

sessment, PloS one, 10, e0118 571, https://doi.org/10.1371/journal.pone.0118571, 2015.

Nicholls, R. J. and Cazenave, A.: Sea-level rise and its impact on coastal zones, Science, 328, 1517–1520, https://doi.org/10.1126/science.1185782, 2010.

Nicholls, R. J., Lincke, D., Hinkel, J., Brown, S., Vafeidis, A. T., Meyssignac, B., Hanson, S. E., Merkens, J.-L., and Fang, J.: A global analysis of subsidence, relative sea-level change and coastal flood exposure, Nature Climate Change, 115, 2022, https://doi.org/10.1038/s41558-021-00993-z, 2021.

Nottage, A. and Robertson, P.: The saltmarsh creation handbook: A project manager's guide to the creation of saltmarsh and intertidal mudflat, Royal Society for the Protection of Birds, Sandy, 2005.

Oosterlee, L., Cox, T. J. S., Vandenbruwaene, W., Maris, T., Temmerman, S., and Meire, P.: Tidal marsh restoration design affects feedbacks between inundation and elevation change, Estuaries and Coasts, 41, 613–625, https://doi.org/10.1007/s12237-017-0314-2, 2018.

Oosterlee, L., Cox, T. J., Temmerman, S., and Meire, P.: Effects of tidal reintroduction design on sedimentation rates in previously embanked tidal marshes, Estuarine, Coastal and Shelf Science, 244, 106 428, https://doi.org/10.1016/j.ecss.2019.106428, 2020.

Oppenheimer, M., Glavovic, B. C., Hinkel, J., van de Wal, R., Magnan, A. K., Abd-Elgawad, A., Cai, R., Cifuentes-Jara, M., DeConto, R. M., Ghosh, T., Hay, J., Isla, F., Marzeion, B., Meyssignac, B., and Sebesvari, Z.: Sea level rise and implications for low-lying islands, coasts and communities, in: Special report on the ocean and the cryosphere in a changing climate, edited by Pörtner, H. O., Roberts, D. C., Masson-Delmotte, V., Zhai, P., Tignor, M., Poloczanska, E., Mintenbeck, K., Alegría, A., Nicolai, M., Okem, A., Petzold, J., Rama, B., and Weyer, N. M., 2019.

Paquier, A.-E., Haddad, J., Lawler, S., and Ferreira, C. M.: Quantification of the attenuation of storm surge components by a coastal wetland of the US mid Atlantic, Estuaries and Coasts, 40, 930–946, https://doi.org/10.1007/s12237-016-0190-1, 2017.

Pethick, J.: Estuarine and tidal wetland restoration in the United Kingdom: policy versus practice, Restoration Ecology, 10, 431–437, 2002.

Pontee, N.: Defining coastal squeeze: A discussion, Ocean & Coastal Management, 84, 204–207, https://doi.org/10.1016/j.ocecoaman.2013.07.010, 2013.

Pontee, N. and Tarrant, O.: Editorial: Promoting coastal resilience using green infrastructure, Proceedings of the Institution of Civil Engineers - Maritime Engineering, 170, 37–38, https://doi.org/10.1680/jmaen.2017.170.2.37, 2017.

Pontee, N., Narayan, S., Beck, M. W., and Hosking, A. H.: Nature-based solutions: Lessons from around the world, Proceedings of the Institution of Civil Engineers - Maritime Engineering, 169, 29–36, https://doi.org/10.1680/jmaen.15.00027, 2016.

Posford Duvivier: The Wash shoreline management plan. Report for the Environment Agency Anglian Region., Anglian Region, 1996.

Pye, K.: Controls on long-term saltmarsh accretion and erosion in The Wash, Eastern England, Journal of Coastal Research, 11, 337–356, 1995.

R Core Team: R: A language and environment for statistical computing, URL URLhttps://www.R-project.org/, 2019.

Reed, D., van Wesenbeeck, B., Herman, P. M., and Meselhe, E.: Tidal flat-wetland systems as flood defenses: Understanding biogeomorphic controls, Estuarine, Coastal and Shelf Science, 213, 269–282, https://doi.org/10.1016/j.ecss.2018.08.017, 2018.

Reed, D. J., Spencer, T., Murray, A. L., French, J. R., and Leonard, L.: Marsh surface sediment deposition and the role of tidal creeks: Implications for created and man-

aged coastal marshes, Journal of Coastal Conservation, 5, 81–90, https://doi.org/10.1007/BF02802742, 1999.

Reguero, B. G., Beck, M. W., Bresch, D. N., Calil, J., and Meliane, I.: Comparing the cost effectiveness of nature-based and coastal adaptation: A case study from the Gulf Coast of the United States, PloS one, 13, e0192 132, https://doi.org/10.1371/journal.pone.0192132, 2018.

Resio, D. T. and Westerink, J. J.: Modeling the physics of storm surges, Physics Today, 61, 33–38, https://doi.org/10.1063/1.2982120, 2008.

Rupprecht, F., Möller, I., Paul, M., Kudella, M., Spencer, T., van Wesenbeeck, B. K., Wolters, G., Jensen, K., Bouma, T. J., Miranda-Lange, M., and Schimmels, S.: Vegetation-wave interactions in salt marshes under storm surge conditions: Ecological Engineering, 100, 301-315, https://doi.org/10.1016/j.ecoleng.2016.12.030, 2017.

Sadat-Noori, M., Rankin, C., Rayner, D., Heimhuber, V., Gaston, T., Drummond, C., Chalmers, A., Khojasteh, D., and Glamore, W.: Coastal wetlands can be saved from sea level rise by recreating past tidal regimes, Scientific reports, 11, 1196, https://doi.org/10.1038/s41598-021-80977-3, 2021.

Saito, Y., Chaimanee, N., Jarupongsakul, T., and Syvitski, J.: Shriking megadeltas in Asia: Sea-Level rise and sediment reduction impacts from case study of the Chao Phraya Delta., Inprint Newsletter of the IGBP/IHDP Land Ocean Interaction in the Coastal Zone, pp. 3–9, 2007.

Schepers, L., Brennand, P., Kirwan, M. L., Guntenspergen, G. R., and Temmerman, S.: Coastal marsh degradation into ponds induces irreversible elevation loss relative to sea level in a microtidal system, Geophysical Research Letters, 47, 1021, https://doi.org/10.1029/2020GL089121, 2020.

Schernewski, G., Bartel, C., Kobarg, N., and Karnauskaite, D.: Retrospective assessment of a managed coastal realignment and lagoon restoration measure:

The Geltinger Birk, Germany, Journal of Coastal Conservation, 22, 157–167, https://doi.org/10.1007/s11852-017-0496-6, 2018a.

Schernewski, G., Schumacher, J., Weisner, E., and Donges, L.: A combined coastal protection, realignment and wetland restoration scheme in the southern Baltic: Planning process, public information and participation, Journal of Coastal Conservation, 22, 533–547, https://doi.org/10.1007/s11852-017-0542-4, 2018b.

Schmid, K. A., Hadley, B. C., and Wijekoon, N.: Vertical accuracy and use of topographic LIDAR data in coastal marshes, Journal of Coastal Research, 275, 116–132, https://doi.org/10.2112/JCOASTRES-D-10-00188.1, 2011.

Schuerch, M., Spencer, T., Temmerman, S., Kirwan, M. L., Wolff, C., Lincke, D., McOwen, C. J., Pickering, M. D., Reef, R., Vafeidis, A. T., Hinkel, J., Nicholls, R. J., and Brown, S.: Future response of global coastal wetlands to sea-level rise, Nature, 561, 231–234, https://doi.org/10.1038/s41586-018-0476-5, 2018.

Scott, D. B., Frail-Gauthier, J., and Mudie, P. J.: Coastal wetlands of the world: Geology, ecology, distribution and applications, Cambridge University Press, Cambridge and New York, 2014.

Sheng, Y. P., Lapetina, A., and Ma, G.: The reduction of storm surge by vegetation canopies: Three–dimensional simulations, Geophysical Research Letters, 39, https://doi.org/10.1029/2012GL053577, 2012.

Shepard, C. C., Crain, C. M., and Beck, M. W.: The protective role of coastal marshes: a systematic review and meta-analysis, PloS one, 6, e27 374, https://doi.org/10.1371/journal.pone.0027374, 2011.

Sigma Plan: URL `https://www.sigmaplan.be/en/`, visited on 2019-11-08, 2011.

Small, C. and Nicholls, R. J.: A global analysis of human settlement in coastal zones, Journal of Coastal Research, 19, 584–599, 2003.

Smolders, S., Plancke, Y., Ides, S., Meire, P., and Temmerman, S.: Role of intertidal wetlands for tidal and storm tide attenuation along a confined estuary: A model study, Natural Hazards and Earth System Sciences, 15, 1659–1675, https://doi.org/10.5194/nhess-15-1659-2015, 2015.

Sousa, A. I., Lillebø, A. I., Caçador, I., and Pardal, M. A.: Contribution of Spartina maritima to the reduction of eutrophication in estuarine systems, Environmental pollution, 156, 628–635, https://doi.org/10.1016/j.envpol.2008.06.022, 2008.

Spencer, K. L. and Harvey, G. L.: Understanding system disturbance and ecosystem services in restored saltmarshes: Integrating physical and biogeochemical processes, Estuarine, Coastal and Shelf Science, 106, 23–32, https://doi.org/10.1016/j.ecss.2012.04.020, 2012.

Spencer, T., Friess, D. A., Möller, I., Brown, S. L., Garbutt, R. A., and French, J. R.: Surface elevation change in natural and re-created intertidal habitats, eastern England, UK, with particular reference to Freiston Shore, Wetlands Ecology and Management, 20, 9–33, https://doi.org/10.1007/s11273-011-9238-y, 2012.

Spencer, T., Brooks, S. M., Evans, B. R., Tempest, J. A., and Möller, I.: Southern North Sea storm surge event of 5 December 2013: Water levels, waves and coastal impacts, Earth-Science Reviews, 146, 120–145, https://doi.org/10.1016/j.earscirev.2015.04.002, 2015.

Spencer, T., Schuerch, M., Nicholls, R. J., Hinkel, J., Lincke, D., Vafeidis, A. T., Reef, R., McFadden, L., and Brown, S.: Global coastal wetland change under sea-level rise and related stresses: The DIVA Wetland Change Model, Global and Planetary Change, 139, 15–30, https://doi.org/10.1016/j.gloplacha.2015.12.018, 2016.

Stark, J., van Oyen, T., Meire, P., and Temmerman, S.: Observations of tidal and storm surge attenuation in a large tidal marsh, Limnology and Oceanography, 60, 1371–1381, https://doi.org/10.1002/lno.10104, 2015.

Stark, J., Plancke, Y., Ides, S., Meire, P., and Temmerman, S.: Coastal flood protection by a combined nature-based and engineering approach: Modeling the effects of marsh geometry and surrounding dikes, Estuarine, Coastal and Shelf Science, 175, 34–45, https://doi.org/10.1016/j.ecss.2016.03.027, 2016.

Stark, J., Smolders, S., Meire, P., and Temmerman, S.: Impact of intertidal area characteristics on estuarine tidal hydrodynamics: A modelling study for the Scheldt Estuary, Estuarine, Coastal and Shelf Science, 198, 138–155, https://doi.org/10.1016/j.ecss.2017.09.004, 2017.

Symonds, A. M. and Collins, M. B.: Sediment dynamics associated with managed realignment; Freiston Shore, The Wash, UK, in: Proceedings of the 29th International Conference, edited by Smith, J. M., pp. 3173–3185, https://doi.org/10.1142/9789812701916{\textunderscore}0256, 2005.

Symonds, A. M. and Collins, M. B.: The development of artificially created breaches in an embankment as part of a managed realignment, Freiston Shore, UK, Journal of Coastal Research, pp. 130–134, 2007a.

Symonds, A. M. and Collins, M. B.: The establishment and degeneration of a temporary creek system in response to managed coastal realignment: The Wash, UK, Earth Surface Processes and Landforms, 32, 1783–1796, https://doi.org/10.1002/esp.1495, 2007b.

Symonds, A. M., Scott, C. R., and Collins, M. B.: Assessing the physical impacts of managed realignment in an estuarine and coastal environment, in: Proceedings of the 31st International Conference, edited by Smith, J. M., pp. 4508–4520, https://doi.org/10.1142/9789814277426{\textunderscore}0374, 2008.

Syvitski, J. P. M., Kettner, A. J., Overeem, I., Hutton, E. W. H., Hannon, M. T., Brakenridge, G. R., Day, J., Vörösmarty, C., Saito, Y., Giosan, L., and Nicholls,

R. J.: Sinking deltas due to human activities, Nature Geoscience, 2, 681–686, https://doi.org/10.1038/ngeo629, 2009.

Temmerman, S., de Vries, M. B., and Bouma, T. J.: Coastal marsh die-off and reduced attenuation of coastal floods: A model analysis, Global and Planetary Change, 92-93, 267–274, https://doi.org/10.1016/j.gloplacha.2012.06.001, 2012.

Temmerman, S., Meire, P., Bouma, T. J., Herman, P. M. J., Ysebaert, T., and de Vriend, H. J.: Ecosystem-based coastal defence in the face of global change, Nature, 504, 79–83, https://doi.org/10.1038/nature12859, 2013.

Tempest, J. A., Möller, I., and Spencer, T.: A review of plant-flow interactions on salt marshes: The importance of vegetation structure and plant mechanical characteristics, Wiley Interdisciplinary Reviews: Water, 2, 669–681, https://doi.org/10.1002/wat2.1103, 2015.

Thorslund, J., Jarsjo, J., Jaramillo, F., Jawitz, J. W., Manzoni, S., Basu, N. B., Chalov, S. R., Cohen, M. J., Creed, I. F., Goldenberg, R., Hylin, A., Kalantari, Z., Koussis, A. D., Lyon, S. W., Mazi, K., Mard, J., Persson, K., Pietro, J., Prieto, C., Quin, A., van Meter, K., and Destouni, G.: Wetlands as large-scale nature-based solutions: Status and challenges for research, engineering and management, Ecological Engineering, 108, 489–497, https://doi.org/10.1016/j.ecoleng.2017.07.012, 2017.

Townend, I. and Pethick, J.: Estuarine flooding and managed retreat, Philosophical transactions. Series A, Mathematical, physical, and engineering sciences, 360, 1477–1495, https://doi.org/10.1098/rsta.2002.1011, 2002.

Townend, I., Wang, Z. B., Stive, M., and Zhou, Z.: Development and extension of an aggregated scale model: Part 1 – Background to ASMITA, China Ocean Engineering, 30, 483–504, https://doi.org/10.1007/s13344-016-0030-x, 2016.

Turner, R. K., Burgess, D., Hadley, D., Coombes, E., and Jackson, N.: A cost–benefit

appraisal of coastal managed realignment policy, Global Environmental Change, 17, 397–407, https://doi.org/10.1016/j.gloenvcha.2007.05.006, 2007.

United States Environmental Protection Agency: San Francisco Bay Delta Watershed, URL `http://www2.epa.gov/sfbay-delta`, visited on 2011-11-08, 2013.

Valiela, I. and Cole, M. L.: Comparative evidence that salt marshes and mangroves may protect seagrass meadows from land-derived nitrogen loads, Ecosystems, 5, 92–102, https://doi.org/10.1007/s10021-001-0058-4, 2002.

van de Koppel, J., van der Wal, D., Bakker, J. P., and Herman, P. M. J.: Self-organization and vegetation collapse in salt marsh ecosystems, The American naturalist, 165, E1–12, https://doi.org/10.1086/426602, 2005.

van der Molen, J.: Tidal distortion and spatial differences in surface flooding characteristics in a salt marsh: Implications for Sea-Level Reconstruction, Estuarine, Coastal and Shelf Science, 45, 221–233, https://doi.org/10.1006/ecss.1997.0179, 1997.

van Goor, M. A., Zitman, T. J., Wang, Z. B., and Stive, M.: Impact of sea-level rise on the morphological equilibrium state of tidal inlets, Marine Geology, 202, 211–227, https://doi.org/10.1016/S0025-3227(03)00262-7, 2003.

van Oyen, T., Lanzoni, S., D'Alpaos, A., Temmerman, S., Troch, P., and Carniello, L.: A simplified model for frictionally dominated tidal flows, Geophysical Research Letters, 39, n/a–n/a, https://doi.org/10.1029/2012GL051949, 2012.

van Oyen, T., Carniello, L., D'Alpaos, A., Temmerman, S., Troch, P., and Lanzoni, S.: An approximate solution to the flow field on vegetated intertidal platforms: Applicability and limitations, Journal of Geophysical Research: Earth Surface, 119, 1682–1703, https://doi.org/10.1002/2013JF003064, 2014.

Vandenbruwaene, W., Schwarz, C., Bouma, T. J., Meire, P., and Temmerman, S.: Landscape-scale flow patterns over a vegetated tidal marsh and an unvegetated

tidal flat: Implications for the landform properties of the intertidal floodplain, Geomorphology, 231, 40–52, https://doi.org/10.1016/j.geomorph.2014.11.020, 2015.

Vousdoukas, M. I., Mentaschi, L., Voukouvalas, E., Bianchi, A., Dottori, F., and Feyen, L.: Climatic and socioeconomic controls of future coastal flood risk in Europe, Nature Climate Change, 8, 776–780, https://doi.org/10.1038/s41558-018-0260-4, 2018.

Vuik, V., Jonkman, S. N., Borsje, B. W., and Suzuki, T.: Nature-based flood protection: The efficiency of vegetated foreshores for reducing wave loads on coastal dikes, Coastal Engineering, 116, 42–56, https://doi.org/10.1016/j.coastaleng.2016.06.001, 2016.

Wadey, M. P., Haigh, I. D., Nicholls, R. J., Brown, J. M., Horsburgh, K., Carroll, B., Gallop, S. L., Mason, T., and Bradshaw, E.: A comparison of the 31 January–1 February 1953 and 5–6 December 2013 coastal flood events around the UK, Frontiers in Marine Science, 2, 793, https://doi.org/10.3389/fmars.2015.00084, 2015.

Wamsley, T. V., Cialone, M. A., Smith, J. M., Ebersole, B. A., and Grzegorzewski, A. S.: Influence of landscape restoration and degradation on storm surge and waves in southern Louisiana, Natural Hazards, 51, 207–224, https://doi.org/10.1007/s11069-009-9378-z, 2009.

Wamsley, T. V., Cialone, M. A., Smith, J. M., Atkinson, J. H., and Rosati, J. D.: The potential of wetlands in reducing storm surge, Ocean Engineering, 37, 59–68, https://doi.org/10.1016/j.oceaneng.2009.07.018, 2010.

Wasson, K., Ganju, N. K., Defne, Z., Endris, C., Elsey-Quirk, T., Thorne, K. M., Freeman, C. M., Guntenspergen, G., Nowacki, D. J., and Raposa, K. B.: Understanding tidal marsh trajectories: Evaluation of multiple indicators of marsh persistence, Environmental Research Letters, 14, 124 073, https://doi.org/10.1088/1748-9326/ab5a94, 2019.

Widdows, J., Pope, N. D., and Brinsley, M. D.: Effect of Spartina anglica stems on near-bed hydrodynamics, sediment erodability and morphological changes on an intertidal mudflat, Marine Ecology Progress Series, 362, 45–57, https://doi.org/10.3354/meps07448, 2008.

Wolters, M., Garbutt, A., and Bakker, J. P.: Salt-marsh restoration: Evaluating the success of de-embankments in north-west Europe, Biological Conservation, 123, 249–268, https://doi.org/10.1016/j.biocon.2004.11.013, 2005.

Ysebaert, T., Yang, S.-L., Zhang, L., He, Q., Bouma, T. J., and Herman, P. M. J.: Wave attenuation by two contrasting ecosystem engineering salt marsh macrophytes in the intertidal pioneer zone, Wetlands, 31, 1043–1054, https://doi.org/10.1007/s13157-011-0240-1, 2011.

Zedler, J. B. and Lindig-Cisneros, R.: Functional equivalency of restored and natural salt marshes, in: Concepts and controversies in tidal marsh ecology, edited by Weinstein, M. P. and Kreeger, D. A., pp. 565–582, Kluwer Academic Publishers, Dordrecht, The Netherlands, 2000.

Appendices

Appendix A

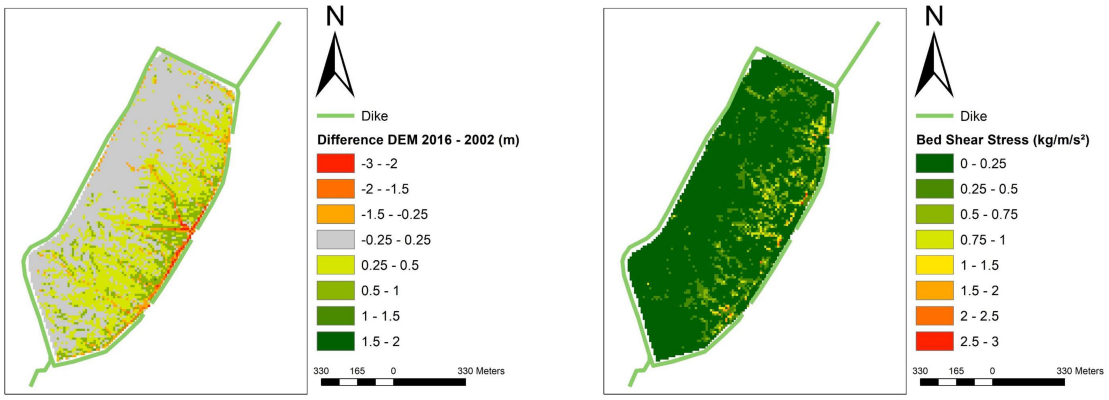

Figure A.1 Left: The difference between two LiDAR derived DEMs (provided by EA). The map shows areas of topographic change within the Freiston Shore managed realignment site between 2002 (year of dike breach) and 2016. Right: Bed shear stress was averaged over the study period, excluding times when the site was not flooded. Areas of topographic development and bed shear stress correspond well and are both limited to locations within and next to the artificial tidal creeks and the dike breaches.

Appendix B

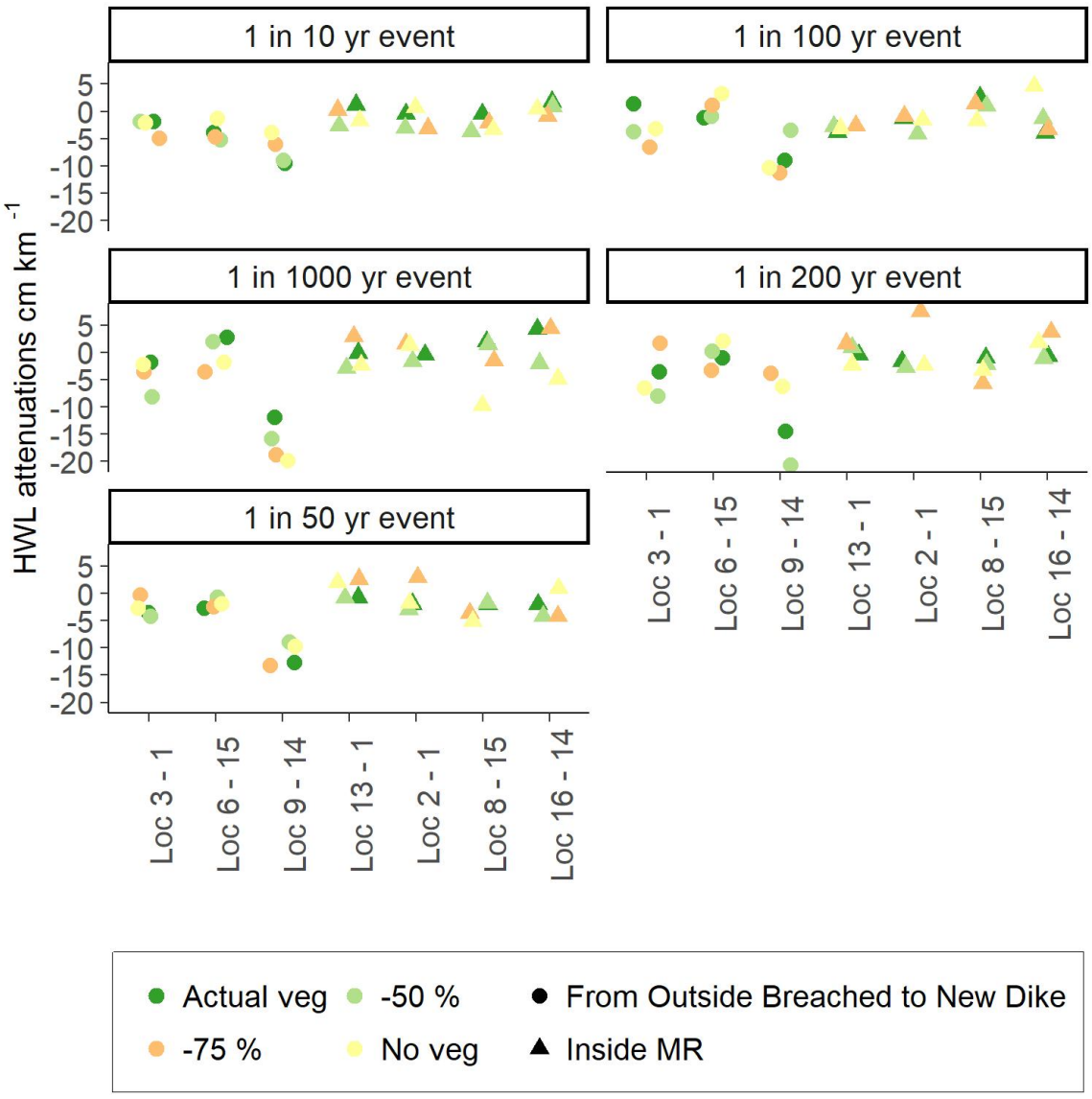

Figure B.1 HWL attenuation rates for the Freiston Shore MR site plotted per transect.

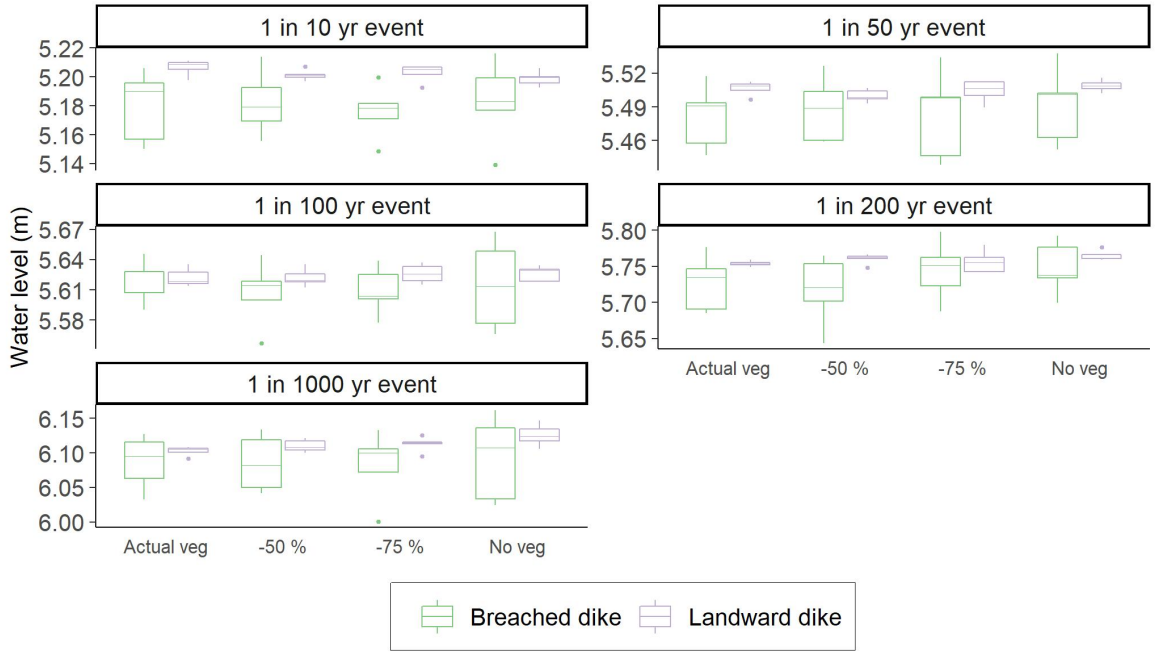

Figure B.2 High water levels (referenced to ODN) in front of the breached, seaward and landward lines of defence of the Freiston Shore MR site.

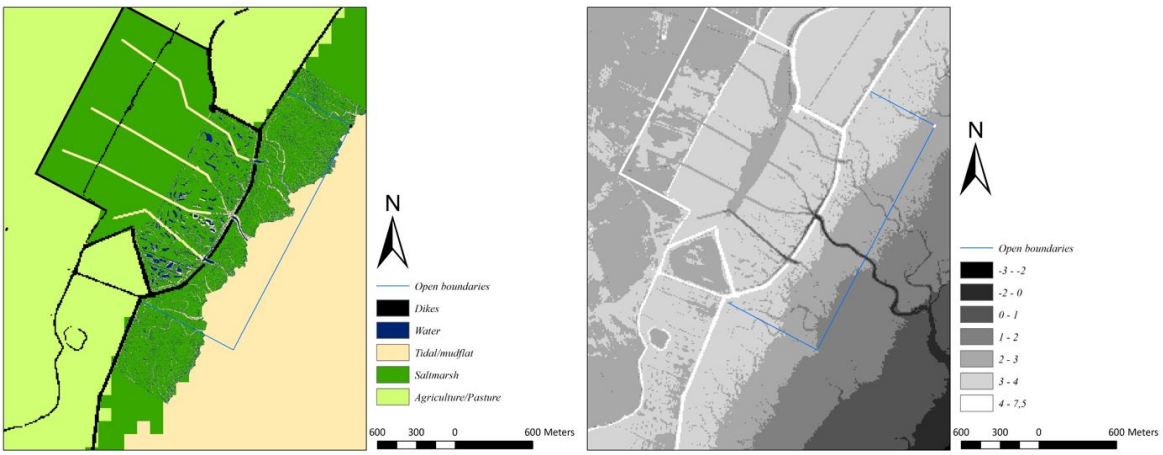

Figure B.3 Elevation and landcover maps of scenario 1.4 with additional tidal creeks. We used this additional scenario to investigate differences in HWL attenuation rates between a large MR site with and without tidal creeks. Tidal creeks were created by extending those of the original Freiston Shore MR site. The new, extended tidal creeks have a width of 10 m and a depth of approximately 1 m for most of the length, but decreasing depths to the landward ends of each creek. Thus, the additional creeks are substantially wider compared to those of the original MR site.

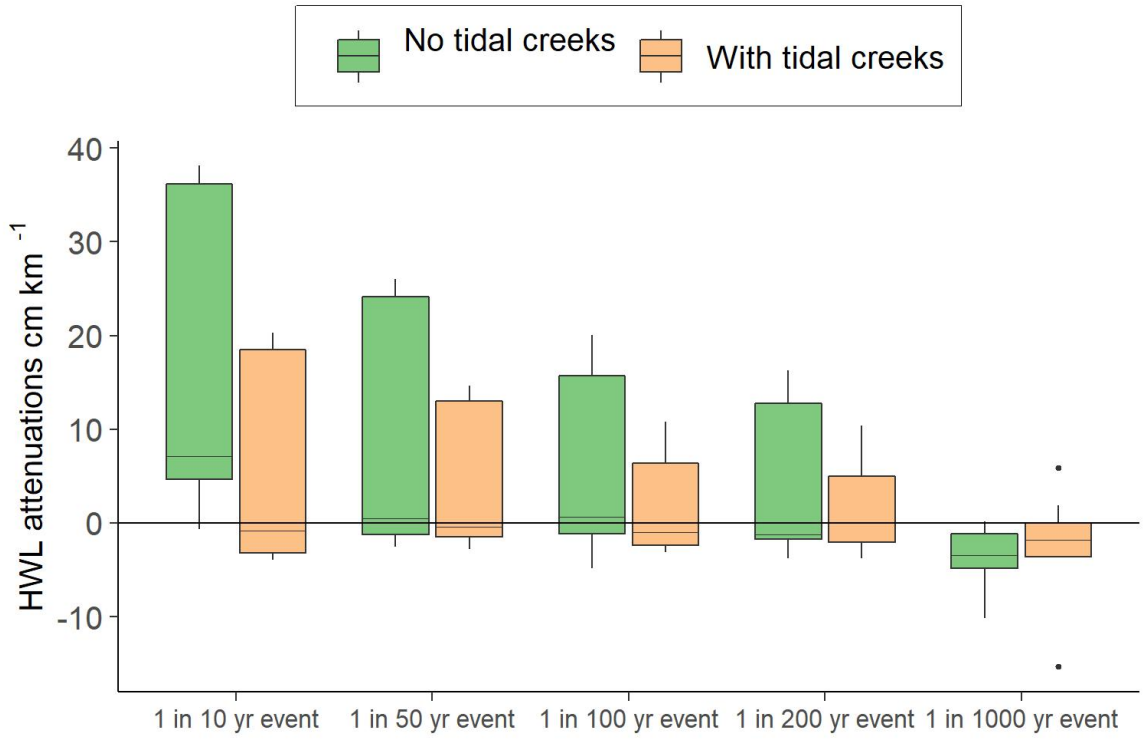

Figure B.4 Boxplots show HWL attenuation rates for scenario 1.4 with and without tidal creeks. Differences between the two scenarios were not statistically significant (Wilcoxon rank sum test p-value = 0.22). Comparing HWL attenuation rates between the Status Quo and scenario 1.4 without tidal creeks suggests statistically significant differences (Wilcoxon-rank-sum-test p-value 0.0008). On the contrary, comparing the Status Quo to scenario 1.4 with tidal creeks indicates no statistical significance (Wilcoxon-rank-sum-test p-value = 0.08, considering only actual (full) vegetation cover).

Table B.1 Average HWL attenuation rates (HWL att., cm km^{-1}), standard deviations (SD, cm km^{-1}) and p-values for statistical tests for all extreme event and vegetation scenarios of Freiston Shore, scenario 1.1, 1.2, 1.3 and 1.4. Superscript a and b indicate whether a two-way ANOVA model was calculated, or the non-parametric Kruskal-Wallis-test, respectively.

		10-year-event				50-year-event				100-year-event				200-year-event				1000-year-event				
		Actual veg	-50 %	-75 %	No veg	Actual veg	-50 %	-75 %	No veg	Actual veg	-50 %	-75 %	No veg	Actual veg	-50 %	-75 %	No veg	Actual veg	-50 %	-75 %	No veg
Status Quo	HWL att.	–2	–3	–3	–2	–4	–3	–3	–3	–2	–2	–3	–2	–3	–5	0	–2	–1	–4	–3	–6
	SD	4	3	2	2	4	3	5	4	4	2	4	5	5	8	5	3	5	6	8	7
	Veg. p-value		0.54[a]				0.94[b]				0.93[a]				0.61[b]				0.27[b]		
	Event p-value									0.27[b]											
1.1	HWL att.	–4				–5				–4				–3				–3			
	SD	4				8				6				5				5			
	Event p-value									0.77[b]											
1.2	HWL att.	–2				–5				–3				–5				–5			
	SD	3				4				6				6				6			
	Event p-value									0.38[b]											
1.3	HWL att.	6				3				0				1				0			
	SD	10				6				4				4				5			
	Event p-value									0.41[a]											
1.4	HWL att.	18	7	5	0	10	3	1	–1	6	1	–2	1	5	3	1	1	–4	–5	–8	–2
	SD	18	12	9	6	14	6	5	4	10	5	4	5	9	4	3	3	4	3	4	5
	Veg. p-value		0.06[a]				0.27[b]				0.41[a]				0.02[b]				0.0488[a]		
	Event p-value									0.02[b]											

Declaration of Authorship

Hiermit erkläre ich an Eides statt, dass ich die vorliegende Dissertation, abgesehen von der Beratung durch meine Betreuer, nach Inhalt und Form selbständig verfasst habe und keine weiteren Quellen und Hilfsmittel als die hier angegebenen verwendet habe. Diese Arbeit hat weder ganz noch in Teilen bereits an anderer Stelle im Rahmen eines Prüfungsverfahrens vorgelegen. Als kumulative Dissertation sind chapter 3 bis chapter 5 wie zu Beginn der Kapitel vermerkt in den genannten Zeitschriften veröffentlicht. Ich erkläre, dass die vorliegende Arbeit unter Einhaltung der Regeln guter wissenschaftlicher Praxis der Deutschen Forschungsgemeinschaft entstanden ist. Ich versichere, dass mir kein akademischer Grad entzogen wurde.

Kiel, Juli 2021